The Metric Space Approach to Quantum Mechanics

Paul Michael Sharp

Doctor of Philosophy

University of York
Physics

July 2015

Abstract

The metric space approach to quantum mechanics is a new, powerful method for deriving metrics for sets of quantum mechanical functions from conservation laws. We develop this approach to show that, from a standard form of conservation law, a universal method exists to generate a metric for the physical functions connected to that conservation law. All of these metric spaces have an "onion-shell" geometry consisting of concentric spheres, with functions conserved to the same value lying on the same sphere. We apply this approach to generate metrics for wavefunctions, particle densities, paramagnetic current densities, and external scalar potentials. In addition, we demonstrate the extensions to our approach that ensure that the metrics for wavefunctions and paramagnetic current densities are gauge invariant.

We use our metric space approach to explore the unique relationship between ground-state wavefunctions, particle densities and paramagnetic current densities in Current Density Functional Theory (CDFT). We study how this relationship is affected by variations in the external scalar potential, pairwise electronic interaction strength, and magnetic field strength. We find that all of the metric spaces exhibit a "band structure", consisting of "bands" of points characterised by the value of the angular momentum quantum number, m. These "bands" were found to either be separated by "gaps" of forbidden distances, or be "overlapping". We also extend this analysis beyond CDFT to explore excited states.

We apply our metrics in order to gain new insight into the Hohenberg-Kohn theorem and the Kohn-Sham scheme of Density Functional Theory. For the Hohenberg-Kohn theorem, we find that the relationship between potential and wavefunction metrics, and between potential and density metrics, is monotonic and includes a linear region. Comparing Kohn-Sham quantities to many-body quantities, we find that the distance between them increases as the electron interaction dominates over the external potential.

Contents

List of Figures

Acknowledgements

First of all, I would like to thank my PhD supervisor Irene D'Amico, for giving me the opportunity to work on a fascinating and challenging project, and providing guidance for my first steps into research.

Throughout my time in York, Phil Hasnip has provided me with an extraordinary amount of advice, support, and friendship. He has seen me through the many ups and downs a PhD inevitably brings with positivity and wise words, and his generosity with his time is matched only by his capacity for coffee.

The condensed matter theory group at York has been blessed with a number of brilliant researchers during my time here, and I would like to thank everyone who has provided excellent company over the last four years. In particular: James Ramsden, Matt Hodgson, Joly Aarons, Aaron Hopkinson, Ed Higgins, Jack Shepherd, Jacob Wilkins, Greta Carangelo and Neville Yee have been great friends and made my working days all the more pleasurable - often with the timely offer of a cup of tea! I am also very grateful for all of the guidance I have received from Matt Probert and Rex Godby.

In addition, a number of project students have enhanced the group during their year with us. It was always a pleasure to see them engage with us and go on to bigger and better things. I would especially like to mention: Jonathan Ledger, Elliot Levi, Nick Ashwin, Tom Durrant, Richard Lynn, Kevin Duff, Suzy Wallace, Alex Foote, Matthew Pickin, Jonathan Hogben, Liam Fitzgerald, Robbie Daniels, Mike Entwistle and Jack Wetherell for their enthusiasm and friendship whilst they were part of the group.

James Sizeland has been a brilliant friend for the last four years, and I'm very grateful for his excellent company and generous spirit. He also achieved what I had long thought impossible, by introducing me to a sport at which I have some ability when taking me to my first session at the Red Goat Climbing Wall. I'd also like to thank all of the friends I have made through climbing, including Steve Holgate, Tom Healey, Dan Wickison, and Tom Walton amongst many others. They have always been reliable for session at the wall followed by a pint, during which they tell me tales of the real world.

I'd like to thank all of my friends in the Department of Physics, all of whom have made sure I will look back fondly on my time at York.

I would like to extend my warmest gratitude to Jonathan Hogben (again), Aaron Long, and Edmund Dable-Heath, for volunteering to proof read this thesis, and for their diligence and valuable feedback. In addition, I am thankful for the enthusiasm and attention to detail shown by Luke Elliot, Daniel

Meilak, and Amy Skelt for assisting me in the final stages of my four year hunt for miscellaneous minus signs and factors of two. Many thanks to Luke Abraham for writing the template on which this thesis is based, I am sure I will never quite realise the amount of work I have been saved because of this.

I have had the pleasure and good fortune to live with some amazing people over the last four years, and I would like to extend my gratitude to all of my housemates at 43A Moorland Road: Matthew Hodgson, Jenefried Gay, Gionni Marchetti, Jon Bean, and Michael Mousley. I will treasure the new perspective on a good number of topics, extraordinary Sunday roasts and, most of all, the feeling of home from my time there.

Finally, and most importantly, I wish to thank my parents and my brother: Mike, Karen, and Adam Sharp, for their unstinting support. None of this would have been remotely possible without their willingness and ability to help me in any way I have ever needed.

Declarations

I declare that the work presented in this thesis, except where otherwise stated, is based on my own research and has not been submitted previously for a degree in this or any other university. Parts of the work reported in this thesis have been published in:

P. M. Sharp & I. D'Amico, "Metric space formulation of quantum mechanical conservation laws", *Phys. Rev. B* **89**, 115137, (2014);

P. M. Sharp & I. D'Amico, "Metric space analysis of systems immersed in a magnetic field" *Phys. Rev. A* **92**, 032509, (2015).

Chapter 1

Introduction

The quantum revolution in physics over the last century has resulted in an impressively detailed understanding of the physical world. The theory of quantum mechanics allows for physical descriptions of fundamental particles and radiation, where the predictions of classical mechanics have been shown to break down. In quantum mechanics, the deterministic description of matter is replaced by a description based on probabilities, with the information about the system given by a wavefunction. The development of quantum mechanics introduced concepts fundamentally different from those of classical physics, in particular: the quantisation of physical quantities such as energy and momentum; the notion of wave-particle duality for radiation and matter; and the uncertainty principle limiting the accuracy to which quantum observables can be measured [1].

Quantum mechanics has had an enormous influence on modern technology, with devices such as lasers and transistors that operate on the quantum scale. The phenomenon of quantum mechanical tunnelling is exploited in scanning tunnelling microscopes and tunnel diodes. In addition, our knowledge of quantum phenomena has led to the development of new fields of physics such as solid state physics and superconductivity.

Quantum mechanics is sufficiently well developed to be applied to describe real materials. However, direct quantum mechanical modelling of materials consisting of 10^{23} interacting atoms is impossible practically, due to the complexity of the many-body wavefunction. This has led to the development of approaches such as Density Functional Theory (DFT), which utilises the density, rather than the wavefunction, in a prominant role [2–4].

Mathematically, there is a deep connection between wavefunctions and vectors. Indeed, the wavefunction describing a quantum system is represented mathematically as a vector in a complex Hilbert space. This strong analogy

extends to defining lengths and scalar products of wavefunctions, as well as basis sets of linearly independent wavefunctions.

The motivation of this thesis is to use metric spaces in order to describe and compare quantum mechanical functions. Metric spaces define the concept of a distance between each of their elements. The use of metric spaces is motivated by the fact that the advantageous structures and operations conferred by the Hilbert space for wavefunctions do not carry over to the set of densities. Therefore, when changing the framework of quantum mechanics from the many-body wavefunction approach to the DFT approach, we lose these properties. However, a metric can be defined on any non-empty set. Thus we can define the concept of a distance for any set of functions, including wavefunctions, densities and any other set of quantum mechanical functions, and treat all of these quantities on the same footing.

1.1 Quantum Mechanics

Quantum mechanics has its origins in Max Planck's work on black-body radiation. In this work he proposed that the frequency of an oscillator, which in this case is the thermal vibration of the atoms making up the black body, can only take discrete values, and the energy of the oscillator is *quantised*. The allowed values of the frequency were hypothesised to be multiples of a fundamental physical constant, now known as Planck's constant, h (in quantum mechanics, it is more common to see $\hbar = \frac{h}{2\pi}$). Planck's hypothesis matched with the experimental data, which could not be explained by classical physics. The notion of quantisation of energy was further developed by Albert Einstein in his quantum interpretation of the photoelectric effect [5]. Einstein proposed that light itself was quantised, such that it is composed of quanta, which were later called photons, of energy $E = \hbar\omega$ [1]. This work suggested that light, which was always considered to be a wave, also has a particle-like nature [1].

In 1923, Louis de Broglie made the hypothesis that, alongside the particle nature of radiation, matter possessed wave-like properties, and hence the concept of wave-particle duality is universal in nature. By considering wave packets, de Broglie proposed that matter waves have an energy given by the Einstein relation, $E = \hbar\omega$, and wavelength

$$\lambda = \frac{h}{p}. \tag{1.1}$$

This hypothesis was confirmed by the electron diffraction experiments of C. J.

Davisson and L. H. Germer, and G. P. Thompson [1].

These ideas were developed into the theory of quantum mechanics between 1925 and 1930 [1]. One of the key postulates of quantum mechanics is that the most complete knowledge of a quantum system is given by the wavefunction, $\psi(\mathbf{r},t)$, and this wavefunction obeys a wave equation known as the Schrödinger equation.

The wavefunction was given a statistical interpretation by Max Born in 1926 [6]. The Born rule states that if we consider a large number of identically prepared systems described by the wavefunction $\psi(\mathbf{r},t)$, it is postulated that if the position of the particle is measured for each of the systems, $|\psi(\mathbf{r},t)|^2 d\mathbf{r}$ represents the probability of finding the particle within the volume element $d\mathbf{r}$. Hence, $|\psi(\mathbf{r},t)|^2$ is known as the position probability density [1].

In non-relativistic quantum mechanics, the wavefunction is obtained by solution of the time-dependent Schrödinger equation, which is given by

$$\hat{H}\psi(\mathbf{r},t) = i\frac{\partial\psi(\mathbf{r},t)}{\partial t}, \tag{1.2}$$

where $\hat{H}$ is the Hamiltonian of the system and, as is the case throughout this thesis, we use atomic units $\hbar = m_e = e = \frac{1}{4\pi\varepsilon_0} = 1$. In this thesis, we will restrict ourselves to the limit of time-independent quantum mechanics, and therefore we consider the time-independent Schrödinger equation,

$$\hat{H}\psi(\mathbf{r}) = E\psi(\mathbf{r}), \tag{1.3}$$

where E is the energy of the system.

The form of the Hamiltonian in Eq. (1.2) and Eq. (1.3) depends on the system under consideration. The most common form of the Hamiltonian is for a particle moving in a potential, $V(\mathbf{r})$, which is given by [1]

$$\hat{H} = -\frac{1}{2}\nabla^2 + V(\mathbf{r}), \tag{1.4}$$

where $V(\mathbf{r})$ is a scalar potential. This potential corresponds to an electric field via $\mathbf{E} = -\nabla V(\mathbf{r})$.

In this thesis, we will study systems subject to external magnetic fields. In this case it is necessary to introduce a dependence on the magnetic field into the Hamiltonian. The magnetic field is represented by a *vector* potential, $\mathbf{A}(\mathbf{r})$, such that $\mathbf{B}(\mathbf{r}) = \nabla \times \mathbf{A}(\mathbf{r})$. Including a vector potential gives us the Pauli Hamilto-

nian [7],

$$\hat{H} = -\frac{1}{2}\left[\nabla + \frac{1}{c}\mathbf{A}(\mathbf{r})\right]^2 + V(\mathbf{r}). \tag{1.5}$$

Quantum mechanics tells us that every observable quantity corresponds to a Hermitian operator, $\hat{O}$. The probabilistic nature of quantum mechanics means that, when measuring an observable for the same state, there is a range of possible results. Each of these results occurs with a well-defined probability.

The mean value of an observable, O, is given by the *expectation value* of the operator $\hat{O}$,

$$\langle O \rangle = \langle \psi | \hat{O} | \psi \rangle = \int \psi^*(\mathbf{r}) \hat{O} \psi(\mathbf{r}) d\mathbf{r}. \tag{1.6}$$

Following Born's interpretation of the wavefunction, the expectation value of an operator should be interpreted as the mean value of measurements of the observable O on a large number of identically prepared systems all represented by the wavefunction $\psi(\mathbf{r})$ [1].

In 1923, Niels Bohr formulated a principle connecting quantum mechanics with classical mechanics, that proved useful in the early development of quantum theory. Bohr's correspondence principle states that the results from quantum mechanics must tend asymptotically to those of classical mechanics, in the limit of large quantum numbers [1]. More precisely, when studying the classical limit of quantum mechanics, the "classical particle" is identified as a quantum mechanical wave packet. In order to specify the state of a system classically, both its position and momentum are required. However, the Heisenberg Uncertainty Principle states that it is impossible to specify position and momentum in quantum mechanics to accuracy better than $\hbar/2$ [1]. Therefore, the classical limit of quantum mechanics is attained when the values of distance and momentum are sufficiently large that the Heisenberg uncertainty principle can be neglected, i.e., for a sharply peaked wave packet [1, 8].

It can be shown that the expectation values of operators provide this connection to classical mechanics. We will now consider the behaviour of the quantum mechanical expectation values of observables with the Ehrenfest theorem.

1.1.1 Ehrenfest's Theorem

Ehrenfest's theorem [9] enables one to obtain the time evolution of the expectation value of physical quantities. Given that, for an operator $\hat{O}$, its expectation

value is given by $\langle O \rangle = \langle \psi | \hat{O} | \psi \rangle$, its time derivative is given by [8, 10]

$$\frac{d}{dt}\langle O \rangle = \left\langle \frac{d\psi}{dt} \middle| \hat{O} \middle| \psi \right\rangle + \left\langle \psi \middle| \frac{d\hat{O}}{dt} \middle| \psi \right\rangle + \left\langle \psi \middle| \hat{O} \middle| \frac{d\psi}{dt} \right\rangle. \tag{1.7}$$

Substituting in the time dependent Schrödinger equation (1.2) and its Hermitian conjugate we get

$$\begin{aligned}\frac{d}{dt}\langle O \rangle =& -\frac{1}{i\hbar}\left\langle \left(\psi \hat{H}\right) | \hat{O} | \psi \right\rangle + \left\langle \psi \middle| \frac{d\hat{O}}{dt} \middle| \psi \right\rangle + \frac{1}{i\hbar}\left\langle \psi | \hat{O} \right| \left(\hat{H}\psi\right) \rangle, \\ =& \frac{1}{i\hbar}\langle \psi | \left(\hat{O}\hat{H} - \hat{H}\hat{O}\right) | \psi \rangle + \left\langle \psi \middle| \frac{d\hat{O}}{dt} \middle| \psi \right\rangle.\end{aligned}$$

By applying the definition of a commutator, we get the result,

$$\frac{d}{dt}\langle O \rangle = \frac{1}{i\hbar}\langle \psi | \left[\hat{O}, \hat{H}\right] | \psi \rangle + \left\langle \psi \middle| \frac{d\hat{O}}{dt} \middle| \psi \right\rangle. \tag{1.8}$$

This is Ehrenfest's theorem. Applying the theorem to the expectation values of position and momentum shows that, in the classical limit, these expectation values obey Newton's equations of motion [1]. Also, if $\frac{d}{dt}\left\langle \hat{O} \right\rangle = 0$ then the operator $\hat{O}$ does not vary with time and is thus stated to be a constant of motion and conserved [8].

1.1.1.1 Noether's Theorem

The importance of conserved quantities in physics was established by the work of Emmy Noether in 1918 [11]. Noether's theorem is a powerful concept in theoretical physics that draws a clear link between the symmetries of a physical system and conservation laws [12].

The proof of the theorem proceeds by considering the Euler-Lagrange equations,

$$\frac{\partial L}{\partial Q} = \frac{d}{dt}\frac{\partial L}{\partial \dot{Q}}, \tag{1.9}$$

where L is the Lagrangian, Q is a generalised coordinate and a dot denotes differentiation with respect to time. We consider a continuous coordinate transformation, s, such that $s = 0$ represents the identity transformation. If $Q(s,t)$ is a solution of the Euler-Lagrange equations for any value of s, the Lagrangian is $L\left(Q(s,t), \dot{Q}(s,t)\right)$ and the Lagrangian after an infinitesimal transformation, ds, is $L'\left(Q(s+ds,t), \dot{Q}(s+ds,t)\right)$. In order for s to represent an invariant coordinate transformation, we require that

$$L'\left(Q(s+ds,t), \dot{Q}(s+ds,t)\right) = L\left(Q(s,t), \dot{Q}(s,t)\right), \tag{1.10}$$

which can also be written as

$$\frac{d}{ds}L\left(Q(s,t),\dot{Q}(s,t)\right)=0. \tag{1.11}$$

Applying the chain rule to Eq. (1.11) gives

$$\frac{dL}{ds}=\frac{\partial L}{\partial Q}\frac{dQ}{ds}+\frac{\partial L}{\partial \dot{Q}}\frac{d\dot{Q}}{ds}. \tag{1.12}$$

Substituting in the Euler-Lagrange equation for $L\left(Q(s,t),\dot{Q}(s,t)\right)$ gives,

$$\begin{aligned}\frac{dL}{ds}=&\frac{d}{dt}\left(\frac{\partial L}{\partial \dot{Q}}\right)\frac{dQ}{ds}+\frac{\partial L}{\partial \dot{Q}}\frac{d}{dt}\left(\frac{dQ}{ds}\right),\\ =&\frac{d}{dt}\left(\frac{\partial L}{\partial \dot{Q}}\frac{dQ}{ds}\right)=0.\end{aligned}$$

This means that

$$I(q,\dot{q})=\left.\frac{\partial L}{\partial \dot{q}}\frac{dQ}{ds}\right|_{s=0}=const, \tag{1.13}$$

where I is a conserved quantity, and $q=Q(0,t)$, $\dot{q}=\dot{Q}(0,t)$. Noether's theorem can hence be stated as: If the Lagrangian is invariant under a continuous symmetry transformation, there are conserved quantities associated with that symmetry [12]. This link between symmetries and conserved quantities holds for both classical and quantum mechanics.

1.1.2 Conservation Laws in Quantum Mechanics

We will now use Ehrenfest's theorem in order to derive conservation laws in quantum mechanics. The operators we consider are time-independent, so we can establish whether an operator is a constant of motion simply by determining whether or not it commutes with the Hamiltonian.

1.1.2.1 Conservation of the Norm of a Wavefunction

The norm of a wavefunction is given by $\langle\psi|\,\psi\rangle$, which we can write as $\langle\psi|\hat{I}|\,\psi\rangle$, where $\hat{I}$ is the identity operator, defined by

$$\hat{I}|\,\psi\rangle=|\,\psi\rangle\,. \tag{1.14}$$

From Eq. (1.14), we note that the identity operator commutes with any other operator by definition, hence

$$\left[\hat{I},\hat{H}\right]=0. \tag{1.15}$$

Therefore,

$$\frac{d}{dt}\langle\psi|\,\psi\rangle = 0 \quad \Longrightarrow \quad \langle\psi|\,\psi\rangle = const, \tag{1.16}$$

with the constant depending on how the wavefunction is normalised. The choice of normalisation is conventionally guided by the Born Rule, which defines $|\psi(\mathbf{r})|^2$ as the position probability density [1]. When calculating this expectation value, we integrate this position probability density over all space. Therefore this sum of all probabilities should be equal to 1.

Thus, the conservation of the norm of a wavefunction is

$$\langle\psi|\,\psi\rangle = 1. \tag{1.17}$$

By writing the definition of the particle density,

$$\rho(\mathbf{r}) = N\int\ldots\int|\psi(\mathbf{r}_1,\mathbf{r}_2\ldots\mathbf{r}_N)|^2\,d\mathbf{r}_2\ldots d\mathbf{r}_N, \tag{1.18}$$

and substituting into Eq. (1.17), we have

$$\begin{aligned}\langle\psi|\,\psi\rangle =& \int\ldots\int|\psi(\mathbf{r}_1,\mathbf{r}_2\ldots\mathbf{r}_N)|^2\,d\mathbf{r}_1 d\mathbf{r}_2\ldots d\mathbf{r}_N,\\ =&\frac{1}{N}\int\rho(\mathbf{r}_1)\,d\mathbf{r}_1 = 1.\end{aligned}$$

Rearranging this gives the conservation of the number of particles

$$\int\rho(\mathbf{r}_1)\,d\mathbf{r}_1 = N. \tag{1.19}$$

1.1.2.2 Conservation of Angular Momentum

The z-component of the angular momentum is given by

$$\hat{L}_z = [\mathbf{r}\times\hat{\mathbf{p}}]_z, \tag{1.20}$$

where $\hat{\mathbf{p}}$ is the linear momentum, $\hat{\mathbf{p}} = -i\nabla$. Hence, the expectation value of $\hat{L}_z$ is,

$$\begin{aligned}\langle L_z\rangle &= \langle\psi|\,[\mathbf{r}\times\hat{\mathbf{p}}]_z\,|\psi\rangle,\\ &= \langle\psi|\,xp_y - yp_x\,|\psi\rangle,\\ &= \left\langle\psi\middle|-i\left[x\frac{\partial}{\partial y} - y\frac{\partial}{\partial x}\right]\middle|\psi\right\rangle.\end{aligned} \tag{1.21}$$

First, we will consider the case where $\mathbf{A}(\mathbf{r}) = 0$ and the Hamiltonian is of the form of Eq. (1.4). In this case, the commutator of $\hat{L}_z$ and $\hat{H}$ is

$$\begin{aligned}
\left[\hat{L}_z, \hat{H}\right]\psi =& \frac{i}{2}\left(x\frac{\partial}{\partial y} - y\frac{\partial}{\partial x}\right)\nabla^2\psi - i\left(x\frac{\partial}{\partial y} - y\frac{\partial}{\partial x}\right)V(\mathbf{r})\,\psi \\
& - \frac{i}{2}\nabla^2\left(x\frac{\partial}{\partial y} - y\frac{\partial}{\partial x}\right)\psi + iV(\mathbf{r})\left(x\frac{\partial}{\partial y} - y\frac{\partial}{\partial x}\right)\psi, \\
=& \frac{1}{2}x\nabla^2\frac{\partial\psi}{\partial y} - \frac{1}{2}y\nabla^2\frac{\partial\psi}{\partial x} - x\frac{\partial\left[V(\mathbf{r})\,\psi\right]}{\partial y} + y\frac{\partial\left[V(\mathbf{r})\,\psi\right]}{\partial x} \\
& - \frac{1}{2}\nabla^2\left(x\frac{\partial\psi}{\partial y}\right) + \frac{1}{2}\nabla^2\left(y\frac{\partial\psi}{\partial x}\right) + xV(\mathbf{r})\frac{\partial\psi}{\partial y} - yV(\mathbf{r})\frac{\partial\psi}{\partial x}, \\
=& \frac{1}{2}x\nabla^2\frac{\partial\psi}{\partial y} - \frac{1}{2}x\nabla^2\frac{\partial\psi}{\partial y} - \nabla x\cdot\nabla\frac{\partial\psi}{\partial y} - \frac{1}{2}\frac{\partial\psi}{\partial y}\nabla^2 x \\
& - \frac{1}{2}y\nabla^2\frac{\partial\psi}{\partial x} + \frac{1}{2}y\nabla^2\frac{\partial\psi}{\partial x} + \nabla y\cdot\nabla\frac{\partial\psi}{\partial x} + \frac{1}{2}\frac{\partial\psi}{\partial x}\nabla^2 y \\
& - xV(\mathbf{r})\frac{\partial\psi}{\partial y} - x\psi\frac{\partial V}{\partial y} + yV(\mathbf{r})\frac{\partial\psi}{\partial x} + y\psi\frac{\partial V}{\partial x} + xV(\mathbf{r})\frac{\partial\psi}{\partial y} - yV(\mathbf{r})\frac{\partial\psi}{\partial x}, \\
=& \frac{\partial}{\partial y}\frac{\partial\psi}{\partial x} - \frac{\partial}{\partial x}\frac{\partial\psi}{\partial y} + y\psi\frac{\partial V}{\partial x} - x\psi\frac{\partial V}{\partial y}, \\
=& y\psi\frac{\partial V}{\partial x} - x\psi\frac{\partial V}{\partial y}, \\
\implies \left[\hat{L}_z, \hat{H}\right] =& y\frac{\partial V}{\partial x} - x\frac{\partial V}{\partial y}
\end{aligned}$$

So, $\left[\hat{L}_z, \hat{H}\right] = 0$ only when $y\frac{\partial V}{\partial x} = x\frac{\partial V}{\partial y}$, i.e., the potential must be rotationally symmetric about the z-axis.

For the Pauli Hamiltonian (1.5), where $\mathbf{A}(\mathbf{r}) \neq 0$, L_z commutes with the Hamiltonian when the scalar potential satisfies the condition of rotational invariance about the z-axis and the vector potential is of the form

$$\mathbf{A} = \left[x\alpha\left(x^2+y^2,z\right) + y\beta\left(x^2+y^2,z\right), y\alpha\left(x^2+y^2,z\right) - x\beta\left(x^2+y^2,z\right), \gamma\left(x^2+y^2,z\right)\right], \tag{1.22}$$

where α, β, γ are arbitrary functions; a proof of this is given in Appendix A.

When $\left[\hat{L}_z, \hat{H}\right] = 0$ is satisfied, we have,

$$\frac{d}{dt}\langle\psi|\hat{L}_z|\psi\rangle = 0 \quad \implies \quad \langle\psi|\hat{L}_z|\psi\rangle = m, \tag{1.23}$$

where m is the angular momentum quantum number.

1.1.2.3 Conservation of Energy

By considering the commutator

$$\left[\hat{H}, \hat{H}\right] = 0, \tag{1.24}$$

in the time-independent case, we obtain the conservation of energy directly,

$$\frac{d}{dt}\langle \psi | \hat{H} | \psi \rangle = 0 \quad \Longrightarrow \quad \left\langle \hat{H} \right\rangle = E. \tag{1.25}$$

1.1.3 The Many-Body Problem

Realistic quantum systems consist of many electrons. If we consider the case of N particles that do not interact with one another and where the confining potential can be written as $V(\mathbf{r}_1, \mathbf{r}_2 \ldots \mathbf{r}_N) = \sum_{i=1}^{N} v(\mathbf{r}_i)$, the Schrödinger equation can be separated into N single-particle Schrödinger equations of the form of Eq. (1.3), with the solution given by [1, 10]

$$\psi(\mathbf{r}_1, \mathbf{r}_2 \ldots \mathbf{r}_N) = \Pi_{i=1}^{N} \phi(\mathbf{r}_i). \tag{1.26}$$

If each coordinate of this wavefunction is determined by p parameters, the entire wavefunction therefore requires Np^3 parameters to be determined, with the particle density requiring only p^3 parameters. The value chosen for p reflects the desired accuracy for the wavefunction and density.

In reality however, the N electrons do interact with one another. Therefore, in order to write the Schrödinger equation for systems of more than one electron, we must introduce into the Hamiltonian a term, $U(\mathbf{r}_i, \mathbf{r}_j)$, that accounts for the pairwise interaction between each of the electrons. This yields the following form for the Schrödinger equation,

$$\left(\hat{T} + \hat{V} + \hat{U}\right) \psi(\mathbf{r}_1, \mathbf{r}_2, \ldots, \mathbf{r}_N) = E\psi(\mathbf{r}_1, \mathbf{r}_2, \ldots, \mathbf{r}_N), \tag{1.27}$$

where $\hat{T}$ is the operator for the kinetic energy, $\hat{V}$ is the operator for the external potential energy, and $\hat{U}$ is the operator for the pairwise electron interaction energy. Typically, the electrons interact via a Coulomb potential, such that

$$\hat{U} = \sum_{i<j} U(\mathbf{r}_i, \mathbf{r}_j) = \sum_{i<j} \frac{1}{|\mathbf{r}_i - \mathbf{r}_j|}. \tag{1.28}$$

This term is non-separable, which means that we cannot write the Schrödinger equation as N single-particle equations, and must instead solve it directly.

Hence, the presence of many-body interactions result in the Schrödinger equation being considerably more difficult to solve as N increases.

In addition, the interaction between electrons results in many-body wavefunctions increasing considerably in complexity as the number of particles in the system increases. For a system of N interacting particles, the number of parameters, M, required to determine the many-body wavefunction is given by [13]

$$M = p^{3N}, \tag{1.29}$$

with p the number of parameters required for each coordinate. The parameter p could, for example, represent the number of meshpoints each coordinate is sampled over. Taking a modest value of 20 meshpoints leads to the result that the wavefunction for a ten-particle system requires 10^{34} times more storage space than storing ten single-particle wavefunctions, and 10^{35} times more storage space than storing the density [3, 13].

1.2 Density Functional Theory

Density Functional Theory is a highly successful approach to the many-body problem in quantum mechanics [14]. The approach of DFT is to promote the density, $\rho(\mathbf{r})$, from being merely one of many observables to taking a central role when modelling many-body systems in the ground state [3]. DFT states that the mapping between the wavefunction and the particle density is *one–to–one* and, therefore, the ground state wavefunction and all ground state expectation values can be written as functionals of the density. As discussed in Sec. 1.1.3, the explicit use of the density rather than the wavefunction serves to reduces the complexity of many-body problems enormously.

In addition, the Kohn-Sham framework of DFT provides a reformulation of the many-body problem, that is in principle exact. The Kohn-Sham scheme replaces the system of N interacting particles with a system of N non-interacting particles confined by an effective potential, that incorporates the interactions present in the many-body system implicitly. The Kohn-Sham system yields the same density as the many-body system. Hence the density of an N-particle interacting system can be obtained by solving N single-particle Schrödinger equations. Despite the fact that approximations are required when implementing DFT practically, the use of DFT has achieved results far beyond what could be obtained by direct solution of the many-body Schrödinger equation.

1.2.1 Hohenberg-Kohn Theorem

The theoretical justification for the prominance of the density in DFT is due to the Hohenberg-Kohn theorem [15]. In 1964, Hohenberg and Kohn proved that a one-to-one map exists between the ground state wavefunction, ψ, and the ground state density, $\rho(\mathbf{r})$, and hence the density, despite being a function of three variables rather than $3N$ variables, contains exactly the same information as the ground state many body wavefunction [3].

The Hohenberg-Kohn theorem was originally proved by showing that two wavefunctions cannot produce the same density by *reductio ad absurdum*. Consider two distinct external potentials $V_1(\mathbf{r}), V_2(\mathbf{r})$ (distinct meaning that they do not merely vary by the addition of a constant) and their corresponding non-degenerate ground state wavefunctions $\psi_1(\mathbf{r}), \psi_2(\mathbf{r})$. We will assume that they both give rise to the same density $\rho(\mathbf{r})$. The Rayleigh-Ritz variational principle [16] tells us that the ground state energy is lowest in energy, i.e., for any arbitrary wavefunction ψ,

$$E_0 \leqslant \langle \psi | \hat{H} | \psi \rangle, \tag{1.30}$$

where E_0 is the ground state energy and the equality applies when ψ is the ground state wavefunction. Hence, for the Hamiltonian $\hat{H}_1$, which differs from $\hat{H}_2$ only by its potential term [15],

$$E_1 = \langle \psi_1 | \hat{H}_1 | \psi_1 \rangle < \langle \psi_2 | \hat{H}_1 | \psi_2 \rangle = \langle \psi_2 | \hat{H}_2 + V_1 - V_2 | \psi_2 \rangle. \tag{1.31}$$

Expanding the final term, with the definition $\langle V \rangle = \int V(\mathbf{r}) \rho(\mathbf{r}) d\mathbf{r}$, gives

$$\begin{aligned} E_1 &< \langle \psi_2 | \hat{H}_2 | \psi_2 \rangle + \langle \psi_2 | V_1 - V_2 | \psi_2 \rangle, \\ E_1 &< E_2 + \int [V_1(\mathbf{r}) - V_2(\mathbf{r})] \rho(\mathbf{r}) d\mathbf{r}. \end{aligned} \tag{1.32}$$

If we now consider the ground state of $\hat{H}_2$,

$$E_2 = \langle \psi_2 | \hat{H}_2 | \psi_2 \rangle < \langle \psi_1 | \hat{H}_2 | \psi_1 \rangle = \langle \psi_1 | \hat{H}_1 + V_2 - V_1 | \psi_1 \rangle. \tag{1.33}$$

Expanding the final term gives

$$\begin{aligned} E_2 &< \langle \psi_1 | \hat{H}_1 | \psi_1 \rangle + \langle \psi_1 | V_2 - V_1 | \psi_1 \rangle, \\ E_2 &< E_1 + \int [V_2(\mathbf{r}) - V_1(\mathbf{r})] \rho(\mathbf{r}) d\mathbf{r}. \end{aligned} \tag{1.34}$$

If we add equations (1.32) and (1.34), we produce the inequality

$$E_1 + E_2 < E_1 + E_2. \tag{1.35}$$

Therefore, two wavefunctions cannot give rise to the same density. We have thus proven that the mapping between wavefunctions and densities is injective, i.e., $\rho_1 = \rho_2 \Longrightarrow \psi_1 = \psi_2$.

In order to establish that the map between wavefunctions and densities is one-to-one, or bijective, we must also establish that the mapping is surjective, that is, whether all physical densities arise from an antisymmetric, N-electron wavefunction, i.e., whether they can be written in the form of Eq. (1.18). This issue is known as the N-representability problem. This problem has been successfully resolved: it was first discussed by Coleman [17] for fermionic density matrices, and then was addressed for arbitrary N-electron densities by Gilbert [18] and Harriman [19]. Harriman begins his proof by considering densities that are positive semidefinite and normalised to the number of particles as in Eq. (1.19) [19]. We show here the proof for N particles in one dimension, the extension to three dimensions is treated in Refs. [2, 4]. The proof begins by constructing a phase function

$$f(x) = \frac{2\pi}{N} \int_{-\infty}^{x} \rho\left(x'\right) dx' \tag{1.36}$$

such that $f(-\infty) = 0$ and $f(\infty) = 2\pi$. The phase function also has the property

$$\frac{df}{dx} = \frac{2\pi}{N} \rho(x) \tag{1.37}$$

Thus, we construct the orbitals

$$\phi_k(x) = \left[\frac{\rho(x)}{N}\right]^{\frac{1}{2}} e^{ikf(x)}. \tag{1.38}$$

We now show that these orbitals are orthonormal,

$$\begin{aligned}
\int_{-\infty}^{\infty} \phi_{k'}^{*}(x)\, \phi_k(x)\, dx &= \frac{1}{N} \int_{-\infty}^{\infty} \rho(x)\, e^{i(k-k')f(x)} dx, \\
&= \frac{1}{2\pi} \int_{-\infty}^{\infty} e^{i(k-k')f(x)} \frac{df}{dx} dx, \\
&= \frac{1}{2\pi} \int_{0}^{2\pi} e^{i(k-k')f} df, \\
&= \delta_{k,k'}
\end{aligned} \tag{1.39}$$

as is required for non-degenerate eigenstates of the Hamiltonian [2, 19]. We

can also show that these orbitals form a complete set [2]

$$\begin{aligned}\sum_k \phi_k^* \left(x'\right) \phi_k \left(x\right) &= \frac{\sqrt{\rho\left(x\right)\rho\left(x'\right)}}{N} \sum_k e^{ik[f(x)-f(x')]}, \\ &= \frac{\sqrt{\rho\left(x\right)\rho\left(x'\right)}}{N} \delta\left(f\left(x\right)-f\left(x'\right)\right), \\ &= \frac{\sqrt{\rho\left(x\right)\rho\left(x'\right)}}{N} \delta\left(x-x'\right)\left(\frac{df}{dx}\right)^{-1}, \\ &= \delta\left(x-x'\right), \end{aligned} \tag{1.40}$$

making use of a series expansion of the Dirac delta function [20].

We can construct an antisymmetric, N-particle wavefunction from the Slater determinant of these orbitals [2]

$$\Phi_{k_1 \ldots k_N} = \frac{1}{\sqrt{N}} \det\left(\phi_{k_1} \ldots \phi_{k_N}\right), \tag{1.41}$$

where the density is given by

$$\begin{aligned}\rho\left(x\right) &= \sum_{i=1}^{N} \left|\phi_{k_i}\left(x\right)\right|^2, \\ &= \frac{\rho\left(x\right)}{N} N, \\ &= \rho\left(x\right). \end{aligned} \tag{1.42}$$

We have therefore constructed an antisymmetric, N-particle wavefunction that yields a given density, resolving the N-representability problem.

In addition to a unique map between wavefunctions and densities, the Hohenberg-Kohn theorem also states that the map between the external potential (modulo a constant) and the wavefunction is also unique. The forward map is demonstrated by Eq. (1.27). In order to prove the reverse map, we consider two potentials, $V_1\left(\mathbf{r}\right)$, $V_2\left(\mathbf{r}\right)$, that give rise to the same ground state wavefunction ψ. From Eq. (1.27)

$$\left(\hat{H}_1 - \hat{H}_2\right)\psi = \left(E_1 - E_2\right)\psi \qquad \left(\hat{H}_1 - \hat{H}_2\right)\psi = \left[V_1\left(\mathbf{r}\right) - V_2\left(\mathbf{r}\right)\right]\psi \tag{1.43}$$

$$\implies \left[V_1\left(\mathbf{r}\right) - V_2\left(\mathbf{r}\right)\right]\psi = \left(E_1 - E_2\right)\psi \tag{1.44}$$

and hence the difference between the potentials $V_1\left(\mathbf{r}\right) - V_2\left(\mathbf{r}\right)$ must be a constant.

By analogy to the case for wavefunctions and densities, the v-representability problem (more precisely the interacting v-representability problem – since $U \neq 0$)

asks whether or not all physical, ground-state densities arise from a potential. In this case there is no clear construction for a potential, and there are known counterexamples [4, 21, 22].

Hohenberg and Kohn [15] have thus proved the following

$$V(\mathbf{r}) \rightleftharpoons \psi(\mathbf{r}, \mathbf{r}_2, \ldots, \mathbf{r}_N) \rightleftharpoons \rho(\mathbf{r}), \tag{1.45}$$

demonstrating the existence of a unique map between the density and the potential. The Hohenberg-Kohn theorem therefore states that the potential, the ground state wavefunction, and hence ground state expectation values of any observable, are all functionals of the ground state density. In particular, the ground state energy can be written as

$$E_0 = E[\rho_0] = \langle \psi[\rho_0] | \hat{H} | \psi[\rho_0] \rangle, \tag{1.46}$$

which, given that the Hamiltonian can be decomposed as $\hat{H} = \hat{T} + \hat{U} + \hat{V}$, can be written

$$E[\rho_0] = \langle \psi[\rho_0] | \hat{T} + \hat{U} | \psi[\rho_0] \rangle + \int V(\mathbf{r}) \rho_0(\mathbf{r}) \, dr = F[\rho_0] + V[\rho_0] \tag{1.47}$$

where $F = T + U$ is a universal functional (in that it does not depend on the external potential), for a given U; whereas V is specified by the system.

This energy is subject to the variational principle,

$$E[\rho_0] \leqslant E[\rho]. \tag{1.48}$$

Thus, after specifying a system, minimising the energy with respect to $\rho(\mathbf{r})$ yields the ground state density $\rho_0(\mathbf{r})$ and hence the ground state energy $E_0 = E[\rho_0]$. Hence, an important implication of the Hohenberg-Kohn theorem is that the ground state density is that which minimises the energy. This statement is sometimes known as the second Hohenberg-Kohn theorem.

However, in practice, minimisation of the functional $E[\rho]$ is itself a difficult problem, particularly since the Hohenberg-Kohn theorem does not provide any indication about the form of the functional $E[\rho]$. The work of Kohn and Sham resolved this difficulty, and set out the approach widely implemented for practical DFT applications.

1.2.2 Kohn-Sham Equations

A major problem in performing the minimisation of the energy is that the form of the universal functional, $F[\rho]$, in Eq. (1.47) is not known. In order to approximate it effectively, Kohn and Sham decomposed it into three parts: the kinetic energy of non-interacting particles of density $\rho(\mathbf{r})$, T_s, the Hartree energy, U_H, which is the classical electrostatic energy of the charge distribution $\rho(\mathbf{r})$ interacting with itself, and the remainder, which is called the exchange-correlation energy, $E_{xc}[\rho]$. We thus rewrite the energy functional as

$$E[\rho] = F[\rho] + V[\rho] = T_s[\rho] + U_H[\rho] + V[\rho] + E_{xc}[\rho] \tag{1.49}$$

where the exchange-correlation energy contains all of the many-body aspects of the system. The first three terms of the right hand side of Eq. (1.49) are known, but $E_{xc}[\rho]$ is an unknown functional of ρ.

Subject to the condition of particle conservation in Eq. (1.19), we minimise the energy in Eq. (1.49) by taking functional derivatives, which gives

$$\frac{\delta E[\rho]}{\delta \rho(\mathbf{r})} = \frac{\delta T_s[\rho]}{\delta \rho(\mathbf{r})} + V_H(\mathbf{r}) + V(\mathbf{r}) + V_{xc}(\mathbf{r}) = 0. \tag{1.50}$$

Consider now Eq. (1.50) for a system of non-interacting particles, i.e., no Hartree or exchange-correlation terms,

$$\frac{\delta E_s[\rho_s]}{\delta \rho(\mathbf{r})} = \frac{\delta T_s[\rho_s]}{\delta \rho(\mathbf{r})} + V_s(\mathbf{r}) = 0. \tag{1.51}$$

By choosing $V_s(\mathbf{r}) = V_H(\mathbf{r}) + V(\mathbf{r}) + V_{xc}(\mathbf{r})$, we find that $\rho_s(\mathbf{r}) = \rho(\mathbf{r})$. Therefore, we see that we can calculate the ground state density, $\rho(\mathbf{r})$, of the interacting N-particle system in an external potential $V(\mathbf{r})$ by solving a system of N non-interacting particles in a potential $V_s(\mathbf{r})$. The Schrödinger equation in this case is

$$\sum_{i=1}^{N} \left[-\frac{1}{2}\nabla^2 + V_s(\mathbf{r}) \right] \phi_i(\mathbf{r}) = \varepsilon_i \phi_i(\mathbf{r}), \tag{1.52}$$

which yields single-particle orbitals, $\phi_i(\mathbf{r})$, that reproduce the density of the interacting system, as

$$\rho(\mathbf{r}) = \sum_{i=1}^{N} |\phi_i(\mathbf{r})|^2, \tag{1.53}$$

where $\sum_{i=1}^{N} \varepsilon_i$ is the energy of the Kohn-Sham system. Eqs. (1.52) and (1.53) are known as the Kohn-Sham equations. Solving these equations yields the ground state density that satisfies the minimisation problem for the ground state energy. The Kohn-Sham scheme has thus replaced the interacting N-

particle system with a system of N non-interacting particles. We note that, as discussed in Sec. 1.1.3, this is a considerably easier problem to solve.

This approach is in principle exact, however, the exchange-correlation energy is an unknown functional and hence must be approximated. Fortunately $E_{xc}[\rho]$ is sufficiently small compared to $T_s[\rho]$ and $U_H[\rho]$ that it is possible to approximate $E_{xc}[\rho]$ with only a small fractional error in E. However, the importance of the exchange-correlation term to DFT should not be underestimated. Typical approximations used for $E_{xc}[\rho]$ are the local density approximation (LDA) [23, 24], generalised gradient approximations (GGA) [25–27], and meta-GGAs [28]. Although all of these approximations have limitations, DFT in the Kohn-Sham scheme has had considerable success in ground-state electronic structure calculations [29], and has even been applied to biological systems [30] and the study of exoplanets [31].

Following this success many extensions to DFT have been developed that extend the applicability of the theory to systems subject to different Hamiltonians. Such extensions include spin densities [32–34], relativistic effects [35, 36] and time-dependence [37, 38] as well as magnetic fields, which we consider next.

1.3 Current Density Functional Theory

In this thesis, we will study systems subject to external magnetic fields. We represent the magnetic field in the Hamiltonian by the vector potential, giving the Pauli Hamiltonian, Eq. (1.5). As a consequence of this vector potential, the wavefunction and all quantum observables will be a functional of another variable in addition to the particle density. Current Density Functional Theory (CDFT) is the extension of DFT that is motivated by the desire to model systems subject to external magnetic fields. Vignale and Rasolt, when deriving CDFT in 1987 [39, 40], showed that this additional basic variable is the paramagnetic current density, given by [4]

$$\mathbf{j}_p(\mathbf{r}) = \frac{1}{2i}\sum_{j=1}^{N}\int \left(\psi^*\nabla_j\psi - \psi\nabla_j\psi^*\right) d\mathbf{r}_2 \ldots d\mathbf{r}_N. \tag{1.54}$$

Vignale and Rasolt then proved the basic theorems of DFT when magnetic fields are present, beginning with the Hohenberg-Kohn theorem.

1.3.1 Hohenberg-Kohn Theorem for CDFT

Vignale and Rasolt showed that a Hohenberg-Kohn type theorem also exists for systems subject to magnetic fields [39]. Specifically, they proved that there is a unique map between the wavefunction and, when taken together, the particle density and the paramagnetic current density. In the spirit of the original proof of the Hohenberg-Kohn theorem for DFT, Vignale and Rasolt proceed by supposing that there are two sets of potentials $V_1(\mathbf{r})$, $A_1(\mathbf{r})$ and $V_2(\mathbf{r})$, $A_2(\mathbf{r})$ that give rise to the same ground state expectation values of the particle density, $\rho(\mathbf{r})$, and paramagnetic current density, $\mathbf{j}_p(\mathbf{r})$, and then proving a contradiction.

We let $\psi_1(\mathbf{r}_1, \mathbf{r}_2 \ldots \mathbf{r}_N)$ and $\psi_2(\mathbf{r}_1, \mathbf{r}_2 \ldots \mathbf{r}_N)$ be the non-degenerate ground states corresponding to the two sets of potentials, with Hamiltonians $\hat{H}_1$, $\hat{H}_2$ and ground state energies E_1 and E_2 respectively. Again, we apply the variational principle to $\hat{H}_1$ and prove the inequality

$$\begin{aligned} E_1 = \langle \psi_1 | \hat{H}_1 | \psi_1 \rangle < \langle \psi_2 | \hat{H}_1 | \psi_2 \rangle = & E_2 + \int \rho(\mathbf{r}) [V_1(\mathbf{r}) - V_2(\mathbf{r})] d^3\mathbf{r} \\ & + \frac{1}{c} \int \mathbf{j}_p(\mathbf{r}) \cdot [A_1(\mathbf{r}) - A_2(\mathbf{r})] d^3\mathbf{r} \\ & + \frac{1}{2c^2} \int \rho(\mathbf{r}) \left[A_1^2(\mathbf{r}) - A_2^2(\mathbf{r})\right] d^3\mathbf{r}. \end{aligned} \tag{1.55}$$

By applying the variational principle to $\hat{H}_2$, we generate the following inequality

$$\begin{aligned} E_2 = \langle \psi_2 | \hat{H}_2 | \psi_2 \rangle < \langle \psi_1 | \hat{H}_2 | \psi_1 \rangle = & E_1 + \int \rho(\mathbf{r}) [V_2(\mathbf{r}) - V_1(\mathbf{r})] d^3\mathbf{r} \\ & + \frac{1}{c} \int \mathbf{j}_p(\mathbf{r}) \cdot [A_2(\mathbf{r}) - A_1(\mathbf{r})] d^3\mathbf{r} \\ & + \frac{1}{2c^2} \int \rho(\mathbf{r}) \left[A_2^2(\mathbf{r}) - A_1^2(\mathbf{r})\right] d^3\mathbf{r}. \end{aligned} \tag{1.56}$$

Adding together equations (1.55) and (1.56) gives the contradiction

$$E_1 + E_2 < E_1 + E_2, \tag{1.57}$$

which proves that two sets of potentials $V_1(\mathbf{r})$, $A_1(\mathbf{r})$ and $V_2(\mathbf{r})$, $A_2(\mathbf{r})$ that give rise to two different ground states $\psi_1(\mathbf{r}_1, \mathbf{r}_2 \ldots \mathbf{r}_N)$ and $\psi_2(\mathbf{r}_1, \mathbf{r}_2 \ldots \mathbf{r}_N)$ cannot give rise to the same set of densities $\rho(\mathbf{r})$, $\mathbf{j}_p(\mathbf{r})$ [39]. We will refer to this theorem as the CDFT-HK theorem.

1.3.2 The Non-Uniqueness Problem

Having proved that there is a unique map between the densities and the wavefunction, Vignale and Rasolt supposed that this proof also extended to the potentials, as is proved for standard DFT. Capelle and Vignale [41] showed that a set of potentials $V(\mathbf{r})$, $\mathbf{A}(\mathbf{r})$ correspond to at most one wavefunction, determined by solution of the Schrödinger equation, but that it is possible to find different scalar and vector potentials that yield the same wavefunction (and hence the same particle and paramagnetic current densities) and thus the map from potentials to wavefunction is many-to-one.

The proof of this proceeds by considering a condition for which two different sets of potentials, $\{V(\mathbf{r}), \mathbf{A}(\mathbf{r})\}$ and $\{V(\mathbf{r}) + \Delta V(\mathbf{r}), A(\mathbf{r}) + \Delta A(\mathbf{r})\}$, yield the same ground-state wavefunction ψ_0. A necessary condition for this is for ψ_0 to satisfy the equation

$$\langle \psi_0 | \Delta \hat{H} | \psi_0 \rangle = \Delta E,$$

$$\int \left\{ \rho_0(\mathbf{r}) \Delta V(\mathbf{r}) + \frac{1}{c} \mathbf{j}_{p_0}(\mathbf{r}) \Delta A(\mathbf{r}) + \frac{1}{2c^2} \rho_0(\mathbf{r}) \Delta \left[A(\mathbf{r})^2 \right] \right\} d\mathbf{r} = \Delta E, \tag{1.58}$$

where $\rho_0(\mathbf{r})$ and $\mathbf{j}_{p_0}(\mathbf{r})$ arise from ψ_0. Particular solutions of Eq. (1.58) can be obtained by constructing linear combinations of the density operators that are constants of motion, and thus have simultaneous eigenfunctions with $\hat{H}$. Provided that the energy difference ΔE satisfies

$$\Delta E < \langle \psi_1 | \hat{H} | \psi_1 \rangle - \langle \psi_0 | \hat{H} | \psi_0 \rangle, \tag{1.59}$$

for the ground state and first excited state of $\hat{H}$, then ψ_0 is the ground-state eigenfunction of both $\hat{H}$ and $\hat{H} + \Delta \hat{H}$.

As was the case for standard DFT in Sec. 1.2.1, Eq. (1.58) is satisfied for $\Delta V = const$, $\Delta A = 0$. Inspection of Eq. (1.58) reveals that this case corresponds to the constant of motion $\hat{N} = \int \rho(\mathbf{r}) d\mathbf{r}$. A non-trivial example of a constant of motion that satisfies Eq. (1.58) is $\hat{L}_z = \int [\mathbf{r} \times \mathbf{j}_p(\mathbf{r})]_z d\mathbf{r}$. In this case, comparing coefficients with Eq. (1.58) gives,

$$\Delta A = \frac{\Delta B}{2} r \hat{\theta}, \qquad \Delta V = -\frac{A^2}{2c^2}, \tag{1.60}$$

with $\Delta B = const$.

This is known as the non-uniqueness problem of potentials, and is present in spin DFT and DFT for superconducting systems as well as CDFT [41]. This problem occurs for both the many-body *and* Kohn-Sham systems, and hence it does not follow that the densities $\rho(\mathbf{r})$, $\mathbf{j}_p(\mathbf{r})$ can be used to construct a Kohn-

Sham scheme for systems subject to vector potentials. This is one of a number of open questions with regards to CDFT, see for example Refs. [42–47].

Hence, the mappings between the wavefunction, basic potentials and basic densities in CDFT are

$$\begin{aligned}
&\{V_1(\mathbf{r}), \mathbf{A}_1(\mathbf{r})\} \searrow \\
&\{V_2(\mathbf{r}), \mathbf{A}_2(\mathbf{r})\} \longrightarrow \psi(\mathbf{r}, \mathbf{r}_2, \ldots, \mathbf{r}_N) \rightleftharpoons \left\{\rho(\mathbf{r}), \mathbf{j}_p(\mathbf{r})\right\} \\
&\qquad\qquad \ldots \\
&\{V_n(\mathbf{r}), \mathbf{A}_n(\mathbf{r})\} \nearrow
\end{aligned}$$

1.4 Metric Spaces

The concept of a metric was first introduced by Maurice Frechét in 1906 [48]. Frechét's motivation was to generalise theorems of functional calculus from cases such as real numbers and functions of one real variable to more abstract sets. Frechét first considered the notion of continuity, for which a definition of neighbouring elements of a set, and of the limit of a sequence of elements was required. This presented a difficulty, since these concepts tended to be defined *ad hoc* for the particular set being considered. Frechét noted that many of the conventional definitions of a limit can be derived by considering, for each pair of elements A, B in the set, a positive semidefinite number (A,B) with properties like that of a distance between two points, such that $(A,B) = 0$ for $A = B$, i.e., the distance between identical points is zero, and $(A,B) \to 0$ as $A \to B$ [48]. This map was called a metric by Felix Hausdorff [49].

By considering continuity, we can gain insight into the concept of the distance between elements for a range of sets. We note that a real-valued function, f, of one real variable is continuous at a point a if given any $\varepsilon > 0$, there exists $\delta > 0$ such that $|f(x) - f(a)| < \varepsilon$ for any x such that $|x - a| < \delta$. In other words, the function is continuous if the distance between $f(x)$ and $f(a)$ can be made as small as desired with an appropriate choice of the distance between x and a. If we now consider f to be a function of two real variables, then our definition of continuity still applies, but we must modify the definition of distance appropriately. A real-valued function, f, of two real variables is continuous at a point (a,b) if given any $\varepsilon > 0$, there exists $\delta > 0$ such that $|f(x) - f(a)| < \varepsilon$ for any x such that $\sqrt{\left[(x-a)^2 + (y-b)^2\right]} < \delta$, i.e., the Pythagorean distance between two points in the plane. From this, it can easily be seen how the definition of continuity can be extended to a real-valued function of three real variables, and then to N real variables [50].

To consider the definition of continuity for a general map $f : X \to Y$, we must define the distance between any two elements of X and Y. Since ε and δ are real numbers, this distance must also be real. We present the properties of the distance next.

1.4.1 Axioms of Metric Spaces

A metric space consists of a non-empty set X and a metric, or distance function, D and is hence written (X, D). The set X forms the "points" of the space whilst the metric is a map $D : X \times X \to \mathbb{R}$ used in order to assign a distance between any two elements of X. In order to describe distances between the elements in the space, the metric must satisfy the following axioms for all $x, y, z \in X$ [50, 51]:

$$D(x,y) \geqslant 0 \text{ and } D(x,y) = 0 \iff x = y, \tag{1.61}$$

$$D(x,y) = D(y,x), \tag{1.62}$$

$$D(x,y) \leqslant D(x,z) + D(z,y). \tag{1.63}$$

These axioms are also known as positivity, symmetry and the triangle inequality respectively. From Eq. (1.63), we also have the reverse triangle inequality [50, 51]

$$D(x,y) \geqslant |D(x,z) - D(y,z)|. \tag{1.64}$$

1.4.2 Examples of Metric Spaces

1.4.2.1 Euclidean Metric

The Euclidean metric is the distance between points in Euclidean space. This metric is intuitively familiar as it is the distance between two points that one would measure with a ruler. In two and three dimensions, the Euclidean metric is simply Pythagoras' theorem. In one dimension, this metric reduces to the absolute value of the difference between two points

$$d_2(x,y) = \left[(x-y)^2\right]^{\frac{1}{2}} = |x-y|. \tag{1.65}$$

For points x, y in N-dimensional space, the Euclidean metric is defined as

$$d_2(x,y) = \left[\sum_{i=1}^{N} (x_i - y_i)^2\right]^{\frac{1}{2}}. \tag{1.66}$$

We will now prove that this metric satisfies the metric axioms (1.61)–(1.63).

The axioms (1.61) and (1.62) hold because $(x_i - y_i)$ is squared, removing the negative and non-symmetric terms. For the axiom (1.63)

$$\left[\sum_{i=1}^{N}(x_i-y_i)^2\right]^{\frac{1}{2}} \leqslant \left[\sum_{i=1}^{N}(x_i-z_i)^2\right]^{\frac{1}{2}} + \left[\sum_{i=1}^{N}(z_i-y_i)^2\right]^{\frac{1}{2}}. \tag{1.67}$$

By writing $r_i = x_i - z_i$ and $s_i = z_i - y_i$ we can write the equivalent inequality

$$\left[\sum_{i=1}^{N}(r_i+s_i)^2\right]^{\frac{1}{2}} \leqslant \left[\sum_{i=1}^{N}r_i^2\right]^{\frac{1}{2}} + \left[\sum_{i=1}^{N}s_i^2\right]^{\frac{1}{2}}. \tag{1.68}$$

If we square both sides,

$$\begin{aligned}
\sum_{i=1}^{N}r_i^2 + \sum_{i=1}^{N}s_i^2 + 2\sum_{i=1}^{N}r_is_i &\leqslant \sum_{i=1}^{N}r_i^2 + \sum_{i=1}^{N}s_i^2 + 2\left[\sum_{i=1}^{N}r_i^2\right]^{\frac{1}{2}}\left[\sum_{i=1}^{N}s_i^2\right]^{\frac{1}{2}}, \\
\sum_{i=1}^{N}r_is_i &\leqslant \left[\sum_{i=1}^{N}r_i^2\right]^{\frac{1}{2}}\left[\sum_{i=1}^{N}s_i^2\right]^{\frac{1}{2}}, \\
\left[\sum_{i=1}^{N}r_is_i\right]^2 &\leqslant \left[\sum_{i=1}^{N}r_i^2\right]\left[\sum_{i=1}^{N}s_i^2\right].
\end{aligned} \tag{1.69}$$

This is Cauchy's inequality [50]. Cauchy's inequality is proved by expanding the left hand side using Lagrange's identity [52]

$$\begin{aligned}
\left[\sum_{i=1}^{N}r_is_i\right]^2 &= \left[\sum_{i=1}^{N}r_i^2\right]\left[\sum_{i=1}^{N}s_i^2\right] - \sum_{1\leqslant i<j\leqslant N}\left(r_is_j - r_js_i\right)^2, \\
\sum_{1\leqslant i<j\leqslant N}\left(r_is_j - r_js_i\right)^2 &= \left[\sum_{i=1}^{N}r_i^2\right]\left[\sum_{i=1}^{N}s_i^2\right] - \left[\sum_{i=1}^{N}r_is_i\right]^2.
\end{aligned} \tag{1.70}$$

The left hand side of Eq. (1.70) is a sum of squares and thus always non-negative, so

$$\begin{aligned}
\left[\sum_{i=1}^{N}r_i^2\right]\left[\sum_{i=1}^{N}s_i^2\right] - \left[\sum_{i=1}^{N}r_is_i\right]^2 &\geqslant 0, \\
\left[\sum_{i=1}^{N}r_i^2\right]\left[\sum_{i=1}^{N}s_i^2\right] &\geqslant \left[\sum_{i=1}^{N}r_is_i\right]^2.
\end{aligned} \tag{1.71}$$

1.4.2.2 Discrete Metric

The discrete metric can be defined on any non-empty set as

$$d_0(x,y) = \begin{cases} 0, & x = y \\ 1, & x \neq y \end{cases} \tag{1.72}$$

The metric (1.72) clearly satisfies axioms (1.61) and (1.62). For the triangle inequality, (1.63), consider

$$d_0(x,y) \leqslant d_0(x,z) + d_0(z,y) \tag{1.73}$$

The left hand side of this equation must equal 0 or 1, and the right hand side must be equal to $0, 1$ or 2. Thus, the only way in which the inequality is violated is in the case that $d_0(x,y) = 1$ and $d_0(x,z) + d_0(z,y) = 0$. For the right hand side to equal 0, $x = z$ and $z = y$. Hence, $x = y$ and $d_0(x,y) = 0$, meaning this situation cannot happen and axiom (1.63) holds.

1.5 Vector Spaces

In quantum mechanics, the state of the quantum system, given by the wavefunction, is represented by a vector in a complex vector space. Vector spaces (also known as linear spaces) are another type of mathematical space, motivated by generalising the properties of vectors in three-dimensional Euclidean space to more abstract sets. Certain vector spaces possess considerable additional structure, which we will detail in this section.

A vector space is a set V of objects called vectors over a field $\mathbb{F}$, which is composed of elements called scalars and could be either the real numbers, $\mathbb{R}$, or complex numbers, $\mathbb{C}$. A vector space is equipped with two laws: a law of combination which associates two vectors $\mathbf{u}, \mathbf{v} \in V$ with a third vector $\mathbf{u} + \mathbf{v} \in V$, and a scalar multiplication law which associates each vector $\mathbf{v} \in V$ and a scalar $\alpha \in \mathbb{F}$ with another vector, $\alpha\mathbf{v} \in V$ [51, 53, 54].

These laws are subject to several axioms. For the vector addition law:

- The addition law is associative for all $\mathbf{u}, \mathbf{v}, \mathbf{w} \in V$, i.e., $\mathbf{u} + (\mathbf{v} + \mathbf{w}) = (\mathbf{u} + \mathbf{v}) + \mathbf{w}$
- There exists a null vector $\mathbf{0}$ such that $\mathbf{v} + \mathbf{0} = \mathbf{v}$ for all $\mathbf{v} \in V$
- For all $\mathbf{v} \in V$ there exists an inverse element $-\mathbf{v}$ such that $\mathbf{v} + (-\mathbf{v}) = \mathbf{0}$

- The addition law is commutative, i.e. $\mathbf{u}+\mathbf{v}=\mathbf{v}+\mathbf{u}$

The scalar multiplication law must obey the following axioms for all $\mathbf{u},\mathbf{v}\in V$ and $\alpha,\beta\in\mathbb{F}$:

$$\alpha(\mathbf{u}+\mathbf{v})=\alpha\mathbf{u}+\alpha\mathbf{v}, \tag{1.74}$$
$$(\alpha+\beta)\mathbf{v}=\alpha\mathbf{v}+\beta\mathbf{v}, \tag{1.75}$$
$$\alpha(\beta\mathbf{v})=(\alpha\beta)\mathbf{v}, \tag{1.76}$$
$$1\mathbf{v}=\mathbf{v}, \tag{1.77}$$
$$0\mathbf{v}=\mathbf{0}. \tag{1.78}$$

We note here that, unlike for metric spaces as described in Sec. 1.4, the axioms for vector spaces above place restrictions on the elements of the set V. As a result, it is not possible to form a vector space from any desired set. Indeed, although the set of all wavefunctions forms a vector space, the set of all densities does not form a vector space, since there are no inverse elements present in the set.

1.5.1 Normed Vector Spaces

A norm on a vector space, V, is a function, $||.||:V\times V\to\mathbb{R}$, that assigns a length to each vector in the space. Although the concept of a norm had been hinted at by various authors in the early 20th century, the norm was first indisputably defined in 1922 by Hahn [55] and Banach [56].

The norm must satisfy the following axioms for all $\mathbf{u},\mathbf{v}\in V$ and $\alpha\in\mathbb{F}$ [51, 53, 54]:

$$||\mathbf{v}||\geqslant 0 \text{ and } ||\mathbf{v}||=0 \iff \mathbf{v}=0, \tag{1.79}$$
$$||\alpha\mathbf{v}||=|\alpha|\,||\mathbf{v}||, \tag{1.80}$$
$$||\mathbf{u}+\mathbf{v}||\leqslant||\mathbf{u}||+||\mathbf{v}||. \tag{1.81}$$

With a function satisfying these axioms, we have the normed vector space $(V,||.||)$.

In all normed vector spaces, a metric is induced by the norm, resulting in a metric space where the metric is defined by [51]

$$D(x,y)=||x-y||. \tag{1.82}$$

We now show that the axioms of a metric are satisfied for any metric induced

from equation (1.82). The axiom (1.61) is clearly satisfied for $D(x,y) = ||x-y||$ given the norm axiom (1.79). Axiom (1.62) is satisfied by considering

$$\begin{aligned} D(x,y) &= ||x-y||\,, \\ &= ||-(y-x)||\,, \\ &= |-1|\,||y-x||\,, \\ &= ||y-x||\,, \\ &= D(y,x). \end{aligned}$$

Making use of the axiom (1.81), the triangle inequality is satisfied since

$$\begin{aligned} D(x,y) &= ||x-y||\,, \\ &= ||(x-z)+(z-y)||\,, \\ &\leqslant ||x-z||+||z-y||\,, \\ &= D(x,z)+D(z,y). \end{aligned}$$

1.5.2 Completeness and Banach Spaces

A metric space (X,D) is *complete* if every Cauchy sequence in X converges to a point in X. A sequence, (x_n), in a metric space is a Cauchy sequence if, for $\varepsilon > 0$ there exists a natural number N such that $D(x_m,x_n) < \varepsilon$ whenever $m,n > N$. For a sequence in a metric space to converge to a point, $x \in X$, for any real number $\varepsilon > 0$, there must exist a natural number N such that x_n is contained in the ball $B(x,\varepsilon)$ whenever $n \geqslant N$. From these definitions it can be seen that any convergent sequence in a metric space is a Cauchy sequence.

If a norm induces a complete metric on its vector space, it is known as a *Banach norm* and the vector space is a *Banach space* [51].

1.5.3 Scalar Product Spaces

For vectors in three-dimensional Euclidean space, a useful concept is the dot product, $\mathbf{u}\cdot\mathbf{v}$, which is a product of two vectors that returns a scalar. This scalar represents the *projection* of the vector $\mathbf{u}$ onto $\mathbf{v}$, i.e., the component of $\mathbf{u}$ in the direction of $\mathbf{v}$. If the dot product of two Euclidean vectors is zero, they must be perpendicular to one another. Indeed, in Euclidean space, the dot product can be used to determine the angle between two vectors. The scalar product is the generalisation of the dot product to general vector spaces.

A scalar product space is a vector space that is also equipped with a scalar

product (or inner product). A scalar product on the vector space V is a map $\langle \cdot, \cdot \rangle : V \times V \to \mathbb{F}$ that satisfies the following axioms for all $\mathbf{u}, \mathbf{v}, \mathbf{w} \in V$ and $\alpha, \beta \in \mathbb{F}$ [53, 54]

$$\langle \mathbf{v} \, , \mathbf{v} \rangle \geqslant 0 \text{ and } \langle \mathbf{v} \, , \mathbf{v} \rangle = 0 \iff \mathbf{v} = 0, \tag{1.83}$$

$$\langle \mathbf{u} \, , \mathbf{v} \rangle = \langle \mathbf{v} \, , \mathbf{u} \rangle^* , \tag{1.84}$$

$$\langle \mathbf{u} \, , (\alpha \mathbf{v} + \beta \mathbf{w}) \rangle = \alpha \langle \mathbf{u} \, , \mathbf{v} \rangle + \beta \langle \mathbf{u} \, , \mathbf{v} \rangle . \tag{1.85}$$

where the * denotes the complex conjugate when considering a complex scalar field.

Returning to the motivating example of three-dimensional Euclidean space, we note that the length of a vector is found from the square root of the scalar product of the vector with itself, i.e., $|\mathbf{v}| = \sqrt{\mathbf{v} \cdot \mathbf{v}}$. This relationship holds for norms and scalar products in general vector spaces, allowing us to define a norm on a scalar product space from [53]

$$||\mathbf{v}|| = \langle \mathbf{v} \, , \mathbf{v} \rangle^{\frac{1}{2}} . \tag{1.86}$$

It can clearly be seen that the function $\langle \mathbf{v} \, , \mathbf{v} \rangle^{\frac{1}{2}}$ obeys the norm axiom (1.79) given the scalar product axiom (1.83). Axiom (1.80) of a norm is satisfied by considering axiom (1.84) and axiom (1.85) of a scalar product,

$$\begin{aligned} ||\alpha \mathbf{v}||^2 &= \langle \alpha \mathbf{v} \, , \alpha \mathbf{v} \rangle , \\ &= \alpha^* \langle \mathbf{v} \, , \mathbf{v} \rangle \alpha , \\ &= \alpha^* \alpha \langle \mathbf{v} \, , \mathbf{v} \rangle , \\ &= |\alpha|^2 \langle \mathbf{v} \, , \mathbf{v} \rangle , \\ &= |\alpha|^2 ||\mathbf{v}||^2 , \\ \implies ||\alpha \mathbf{v}|| &= |\alpha| \, ||\mathbf{v}|| . \end{aligned}$$

For the triangle inequality, we use the Schwarz inequality [53],

$$|\langle \mathbf{u} \, , \mathbf{v} \rangle| \leqslant \langle \mathbf{u} \, , \mathbf{u} \rangle^{\frac{1}{2}} \langle \mathbf{v} \, , \mathbf{v} \rangle^{\frac{1}{2}} , \tag{1.87}$$

and consider the sum of two vectors,

$$\begin{aligned}
\langle \mathbf{u}+\mathbf{v}\,,\mathbf{u}+\mathbf{v}\rangle &= \langle \mathbf{u}\,,\mathbf{u}\rangle + \langle \mathbf{v}\,,\mathbf{v}\rangle + \langle \mathbf{u}\,,\mathbf{v}\rangle + \langle \mathbf{v}\,,\mathbf{u}\rangle\,,\\
&= \langle \mathbf{u}\,,\mathbf{u}\rangle + \langle \mathbf{v}\,,\mathbf{v}\rangle + \langle \mathbf{u}\,,\mathbf{v}\rangle + \langle \mathbf{u}\,,\mathbf{v}\rangle^*\,,\\
&= \langle \mathbf{u}\,,\mathbf{u}\rangle + \langle \mathbf{v}\,,\mathbf{v}\rangle + 2\mathrm{Re}\langle \mathbf{u}\,,\mathbf{v}\rangle,\\
&\leqslant \langle \mathbf{u}\,,\mathbf{u}\rangle + \langle \mathbf{v}\,,\mathbf{v}\rangle + 2\,|\langle \mathbf{u}\,,\mathbf{v}\rangle|\,,\\
&\leqslant \langle \mathbf{u}\,,\mathbf{u}\rangle + \langle \mathbf{v}\,,\mathbf{v}\rangle + 2\,\langle \mathbf{u}\,,\mathbf{u}\rangle^{\frac{1}{2}}\,\langle \mathbf{v}\,,\mathbf{v}\rangle^{\frac{1}{2}}\,,\\
&= \left(\langle \mathbf{u}\,,\mathbf{u}\rangle^{\frac{1}{2}} + \langle \mathbf{v}\,,\mathbf{v}\rangle^{\frac{1}{2}}\right)^2,\\
\Longrightarrow \langle \mathbf{u}+\mathbf{v}\,,\mathbf{u}+\mathbf{v}\rangle^{\frac{1}{2}} &\leqslant \langle \mathbf{u}\,,\mathbf{u}\rangle^{\frac{1}{2}} + \langle \mathbf{v}\,,\mathbf{v}\rangle^{\frac{1}{2}}\,,\\
||\mathbf{u}+\mathbf{v}|| &\leqslant ||\mathbf{u}|| + ||\mathbf{v}||\,.
\end{aligned}$$

Therefore, we can state that all scalar product spaces are normed vector spaces, with the norm induced by the scalar product.

Two vectors $\mathbf{u},\mathbf{v}$ in a vector space are said to be *orthogonal* if their scalar product is zero, and *normalised* if the inner product of the vector with itself is equal to one. A set of vectors, $\{\mathbf{e}_1 \ldots \mathbf{e}_N\}$, for which the following holds,

$$\left\langle \mathbf{e}_i\,,\mathbf{e}_j\right\rangle = \delta_{ij}, \tag{1.88}$$

for all $i,j = 1\ldots N$ form an orthonormal basis of the vector space [53]. An orthonormal basis is extremely useful for a vector space, because, provided the basis spans the entire vector space, *any* vector can be written in terms of the basis vectors as

$$\mathbf{v} = \sum_{i=1}^{N} v_i \mathbf{e}_i. \tag{1.89}$$

1.6 Spaces of Quantum Mechanical Functions

1.6.1 Hilbert Spaces

The mathematical framework used to describe quantum mechanics states that all wavefunctions are represented by vectors in a Hilbert space. A Hilbert space is a scalar product space where the scalar product is complete. If we recall that scalar products induce norms, and norms induce metrics, we can use the same definition of completeness as for Banach spaces in Sec. 1.5.2.

The scalar product of wavefunctions is defined as

$$\langle \phi \,|\, \psi\rangle = \int \phi^*(\mathbf{r})\,\psi(\mathbf{r})\,d\mathbf{r}, \tag{1.90}$$

which satisfies the axioms (1.83)–(1.85). In the language of Hilbert spaces, an observable is represented by a Hermitian operator acting on the Hilbert space of all states [53]. An operator is a map from $\mathscr{H}$ onto itself; $\hat{O} : \mathscr{H} \to \mathscr{H}$. This operator is linear, which means that

$$\hat{O}(\alpha\psi + \beta\phi) = \alpha\hat{O}\psi + \beta\hat{O}\phi \tag{1.91}$$

for all complex numbers α, β and all $\psi, \phi \in \mathscr{H}$ [53].

1.6.2 L^p Spaces

One class of vector spaces that is of particular importance to this thesis are the L^p spaces. These spaces consist of functions, f, for which

$$\int |f(x)|^p \, dx < \infty, \tag{1.92}$$

applies. The L^p spaces are Banach spaces, with the usual norm given by

$$||f(x)||_p = \left[\int |f(x)|^p \, dx\right]^{\frac{1}{p}}. \tag{1.93}$$

This norm is known as the p-norm. Inspection of Eq. (1.19) shows that the space of all densities is an L^p space, with $p = 1$.

1.6.3 Metric Spaces for Quantum Mechanical Functions

Longpré and Kreinovich [57] developed a metric for the wavefunction in order to consider a question raised by Pauli – to what extent can we determine the wavefunction from the measurements? Longpré and Kreinovich noted that for every state ψ, and real number α, the probability of obtaining the measurement result ζ is the same for $e^{i\alpha}\psi$ as it is for ψ, i.e., the constant global phase factor $e^{i\alpha}$ is physically trivial. Thus, they stated that a quantum state is associated with an equivalence class of states in the Hilbert space, with the class characterised by wavefunctions of the same magnitude but different global phase factors, and hence that the actual space of possible quantum states is the projective Hilbert space constructed from the union of the equivalence classes. Given this, Longpré and Kreinovich noted that the standard Hilbert metric is not a sufficient way of determining the distance between two physical states as it discriminates between wavefunctions ψ and $e^{i\alpha}\psi$ that describe the same physical state. Longpré and Kreinovich thus chose to define a metric between a wavefunction ψ and *all* wavefunctions representing the physical state ψ' [57].

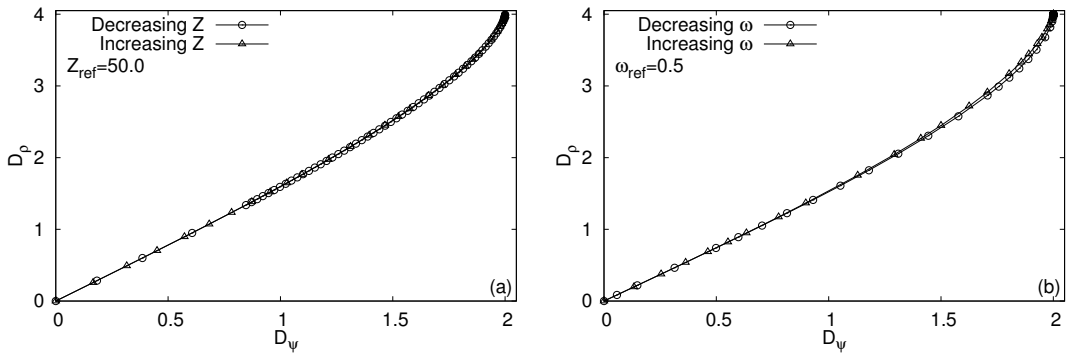

Figure 1.1: Plots of density distance against wavefunction distance for (a) Helium-like atoms, and (b) Hooke's Atom.

They then used this metric to give a definition for distinguishability of states.

The groundwork for the metric space approach to quantum mechanics was laid in the work of D'Amico *et al.* in 2011 [58]. Some of their results, previously published in Ref. [58], have been reproduced in Fig. 1.1. This work introduced the Longpré and Kreinovich metric for wavefunctions along with a metric for particle densities, and observed that both of these metric spaces could be characterised by an "onion-shell" geometry that consists of concentric spheres in the metric space. When focusing on ground states, it was shown that the Hohenberg-Kohn mapping between wavefunctions and particle densities is a mapping between the associated metric spaces. By studying model systems, additional properties of this mapping were discovered, namely that it is monotonic and almost linear, with nearby wavefunctions mapped onto nearby densities, and distant wavefunctions mapped onto distant densities. D'Amico *et al.* studied three model systems of two electrons, and found that the relationship between the metrics for wavefunctions and particle densities could be almost superimposed onto one another, which suggested a universality of this relationship for different systems. In their studies of the Hubbard model [59, 60] (not shown), it was observed that different values of the on-site interaction parameter made little difference to the relationship between the wavefunction and particle density metrics, but studies involving different numbers of particles resulted in different curves for this relationship. These findings were complemented by analysis of a different model system by Nagy and Aldazabal [61].

Chapter 2

Introducing the Metric Space Approach to Quantum Mechanics

The axioms of a metric (1.61)–(1.63) are sufficiently general to allow a number of valid metrics to be introduced for any set. Indeed, the discrete metric (1.72) is a metric for any non-empty set. The question that immediately arises therefore is: which choice of metric is best for the set under consideration?

The metric space approach to quantum mechanics provides an answer to this question for sets of quantum mechanical functions subject to conservation laws. The metric space approach involves deriving a metric that applies to the set of functions subject to the conservation law from the law itself. Thus, we ensure that the proposed metric stems from core characteristics of the systems analysed and contains the related physics, and is therefore a "natural" metric for the particular set of functions.

With the metric space approach to quantum mechanics, we have both a unified theoretical grounding for the metrics for wavefunctions and particle densities introduced in Refs. [57, 58], as well as a method to derive new metrics, which we apply to paramagnetic current densities and scalar potentials.

We published the general approach for deriving metrics presented in this chapter in Ref. [62], along with the paramagnetic current density metric. The discussions of gauge theory with regard to the metrics was published in Ref. [63], and the metric for scalar potentials is ongoing research [64].

2.1 Derivation of Metric Spaces from Conservation Laws

In quantum mechanics, many conservation laws take the form

$$\int |f(x)|^p \, dx = c, \tag{2.1}$$

for $0 < c < \infty$. For each value of $1 \leqslant p < \infty$, the entire set of functions that satisfy Eq. (2.1) belong to the L^p vector space, where the standard norm is the p-norm [51]

$$||f(x)||_p = \left[\int |f(x)|^p \, dx \right]^{\frac{1}{p}}. \tag{2.2}$$

From *any* norm a metric can be introduced in a standard way via Eq. (1.82) so that with p-norms we get

$$D_f(f_1, f_2) = \left[\int |f_1(x) - f_2(x)|^p \, dx \right]^{\frac{1}{p}}. \tag{2.3}$$

However before assuming this metric for the physical functions related to the conservation laws, an important consideration must be made: Eq. (2.3) has been derived assuming the ensemble $\{f\}$ to be a vector space; this is in fact necessary to introduce a norm. If we want to retain the metric (2.3), but restrict it to the ensemble of *physical* functions satisfying Eq. (2.1), which does not necessarily form a vector space, we must show that Eq. (2.3) is a metric for this restricted function set. This can be done using the general theory of metric spaces: given a metric space (X, D) and S, a non empty subset of X, (S, D) is itself a metric space with the metric D inherited from (X, D). The metric axioms (1.61)–(1.63) automatically hold for (S, D) because they hold for (X, D) [50, 51]. Hence, we have a metric for the functions of interest, as their sets are non-empty subsets of the respective L^p sets.

This procedure can be extended to conservation laws of the form

$$\sum_{i=1}^{n} |f_i|^p = c, \tag{2.4}$$

as the l^p vector spaces for sums are directly analogous to the L^p spaces for integrals [51]. In this case the induced metric will be

$$D_f(f_1, f_2) = \left[\sum_{i=1}^{n} |f_{1_i} - f_{2_i}|^p \right]^{\frac{1}{p}}. \tag{2.5}$$

Thus, we have a general procedure to construct a metric for any conservation law that is, or can be cast, in the form of Eq. (2.1) or Eq. (2.4).

Eqs. (2.3) and (2.5) are then the metrics that *directly descend* from the conservation laws (2.1) and (2.4) respectively. Conversely any conservation law which can be recast as Eq. (2.1) (for example conservation of quantum numbers) or Eq. (2.4) can be interpreted as inducing a metric on the appropriate, physically relevant, subset of L^p or l^p functions. This provides a general procedure to derive "natural" metrics from physical conservation laws. As they descend directly from conservation laws, these "natural" metrics are non-trivial and contain the relevant physics.

2.2 Geometry of the Metric Spaces

Now that we have derived "natural" metrics from conservation laws, we can examine the properties of these metrics. By considering spheres in the metric spaces, the geometry of the space can be determined. A sphere in a metric space (X, D) is the set of elements in the space that satisfy the condition

$$S(x_0, r) = \{x \in X : D(x, x_0) = r\}, \tag{2.6}$$

where x_0 is the centre and r is the radius of the sphere [51]. In order to construct our metric space geometry, we will consider the centre of a sphere to be the zero function, i.e., $f^{(0)}(x) \equiv 0$. It can be seen that when we consider the distance between the zero function and any other element in the metric space, we recover the p-norm, Eq. (2.2), defined from the conservation law, and therefore the distance of any function from the zero function is one of a set of values $c_i^{\frac{1}{p}}$. A sphere of radius $c_i^{\frac{1}{p}}$ consists of all the functions which are conserved to the same value c_i. From this it can be seen that the conservation law has induced a geometry consisting of a series of concentric spheres with radii $c_i^{\frac{1}{p}}$, and centred at the zero function, forming an "onion-shell" geometry [58, 62]. This is pictorially shown in Fig. 2.1.

With the onion geometry in mind, we can find the extreme values that the metric (2.3) can take. When considering points on different spheres in the onion geometry, the minimum value of the metric can be found from the reverse triangle inequality, Eq. (1.64),

$$D_f(f_A, f_B) \geqslant \left| D_f(f_A, f^{(0)}) - D_f(f_B, f^{(0)}) \right| = \left| c_A^{\frac{1}{p}} - c_B^{\frac{1}{p}} \right|. \tag{2.7}$$

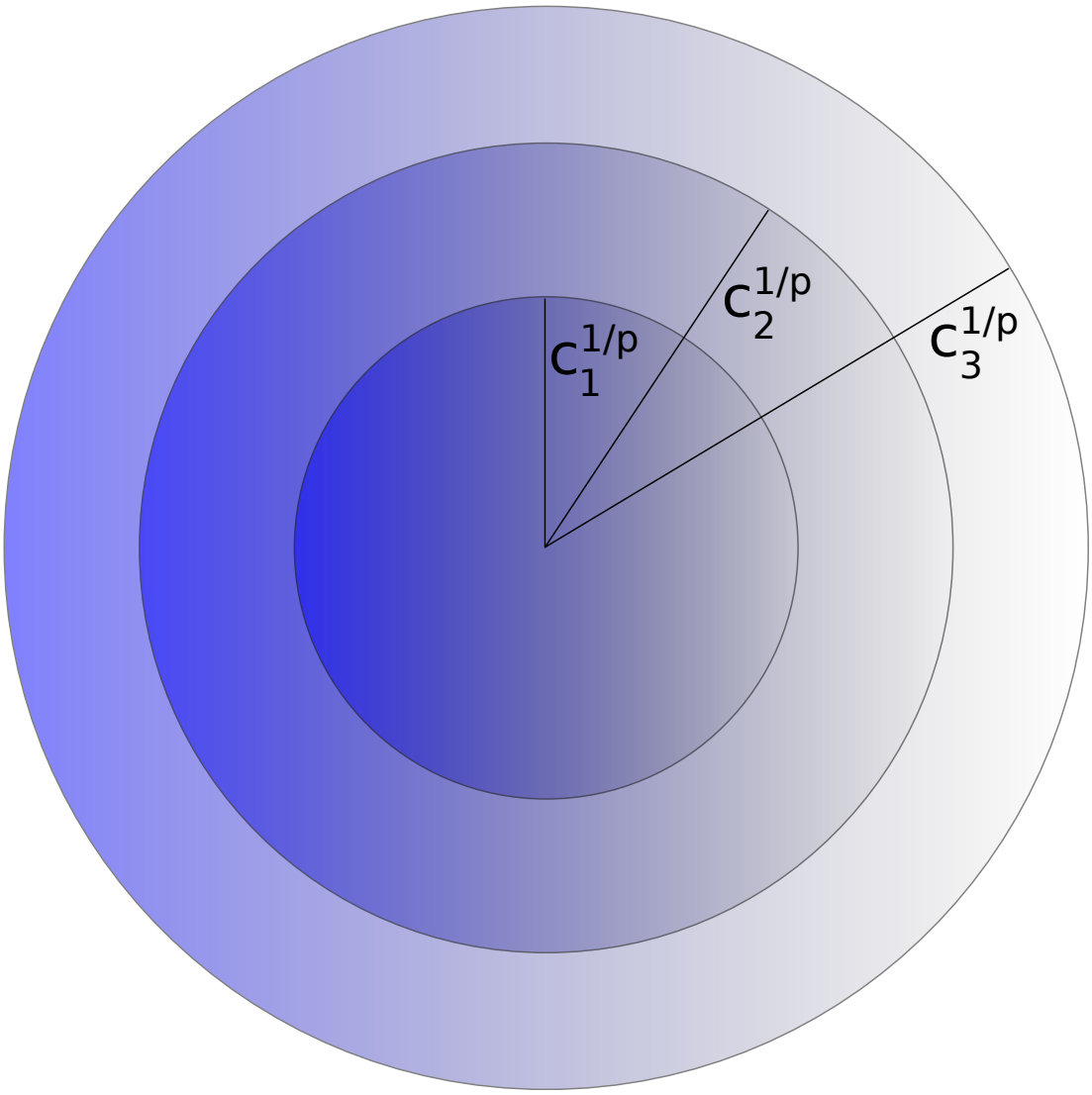

Figure 2.1: Sketch of the "onion-shell" geometry, consisting of a series of concentric spheres. The first three spheres are shown, with radii $c_i^{\frac{1}{p}}, i = 1,2,3$.

This value is the difference in the radii of the two spheres representing f_A and f_B in the geometry. When considering the same sphere, we obtain an absolute minimum value of zero, as required by axiom (1.61). The maximum value of the metric for functions f_A and f_B is found from the triangle inequality, Eq. (1.63),

$$D_f(f_A, f_B) \leqslant D_f(f_A, f^{(0)}) + D_f(f^{(0)}, f_B) = c_A^{\frac{1}{p}} + c_B^{\frac{1}{p}}. \tag{2.8}$$

On a single sphere in the geometry this reduces to $2c^{\frac{1}{p}}$, which is the diameter of the sphere. There is no absolute maximum for the metric in general because there is not necessarily an upper limit to the value of c, and therefore to the number of spheres in the onion geometry.

From the metric (2.3) and conditions in Eqs. (2.7) and (2.8), it can be seen that maximally distant functions are those which do not overlap at all and when

the functions overlap exactly everywhere, i.e., they are the same function, they are minimally distant [as required by axiom (1.61)]. Given this, we can interpret physically that the distance is inversely related to a measure of the spatial overlap of the two functions.

2.3 Applying the Metric Space Approach to Quantum Mechanical Functions

We now show how to apply the metric space approach to quantum mechanics in order to obtain metrics for the fundamental quantities in DFT and CDFT. In order to do so, we will use the conservation laws derived in Sec. 1.1.2 to obtain metrics for paramagnetic current densities and scalar potentials, and show how the metrics presented in recent literature for wavefunctions and particle densities [57, 58] arise from their respective conservation laws.

2.3.1 Particle Densities

The particle density metric is derived from the conservation of the number of particles, Eq. (1.19), which can be written as

$$\int |\rho(\mathbf{r})|\, d\mathbf{r} = N. \tag{2.9}$$

Thus, as stated in Sec. 1.6.2, it can be seen that the particle density is an L^1 function. Hence, the metric is given by [58]

$$D_\rho(\rho_1, \rho_2) = \int |\rho_1(\mathbf{r}) - \rho_2(\mathbf{r})|\, d\mathbf{r}. \tag{2.10}$$

From Eq. (2.9), it can be seen that the geometry of the particle density metric space consists of concentric spheres of radius N, such that the densities of one-particle systems lie on a sphere of radius 1, two-particle densities lie on a sphere of radius 2 and so on, as shown in Fig. 2.2.

2.3.2 Wavefunctions

In order to derive a metric for wavefunctions, we begin with the conservation of the norm of the wavefunction.

$$\int \left| \frac{\psi(\mathbf{r}, \mathbf{r}_2, \ldots, \mathbf{r}_N)}{\sqrt{N}} \right|^2 d\mathbf{r}_1 \ldots d\mathbf{r}_N = 1, \tag{2.11}$$

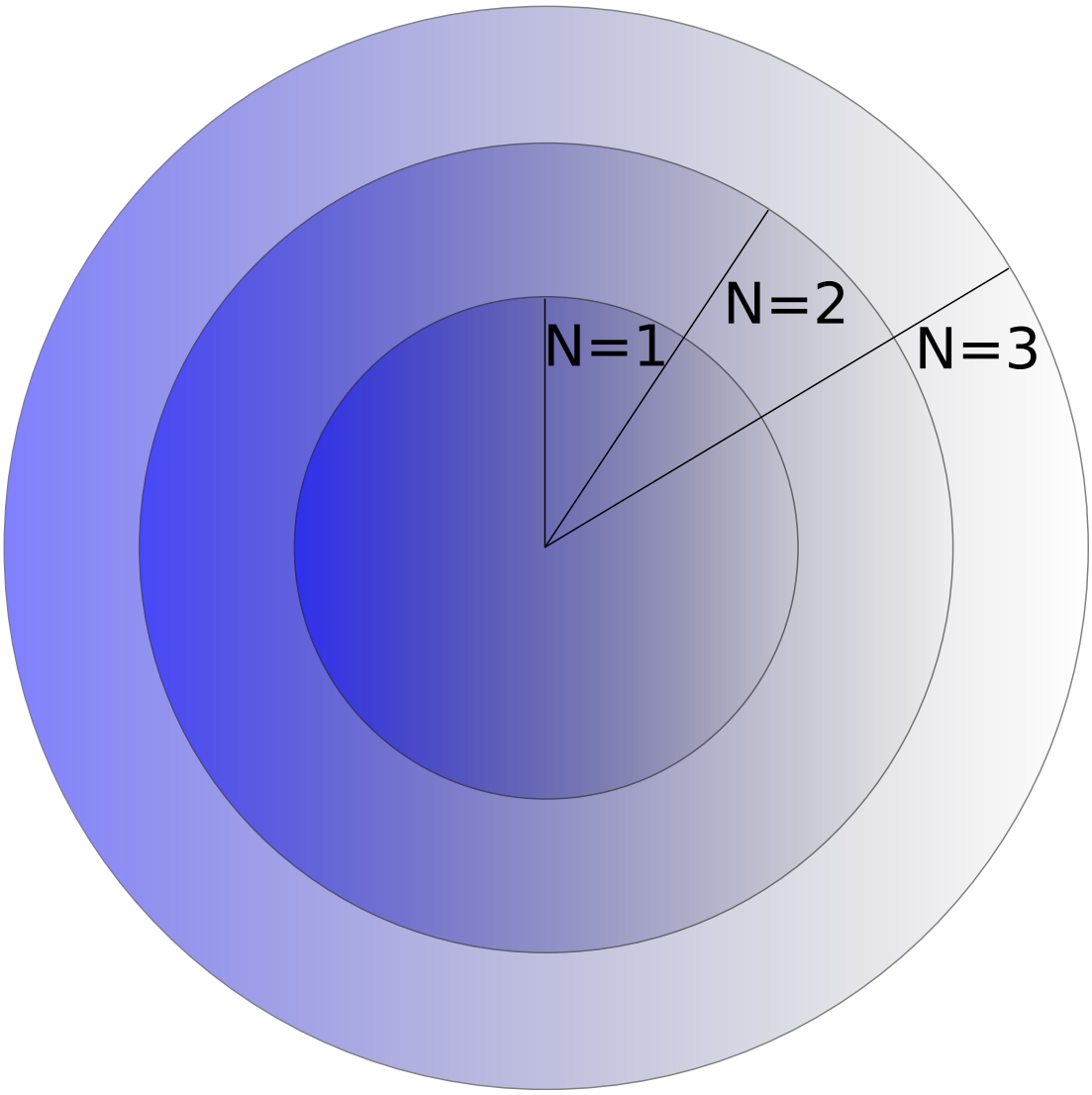

Figure 2.2: The first three spheres of the "onion-shell" geometry for particle densities, with radii $N = 1, 2, 3$.

where we follow the convention of Refs. [58, 62] and normalise wavefunctions to the particle number, N. This ensures that, rather than a single sphere representing all wavefunctions, wavefunctions describing systems of different particle numbers lie on different spheres in the "onion-shell" geometry and thus the wavefunction metric space has a geometry similar to that for particle densities [58].

Equation (2.11) is of the form of Eq. (2.1), so following the procedure in Sec. 2.1 we note that the wavefunction is an L^2 function, and derive the metric

$$\widetilde{D}_{\psi}(\psi_1, \psi_2) = \left[\int |\psi_1 - \psi_2|^2 \, d\mathbf{r}_1 \ldots d\mathbf{r}_N \right]^{\frac{1}{2}}, \tag{2.12}$$

which is the standard Hilbert space metric [57]. However, as first noted by Longpré and Kreinovich [57], the metric (2.12) induced by the norm is not a

sufficient measure of the distance between wavefunctions. This is because the distance between the states ψ and $\psi' = e^{i\phi}\psi$, which differ only by a constant global phase factor, is non-zero. However, wavefunctions differing by such a phase factor describe the same physics, as the solutions of the Schrödinger equation are only defined up to a constant global phase factor. To have physically meaningful metrics, it is therefore important to define equivalence classes such that the metric assigns zero distance to wavefunctions differing only by a constant global phase factor.

An equivalence class for an element $x \in X$ is defined as [65]

$$[x] = \left\{x' \in X : x \sim x'\right\}, \tag{2.13}$$

where $\sim$ is the equivalence relation characterising the class. Each element of the set X belongs to a single equivalence class [65].

In order to account for an equivalence relation between elements, $x \sim x'$, we follow a general procedure for introducing an equivalence relation into a metric space (X, D). We define the following function [66]

$$D_{\sim}(x,y) = \inf\left\{\sum_{i=1}^{k} D(p_i, q_i) : p_1 = x, q_k = y, k \in \mathbb{N}\right\}, \tag{2.14}$$

where the infimum is taken over all choices of $\{p_i\}, \{q_i\}$ such that $p_{i+1} \sim q_i$. This implies that if $x \sim y$, $D_{\sim}(x,y) = D(x,x) + D(y,y) = 0$ even if $D(x,y) \neq 0$ [66]. This function is a *semi-metric* (or pseudometric) on the set X, known as the quotient semi-metric associated to the relation $\sim$. A semi-metric is a distance function that obeys all of the axioms of a metric except axiom (1.61): $D(x,y) = 0 \iff x = y$, replacing it with: $D(x,y) = 0$ for $x = y$, i.e., we allow zero distance between non-identical elements as well as identical ones.

For Eq. (2.12) we have in general that $\widetilde{D}_{\psi}\left(\psi, e^{i\phi}\psi\right) \neq 0$. If we introduce an equivalence relation between wavefunctions differing by only a global phase factor, and take $k = 2$ in Eq. (2.14), we find

$$D_{\psi}(\psi_1, \psi_2) = \inf\left\{\widetilde{D}_{\psi}\left(\psi_1, \psi'\right) + \widetilde{D}_{\psi}\left(\psi_2, \psi_2\right)\right\}, \tag{2.15}$$

$$= \inf\left\{\widetilde{D}_{\psi}\left(\psi_1, \psi'\right)\right\}, \tag{2.16}$$

where $\psi' = e^{i\phi}\psi_2 \sim \psi_2$ and we have used the positivity axiom of the metric. The choice of ψ' that will minimise the value of the semi-metric is determined

by the phase factor, hence [57]

$$D_\psi(\psi_1,\psi_2) = \min_\phi \left\{ \widetilde{D}_\psi\left(\psi_1, e^{i\phi}\psi_2\right)\right\}. \tag{2.17}$$

With this semi-metric space $\left(\{\psi\}, D_\psi\right)$, we can recover a metric space in a natural way, by "gluing" equivalent elements to form a set of equivalence classes. By considering the set of equivalence classes of wavefunctions, rather than the set of all wavefunctions, wavefunctions differing only by a constant global phase factor are identified with one another. Thus, the set of equivalent wavefunctions with D_ψ is a metric space, with the metric defined between each of the equivalence classes, as required [65].

Longpré and Kreinovich showed that we do not need to perform this minimisation explicitly, and instead we can simplify the metric (2.17) by writing [57]

$$\begin{aligned}
D_\psi &= \min_\phi \left[\int \left|\psi_1 - e^{i\phi}\psi_2\right|^2 d\mathbf{r}_1 \ldots d\mathbf{r}_N\right]^{\frac{1}{2}}, \\
&= \min_\phi \left[\int \left(\psi_1 - e^{i\phi}\psi_2\right)^* \left(\psi_1 - e^{i\phi}\psi_2\right) d\mathbf{r}_1 \ldots d\mathbf{r}_N\right]^{\frac{1}{2}}, \\
&= \min_\phi \left[\int \left(\psi_1^* - e^{-i\phi}\psi_2^*\right) \left(\psi_1 - e^{i\phi}\psi_2\right) d\mathbf{r}_1 \ldots d\mathbf{r}_N\right]^{\frac{1}{2}}, \\
&= \min_\phi \left[\int \left(\psi_1^*\psi_1 + \psi_2^*\psi_2 - e^{i\phi}\psi_1^*\psi_2 - e^{-i\phi}\psi_2^*\psi_1\right) d\mathbf{r}_1 \ldots d\mathbf{r}_N\right]^{\frac{1}{2}}, \\
&= \min_\phi \left[\int |\psi_1|^2 + |\psi_2|^2 d\mathbf{r}_1 \ldots d\mathbf{r}_N - \int e^{i\phi}\psi_1^*\psi_2 d\mathbf{r}_1 \ldots d\mathbf{r}_N - \int e^{-i\phi}\psi_2^*\psi_1 d\mathbf{r}_1 \ldots d\mathbf{r}_N\right]^{\frac{1}{2}}, \\
&= \min_\phi \left[\int |\psi_1|^2 + |\psi_2|^2 d\mathbf{r}_1 \ldots d\mathbf{r}_N - \int e^{i\phi}\psi_1^*\psi_2 d\mathbf{r}_1 \ldots d\mathbf{r}_N - \left(\int e^{i\phi}\psi_2\psi_1^* d\mathbf{r}_1 \ldots d\mathbf{r}_N\right)^*\right]^{\frac{1}{2}}, \\
&= \min_\phi \left[\int |\psi_1|^2 + |\psi_2|^2 d\mathbf{r}_1 \ldots d\mathbf{r}_N - 2\mathrm{Re}\left(\int e^{i\phi}\psi_1^*\psi_2 d\mathbf{r}_1 \ldots d\mathbf{r}_N\right)\right]^{\frac{1}{2}}.
\end{aligned}$$

It can now be seen that the distance is at a minimum when the real part of $\int e^{i\phi}\psi_1^*\psi_2 d\mathbf{r}_1 \ldots d\mathbf{r}_N$ is at a maximum.

For any complex number, z,

$$|z|^2 = \mathrm{Re}(z)^2 + Im(z)^2.$$

Since $Im(z)^2$ is always positive,

$$|z|^2 \geqslant Re(z)^2 \Longrightarrow |z| \geqslant |\mathrm{Re}(z)| \geqslant \mathrm{Re}(z),$$

so it can be seen that the real part of any complex number is at a maximum when it is equal to the magnitude of the complex number.

This allows us to write the wavefunction metric as [57, 58, 62]

$$D_\psi(\psi_1,\psi_2) = \left[\int |\psi_1|^2 + |\psi_2|^2 d\mathbf{r}_1 \ldots d\mathbf{r}_N - 2\left|\int \psi_1^* \psi_2 d\mathbf{r}_1 \ldots d\mathbf{r}_N\right|\right]^{\frac{1}{2}}, \qquad (2.18)$$

which is the form we use.

2.3.2.1 Orthogonal Wavefunctions

The term $\int \psi_1^* \psi_2 d\mathbf{r}_1 \ldots d\mathbf{r}_N$ in the wavefunction metric (2.18) shows a connection between the wavefunction metric and the Born Rule of quantum mechanics [6], which, as discussed in Chapter 1, interprets the wavefunction as a statistical quantity, such that $|\psi(\mathbf{r})|^2 d\mathbf{r}$ represents the probability of finding a particle within the volume element $d\mathbf{r}$ [1].

To consider the Born Rule for two different wavefunctions, ϕ and ψ, we expand ϕ in the complete set of eigenfunctions of a Hermitian operator $\hat{O}$, $\phi = \sum_n c_n \phi_n$. The Born Rule states that the inner product of the one of the eigenfunctions ϕ_n with ψ represents the probability of measuring the state ψ with the operator $\hat{O}$ and obtaining the eigenvalue corresponding to the eigenstate ϕ_n. In the case that $\langle \phi_n | \psi \rangle = 0$, the wavefunctions are orthogonal, and represent mutually exclusive physical states [1, 67].

The principal consequence of this with regards to the wavefunction metric is that whenever two wavefunctions ψ_1 and ψ_2 are orthogonal, they will always be assigned the maximum distance by the wavefunction metric, which is $\sqrt{N_1 + N_2}$, where N_i is the number of particles in the system described by the state ψ_i. This point was first raised by Artacho [68, 69] with regards to wavefunctions corresponding to systems of different numbers of particles, but also applies in any other situation where wavefunctions are orthogonal, for example, when considering a ground state and an excited state of the same system.

For the case of systems of different particle numbers, the wavefunction metric (2.18) will always assign their wavefunctions as maximally distant. For this reason, we restrict our use of the the metric (2.18) to systems with the same number of particles, N.

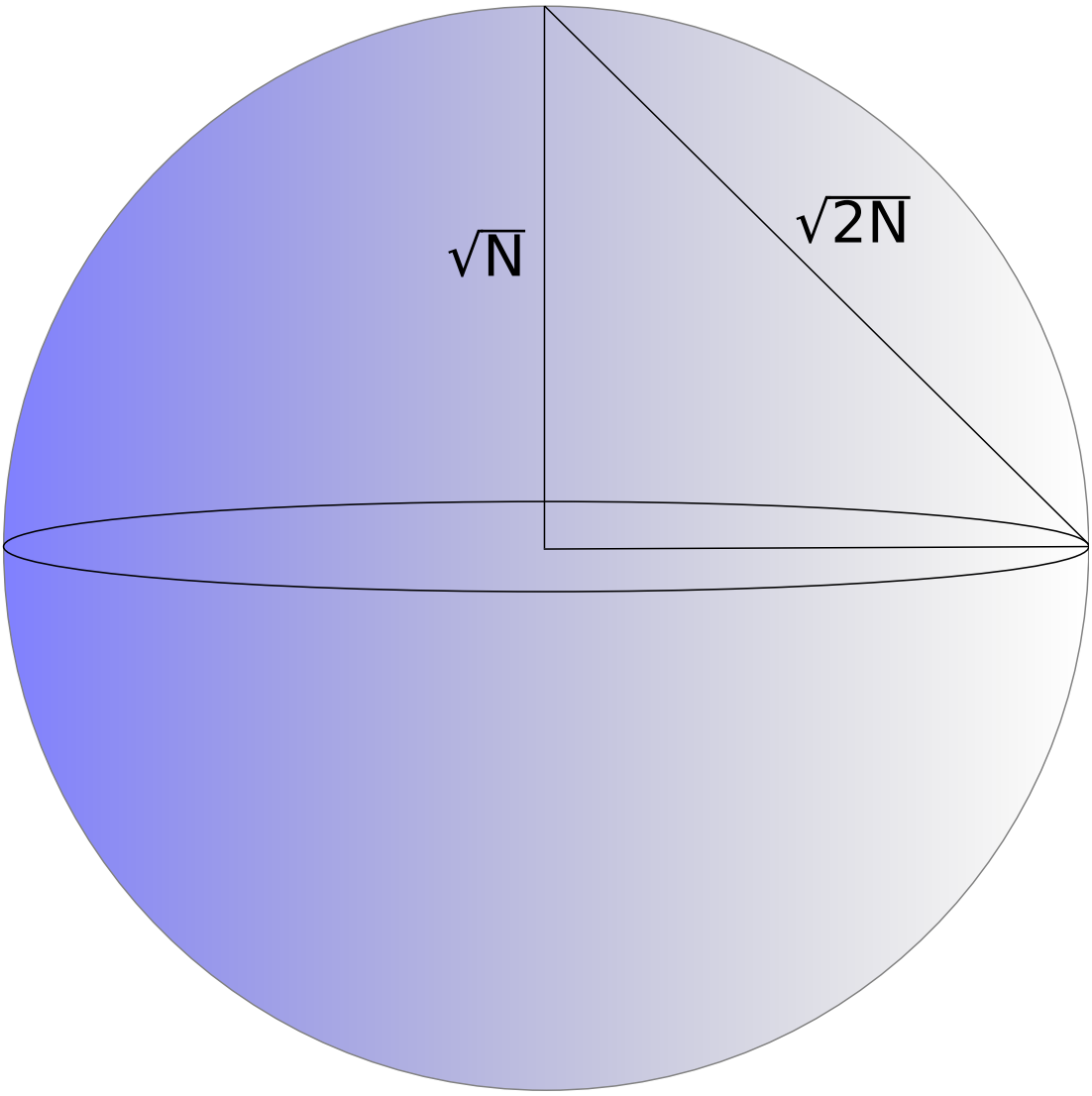

Figure 2.3: A sphere of the "onion-shell" geometry for wavefunctions, with radius $\sqrt{N}$ and maximum value $\sqrt{2N}$.

2.3.2.2 Geometry of the Metric Space

Writing the metric in the form of Eq. (2.18) has interesting consequences for the "onion-shell" geometry of the wavefunction metric space [58]. From Eq. (2.8), it can be seen that the maximum distance between two N-particle wavefunctions is $2\sqrt{N}$, which corresponds to the maximum value obtained when writing the wavefunction metric in the form of Eq. (2.12). However, it can be seen that the maximum value of the metric (2.18) is obtained for orthogonal wavefunctions, and is $\sqrt{2N} < 2\sqrt{N}$.

As far as the "onion-shell" geometry is concerned, we can find the angle be-

tween two wavefunctions with a distance of $\sqrt{2N}$ from the cosine rule,

$$\cos\theta = \frac{\left(\sqrt{N}\right)^2 + \left(\sqrt{N}\right)^2 - 2\left(\sqrt{N}\right)^2}{2\left(\sqrt{N}\right)^2} = 0 \quad \Rightarrow \quad \theta = \frac{\pi}{2}, \tag{2.19}$$

i.e., one wavefunction is located halfway around the sphere from the other. In other words, if we consider an arbitrary wavefunction to lie on the north pole of the sphere, a wavefunction that is maximally distant, according to Eq. (2.18), lies on the equator. This is shown in Fig 2.3.

2.3.3 Paramagnetic Current Densities

In Ref. [62] we derived a metric for the paramagnetic current density, $\mathbf{j}_p(\mathbf{r})$. In order to apply the metric space approach to generate a metric for the paramagnetic current density, we must first relate it to a conservation law of the form of Eq. (2.1). We will show that the paramagnetic current density obeys

$$\int \left[\mathbf{r} \times \mathbf{j}_p(\mathbf{r})\right]_z d\mathbf{r} = \langle \psi | \hat{L}_z | \psi \rangle, \tag{2.20}$$

where $\hat{L}_z$ is defined as in Eq. (1.20), and $\mathbf{j}_p(\mathbf{r}) = \left\langle \hat{\mathbf{j}}_p \right\rangle$. The form of the paramagnetic current density operator is [7]

$$\hat{\mathbf{j}}_p = \frac{1}{2}\sum_{i=1}^{N}\left[\delta(\mathbf{r}-\mathbf{r}_i)\,\hat{\mathbf{p}}_{r_i} + \hat{\mathbf{p}}_{r_i}\delta(\mathbf{r}-\mathbf{r}_i)\right]. \tag{2.21}$$

The expectation value of $\mathbf{r}\times\hat{\mathbf{j}}_p$ is,

$$\begin{aligned}
\left\langle \mathbf{r}\times\hat{\mathbf{j}}_p \right\rangle =& \left\langle \psi(\mathbf{r}_1,\mathbf{r}_2,\ldots,\mathbf{r}_N) \left| \mathbf{r}\times\hat{\mathbf{j}}_p \right| \psi(\mathbf{r}_1,\mathbf{r}_2,\ldots,\mathbf{r}_N) \right\rangle, \\
=& \frac{1}{2}\sum_{i=1}^{N}\left\{ \int\int\ldots\int \psi^*(\mathbf{r}_1,\mathbf{r}_2,\ldots,\mathbf{r}_N)\left[\mathbf{r}\times\delta(\mathbf{r}-\mathbf{r}_i)\,\hat{\mathbf{p}}_{r_i}\right]\psi(\mathbf{r}_1,\mathbf{r}_2,\ldots,\mathbf{r}_N)\,d\mathbf{r}_1 d\mathbf{r}_2\ldots d\mathbf{r}_N \right. \\
& \left. + \int\int\ldots\int \psi^*(\mathbf{r}_1,\mathbf{r}_2,\ldots,\mathbf{r}_N)\left[\mathbf{r}\times\hat{\mathbf{p}}_{r_i}\delta(\mathbf{r}-\mathbf{r}_i)\right]\psi(\mathbf{r}_1,\mathbf{r}_2,\ldots,\mathbf{r}_N)\,d\mathbf{r}_1 d\mathbf{r}_2\ldots d\mathbf{r}_N \right\}, \\
=& \frac{1}{2}\sum_{i=1}^{N}\left\{ \int\int\ldots\int \psi^*(\mathbf{r}_1,\mathbf{r}_2,\ldots,\mathbf{r}_N)\,\delta(\mathbf{r}-\mathbf{r}_i)\left[\mathbf{r}\times\hat{\mathbf{p}}_{r_i}\right]\psi(\mathbf{r}_1,\mathbf{r}_2,\ldots,\mathbf{r}_N)\,d\mathbf{r}_1 d\mathbf{r}_2\ldots d\mathbf{r}_N \right. \\
& \left. + \int\int\ldots\int \psi^*(\mathbf{r}_1,\mathbf{r}_2,\ldots,\mathbf{r}_N)\left[\mathbf{r}\times\hat{\mathbf{p}}_{r_i}\right]\delta(\mathbf{r}-\mathbf{r}_i)\,\psi(\mathbf{r}_1,\mathbf{r}_2,\ldots,\mathbf{r}_N)\,d\mathbf{r}_1 d\mathbf{r}_2\ldots d\mathbf{r}_N \right\}.
\end{aligned}$$

We rewrite the second integral by noting that the operators $\mathbf{r}\times\hat{\mathbf{p}}_{\mathbf{r}_i}$ and $\delta(\mathbf{r}-\mathbf{r}_i)$ are both Hermitian. Therefore, we can apply the relation [8],

$$\langle\phi|\hat{A}\hat{B}|\psi\rangle = \langle\phi|\hat{B}\hat{A}|\psi\rangle^*. \tag{2.22}$$

This gives,

$$\begin{aligned}\left\langle \mathbf{r}\times\hat{\mathbf{j}}_p\right\rangle =& \frac{1}{2}\sum_{i=1}^{N}\left\{\int\int\ldots\int\psi^*(\mathbf{r}_1,\mathbf{r}_2,\ldots,\mathbf{r}_N)\,\delta(\mathbf{r}-\mathbf{r}_i)\,[\mathbf{r}\times\hat{\mathbf{p}}_{r_i}]\,\psi(\mathbf{r}_1,\mathbf{r}_2,\ldots,\mathbf{r}_N)\,d\mathbf{r}_1 d\mathbf{r}_2\ldots d\mathbf{r}_N\right.\\ &\left.+\int\int\ldots\int\psi(\mathbf{r}_1,\mathbf{r}_2,\ldots,\mathbf{r}_N)\,\delta(\mathbf{r}-\mathbf{r}_i)\,[\mathbf{r}\times\hat{\mathbf{p}}_{r_i}]^*\,\psi^*(\mathbf{r}_1,\mathbf{r}_2,\ldots,\mathbf{r}_N)\,d\mathbf{r}_1 d\mathbf{r}_2\ldots d\mathbf{r}_N\right\}.\end{aligned}$$

We now have a series of $2N$ N-dimensional integrals. The delta function removes one integral from each term in this series, resulting in $2N$ $N-1$-dimensional integrals. By renaming each set of dummy variables as $\mathbf{r}_2\ldots\mathbf{r}_N$, we have,

$$\begin{aligned}\left\langle \mathbf{r}\times\hat{\mathbf{j}}_p\right\rangle =& \frac{1}{2}\sum_{i=1}^{N}\left\{\int\ldots\int\psi^*(\mathbf{r},\mathbf{r}_2,\ldots,\mathbf{r}_N)\,[\mathbf{r}\times\hat{\mathbf{p}}_r]\,\psi(\mathbf{r},\mathbf{r}_2,\ldots,\mathbf{r}_N)\,d\mathbf{r}_2\ldots d\mathbf{r}_N\right.\\ &\left.+\int\ldots\int\psi(\mathbf{r},\mathbf{r}_2,\ldots,\mathbf{r}_N)\,[\mathbf{r}\times\hat{\mathbf{p}}_r]^*\,\psi^*(\mathbf{r},\mathbf{r}_2,\ldots,\mathbf{r}_N)\,d\mathbf{r}_2\ldots d\mathbf{r}_N\right\}.\end{aligned}$$

Integrating over $\mathbf{r}$ gives

$$\begin{aligned}\int\left\langle \mathbf{r}\times\hat{\mathbf{j}}_p\right\rangle d\mathbf{r} =& \frac{1}{2}\sum_{i=1}^{N}\int\left\{\int\ldots\int\psi^*(\mathbf{r},\mathbf{r}_2,\ldots,\mathbf{r}_N)\,[\mathbf{r}\times\hat{\mathbf{p}}_r]\,\psi(\mathbf{r},\mathbf{r}_2,\ldots,\mathbf{r}_N)\,d\mathbf{r}_2\ldots d\mathbf{r}_N\right.\\ &\left.+\int\ldots\int\psi(\mathbf{r},\mathbf{r}_2,\ldots,\mathbf{r}_N)\,[\mathbf{r}\times\hat{\mathbf{p}}_r]^*\,\psi^*(\mathbf{r},\mathbf{r}_2,\ldots,\mathbf{r}_N)\,d\mathbf{r}_2\ldots d\mathbf{r}_N\right\}d\mathbf{r}.\end{aligned} \tag{2.23}$$

Since the vector $\mathbf{r}$ is independent of the coordinates $(\mathbf{r}_2\ldots\mathbf{r}_N)$, and the cross product is a linear operation, we can remove the vector $\mathbf{r}$ from the integrals over the coordinates $(\mathbf{r}_2\ldots\mathbf{r}_N)$,

$$\begin{aligned}\int\left\langle \mathbf{r}\times\hat{\mathbf{j}}_p\right\rangle d\mathbf{r} =& \frac{1}{2}\sum_{i=1}^{N}\int\mathbf{r}\times\left\{\int\ldots\int\psi^*(\mathbf{r},\mathbf{r}_2,\ldots,\mathbf{r}_N)\,\hat{\mathbf{p}}_r\psi(\mathbf{r},\mathbf{r}_2,\ldots,\mathbf{r}_N)\,d\mathbf{r}_2\ldots d\mathbf{r}_N\right.\\ &\left.+\int\ldots\int\psi(\mathbf{r},\mathbf{r}_2,\ldots,\mathbf{r}_N)\,\hat{\mathbf{p}}_r^*\psi^*(\mathbf{r},\mathbf{r}_2,\ldots,\mathbf{r}_N)\,d\mathbf{r}_2\ldots d\mathbf{r}_N\right\}d\mathbf{r},\\ =&\int\mathbf{r}\times-\frac{i}{2}\sum_{i=1}^{N}\left\{\int\ldots\int\psi^*(\mathbf{r},\mathbf{r}_2,\ldots,\mathbf{r}_N)\,\nabla_r\psi(\mathbf{r},\mathbf{r}_2,\ldots,\mathbf{r}_N)\,d\mathbf{r}_2\ldots d\mathbf{r}_N\right.\\ &\left.-\int\ldots\int\psi(\mathbf{r},\mathbf{r}_2,\ldots,\mathbf{r}_N)\,\nabla_r\psi^*(\mathbf{r},\mathbf{r}_2,\ldots,\mathbf{r}_N)\,d\mathbf{r}_2\ldots d\mathbf{r}_N\right\}d\mathbf{r},\\ =&\int\mathbf{r}\times\mathbf{j}_p(\mathbf{r})\,d\mathbf{r}.\end{aligned}$$

Returning to Eq. (2.23), and noting that $\mathbf{r}\times\hat{\mathbf{p}}_r$ is Hermitian,

$$\begin{aligned}\int\left\langle \mathbf{r}\times\hat{\mathbf{j}}_p\right\rangle d\mathbf{r} =& \frac{1}{2}\sum_{i=1}^{N}\int\left\{\int\ldots\int\psi^*\left(\mathbf{r},\mathbf{r}_2,\ldots,\mathbf{r}_N\right)\left[\mathbf{r}\times\hat{\mathbf{p}}_r\right]\psi\left(\mathbf{r},\mathbf{r}_2,\ldots,\mathbf{r}_N\right)d\mathbf{r}_2\ldots d\mathbf{r}_N\right.\\ &\left.+\int\ldots\int\psi^*\left(\mathbf{r},\mathbf{r}_2,\ldots,\mathbf{r}_N\right)\left[\mathbf{r}\times\hat{\mathbf{p}}_r\right]\psi\left(\mathbf{r},\mathbf{r}_2,\ldots,\mathbf{r}_N\right)d\mathbf{r}_2\ldots d\mathbf{r}_N\right\}d\mathbf{r},\\ =&\int\sum_{i=1}^{N}\int\ldots\int\psi^*\left(\mathbf{r},\mathbf{r}_2,\ldots,\mathbf{r}_N\right)\left[\mathbf{r}\times\hat{\mathbf{p}}_r\right]\psi\left(\mathbf{r},\mathbf{r}_2,\ldots,\mathbf{r}_N\right)d\mathbf{r}_2\ldots d\mathbf{r}_N d\mathbf{r},\\ =&\int\int\ldots\int\sum_{i=1}^{N}\psi^*\left(\mathbf{r},\mathbf{r}_2,\ldots,\mathbf{r}_N\right)\left[\mathbf{r}\times\hat{\mathbf{p}}_r\right]\psi\left(\mathbf{r},\mathbf{r}_2,\ldots,\mathbf{r}_N\right)d\mathbf{r}d\mathbf{r}_2\ldots d\mathbf{r}_N,\\ =&\left\langle\hat{\mathbf{L}}\right\rangle.\end{aligned}$$

We have thus proved that

$$\int\left\langle\mathbf{r}\times\hat{\mathbf{j}}_p\right\rangle d\mathbf{r}=\left\langle\hat{\mathbf{L}}\right\rangle=\int\left[\mathbf{r}\times\mathbf{j}_p\left(\mathbf{r}\right)\right]d\mathbf{r}. \tag{2.24}$$

Since Eq. (2.24) applies to the vectors $\left[\mathbf{r}\times\mathbf{j}_p\left(\mathbf{r}\right)\right]$ and $\hat{\mathbf{L}}$, it must also apply to each component of these vectors, hence

$$\int\left[\mathbf{r}\times\mathbf{j}_p\left(\mathbf{r}\right)\right]_z d\mathbf{r}=\left\langle\hat{L}_z\right\rangle=m, \tag{2.25}$$

provided that $\hat{L}_z$ is a constant of motion. In order to turn Eq. (2.25) into a conservation law of the form of Eq. (2.1), we note that m can be any positive or negative integer, hence we take the absolute value to ensure that the final constant is positive,

$$\left|\int\left[\mathbf{r}\times\mathbf{j}_p\left(\mathbf{r}\right)\right]_z d\mathbf{r}\right|=\left|\left\langle\hat{L}_z\right\rangle\right|=\left|m\right|. \tag{2.26}$$

Provided that $\left[\mathbf{r}\times\mathbf{j}_p\left(\mathbf{r}\right)\right]_z$ has the same sign everywhere, which applies when the system under consideration is rotationally invariant about the z axis (i.e., $\mathbf{j}_p\left(\mathbf{r}\right)$ has no θ dependence), we can write,

$$\int\left|\left[\mathbf{r}\times\mathbf{j}_p\left(\mathbf{r}\right)\right]_z\right|d\mathbf{r}=\left|m\right|, \tag{2.27}$$

giving us the form of conservation law required. From this, we can now follow our procedure and derive the metric,

$$D_{\mathbf{j}_{p_\perp}}\left(\mathbf{j}_{p_1},\mathbf{j}_{p_2}\right)=\int\left|\left\{\mathbf{r}\times\left[\mathbf{j}_{p_1}\left(\mathbf{r}\right)-\mathbf{j}_{p_2}\left(\mathbf{r}\right)\right]\right\}_z\right|d\mathbf{r}. \tag{2.28}$$

The radii of the concentric spheres in the "onion-shell" geometry for the para-

magnetic current density metric space are $|m|$, with the paramagnetic current densities located on the spheres corresponding to the value of $|m|$ given by Eq. (2.25).

As we take the z-component of the cross product in the paramagnetic current density metric (2.28), it is clear that the z-component of the paramagnetic current density itself does not affect the value of the metric. Therefore, $D_{\mathbf{j}_{p_\perp}}$ is a distance between equivalence classes of paramagnetic currents, each class characterized by current densities having the same transverse component $\mathbf{j}_{p_\perp} \equiv (j_{p_x}, j_{p_y})$.

It transpires that a metric for the transverse components of the current density is well suited for studying systems subject to longitudinal magnetic fields. Classically, it is well known that a particle moving in a magnetic field experiences the Lorentz force, which is given by [12]

$$\mathbf{F} = \mathbf{E} + \frac{1}{c}\mathbf{v} \times \mathbf{B}, \tag{2.29}$$

where $\mathbf{F}$ is the force, $\mathbf{v}$ is the velocity and $\mathbf{E}$ and $\mathbf{B}$ are the electric and magnetic fields. By virtue of the cross product in Eq. (2.29), the particle experiences a force perpendicular to the direction of the magnetic field, which will act to induce motion in the plane transverse to direction of the field.

Quantum mechanically, the physical current density is given by [7],

$$\hat{\mathbf{j}}(\mathbf{r}) = \frac{1}{2}\sum_{i=1}^{N}\left\{\delta(\mathbf{r}-\mathbf{r}_i)\left[\hat{\mathbf{p}}_{r_i} + \frac{1}{c}\mathbf{A}(\mathbf{r}_i)\right] + \left[\hat{\mathbf{p}}_{r_i} + \frac{1}{c}\mathbf{A}(\mathbf{r}_i)\right]\delta(\mathbf{r}-\mathbf{r}_i)\right\}. \tag{2.30}$$

The physical current density can be written as a superposition of transverse and longitudinal components,

$$\hat{\mathbf{j}}(\mathbf{r}) = \hat{\mathbf{j}}_T(\mathbf{r}) + \hat{\mathbf{j}}_L(\mathbf{r}), \tag{2.31}$$

where the components are defined by the identities,

$$\nabla \cdot \hat{\mathbf{j}}_T(\mathbf{r}) = 0, \qquad \nabla \times \hat{\mathbf{j}}_L(\mathbf{r}) = 0. \tag{2.32}$$

We can also split the vector potential, $\mathbf{A}(\mathbf{r})$, into transverse and longitudinal components obeying the same identities,

$$\mathbf{A}(\mathbf{r}) = \mathbf{A}_T(\mathbf{r}) + \mathbf{A}_L(\mathbf{r}), \qquad \nabla \cdot \mathbf{A}_T(\mathbf{r}) = 0, \qquad \nabla \times \mathbf{A}_L(\mathbf{r}) = 0. \tag{2.33}$$

We can see immediately from Eq. (2.33) that the longitudinal component of the vector potential cannot contribute to the magnetic field. Therefore, the

magnetic field is entirely captured by the transverse component of the vector potential. Thus, changes in the magnetic field correspond to changes in the transverse component of the vector potential, which is captured in the transverse component of the physical current density.

2.3.4 Scalar Potentials

For scalar potentials, we consider the conservation of energy, Eq. (1.25), in order to derive a metric [64]. The expectation value of the Hamiltonian is

$$\int\int\ldots\int \psi^*(\mathbf{r},\mathbf{r}_2,\ldots,\mathbf{r}_N)\hat{H}\psi(\mathbf{r},\mathbf{r}_2,\ldots,\mathbf{r}_N)\,d\mathbf{r}_1 d\mathbf{r}_2\ldots d\mathbf{r}_N = E. \tag{2.34}$$

In order to ensure that the resulting metric will satisfy the positivity axiom (1.61), we must take the absolute value of the energy,

$$\left|\int\int\ldots\int \psi^*(\mathbf{r},\mathbf{r}_2,\ldots,\mathbf{r}_N)\hat{H}\psi(\mathbf{r},\mathbf{r}_2,\ldots,\mathbf{r}_N)\,d\mathbf{r}_1 d\mathbf{r}_2\ldots d\mathbf{r}_N\right| = |E|. \tag{2.35}$$

To derive a non-trivial metric, we must ensure that the conservation law is of the form of Eq. (2.1), i.e., be able to "move" the absolute value signs inside the integral, taking the absolute value of the integrand. This can be done only if the integrand always has the same sign throughout its domain. Writing the Hamiltonian explicitly, we have:

$$\begin{gathered}\int\int\ldots\int \psi^*\sum_{i=1}^{N}\left[-\frac{\nabla_i^2}{2}+\sum_{j<i}\frac{1}{|\mathbf{r}_i-\mathbf{r}_j|}+V(\mathbf{r}_i)\right]\psi\, d\mathbf{r}_1 d\mathbf{r}_2\ldots d\mathbf{r}_N = E \\ \int\int\ldots\int \sum_{i=1}^{N}\left[-\frac{\psi^*\nabla_i^2\psi}{2}+\sum_{j<i}\frac{|\psi|^2}{|\mathbf{r}_i-\mathbf{r}_j|}+|\psi|^2 V(\mathbf{r}_i)\right] d\mathbf{r}_1 d\mathbf{r}_2\ldots d\mathbf{r}_N = E\end{gathered} \tag{2.36}$$

where the three terms on the left hand side correspond to the kinetic energy, the energy of the Coulomb interaction between the electrons and the potential energy respectively. We will now demonstrate that each of the terms in the integrand can be written such that they are positive semidefinite everywhere. The integrand of the Coulomb term clearly satisfies this requirement already, so we need only consider the remaining two terms.

2.3.4.1 Kinetic Energy

The kinetic energy of the ith particle is given by

$$T = -\frac{1}{2}\int \psi^*(\mathbf{r},\mathbf{r}_2,\ldots,\mathbf{r}_N)\nabla_i^2\psi(\mathbf{r},\mathbf{r}_2,\ldots,\mathbf{r}_N)\,d\mathbf{r}_1 d\mathbf{r}_2\ldots d\mathbf{r}_N. \tag{2.37}$$

Writing this integral explicitly gives:

$$\begin{aligned}-\frac{1}{2}\int \psi^*\nabla_i^2\psi d\mathbf{r}_i &= -\frac{1}{2}\int_0^\infty\int_0^\pi\int_0^{2\pi}\left(\psi^*\nabla_i^2\psi\right) r_i^2\sin\theta_i dr_i d\theta_i d\phi_i,\\ &= -\frac{1}{2}\int_0^\infty\int_0^\pi\int_0^{2\pi}\psi^*\left[\frac{1}{r_i^2}\frac{\partial}{\partial r_i}\left(r_i^2\frac{\partial\psi}{\partial r_i}\right)+\frac{1}{r_i^2\sin\theta_i}\frac{\partial}{\partial\theta_i}\left(\sin\theta_i\frac{\partial\psi}{\partial\theta_i}\right)\right.\\ &\quad\left.+\frac{1}{r_i^2\sin^2\theta_i}\frac{\partial^2\psi}{\partial\phi_i^2}\right] r_i^2\sin\theta_i dr_i d\theta_i d\phi_i.\end{aligned}$$

Taking each of the three terms in turn, we will perform integration by parts in order to rewrite the kinetic energy. For the first term, we will evaluate the radial integral by parts,

$$\begin{aligned}-\frac{1}{2}\int_0^\infty\psi^*\left[\frac{1}{r_i^2}\frac{\partial}{\partial r_i}\left(r_i^2\frac{\partial\psi}{\partial r_i}\right)\right] r_i^2 dr_i &= -\frac{1}{2}\left[r_i^2\psi^*\frac{\partial\psi}{\partial r_i}\right]_0^\infty+\frac{1}{2}\int_0^\infty r_i^2\left(\frac{\partial\psi*}{\partial r_i}\frac{\partial\psi}{\partial r_i}\right)dr_i,\\ &= \frac{1}{2}\int_0^\infty\left|\frac{\partial\psi}{\partial r_i}\right|^2 r_i^2 dr_i,\end{aligned}$$

where we have used that $\psi\to 0$ as $r_i\to\infty$. For the second term, we calculate the θ integral by parts,

$$\begin{aligned}-\frac{1}{2}\int_0^\pi\psi^*\left[\frac{1}{r_i^2\sin\theta_i}\frac{\partial}{\partial\theta_i}\left(\sin\theta_i\frac{\partial\psi}{\partial\theta_i}\right)\right]\sin\theta_i d\theta_i &= -\frac{1}{2}\left[\frac{\psi^*}{r_i^2}\sin\theta_i\frac{\partial\psi}{\partial r_i}\right]_0^\pi\\ &\quad+\frac{1}{2}\int_0^\pi\frac{1}{r_i^2}\sin\theta_i\left(\frac{\partial\psi*}{\partial\theta_i}\frac{\partial\psi}{\partial\theta_i}\right)d\theta_i,\\ &= \frac{1}{2}\int_0^\pi\left|\frac{1}{r_i}\frac{\partial\psi}{\partial\theta_i}\right|^2\sin\theta_i d\theta_i.\end{aligned}$$

Finally, we perform the ϕ integral by parts for the third term,

$$\begin{aligned}-\frac{1}{2}\int_0^{2\pi}\psi^*\left[\frac{1}{r_i^2\sin^2\theta_i}\frac{\partial^2\psi}{\partial\phi_i^2}\right]d\phi_i &= -\frac{1}{2}\left[\frac{\psi^*}{r_i^2\sin^2\theta_i}\frac{\partial\psi}{\partial\phi_i}\right]_0^{2\pi}+\frac{1}{2}\int_0^{2\pi}\frac{1}{r_i^2\sin^2\theta_i}\left(\frac{\partial\psi*}{\partial\phi_i}\frac{\partial\psi}{\partial\phi_i}\right)d\phi_i,\\ &= \frac{1}{2}\int_0^{2\pi}\left|\frac{1}{r_i\sin\theta_i}\frac{\partial\psi}{\partial\phi_i}\right|^2 d\phi_i,\end{aligned}$$

where we use the fact that the wavefunction and its derivatives must be continuous in order to eliminate the first term.

Therefore, for the full integral, we have,

$$-\frac{1}{2}\int \psi^* \nabla_i^2 \psi d\mathbf{r}_i = \frac{1}{2}\int_0^\infty \int_0^\pi \int_0^{2\pi} \left[\left| \frac{\partial \psi}{\partial r_i} \right|^2 + \left| \frac{1}{r_i} \frac{\partial \psi}{\partial \theta_i} \right|^2 + \left| \frac{1}{r_i \sin\theta_i} \frac{\partial \psi}{\partial \phi_i} \right|^2 \right] r_i^2 \sin\theta_i dr_i d\theta_i d\phi_i,$$
$$= \frac{1}{2}\int |\nabla \psi|^2 d\mathbf{r}_i,$$

and the kinetic energy is given by

$$T = \frac{1}{2}\int\int \ldots \int |\nabla \psi|^2 d\mathbf{r}_1 d\mathbf{r}_2 \ldots d\mathbf{r}_N. \tag{2.38}$$

Thus, the integrand of the kinetic energy term is positive semidefinite everywhere.

2.3.4.2 Potential Energy

The potential energy is given by

$$V = \sum_{i=1}^{N} \int\int \ldots \int \psi^* (\mathbf{r}, \mathbf{r}_2, \ldots, \mathbf{r}_N) V(\mathbf{r}_i) \psi (\mathbf{r}, \mathbf{r}_2, \ldots, \mathbf{r}_N) d\mathbf{r}_1 d\mathbf{r}_2 \ldots d\mathbf{r}_N, \tag{2.39}$$

where $V(\mathbf{r}_i)$ is defined by the system under consideration. Although we cannot guarantee the sign of $V(\mathbf{r}_i)$, we can make use of a gauge transformation. If the potential is modified by a constant, $V(\mathbf{r}_i) \to V(\mathbf{r}_i) + c$, then the solution to the Schrödinger equation is unaffected. Thus, when considering potentials that have a single minimum, we can choose a constant c such that the value of the integrand is positive everywhere for all of the potentials that we consider. Hence, when studying systems with the potential metric, we must always work in the same gauge *and* that gauge must be chosen in order to allow the expectation value of the Hamiltonian to be written as a well-defined norm. This approach works well for potentials with a single minimum, but we are aware of some cases where more care must be taken in order to ensure that the potential metric gives physically relevant results.

2.3.4.3 Forming the Potential Metric

Our expectation value is now given by

$$\int\int \ldots \int \sum_{i=1}^{N} \left[\frac{1}{2} |\nabla \psi|^2 + \sum_{j<i} \frac{\psi^* \psi}{|\mathbf{r}_i - \mathbf{r}_j|} + \psi^* [V(\mathbf{r}_i) + c] \psi \right] d\mathbf{r}_1 d\mathbf{r}_2 \ldots d\mathbf{r}_N = E + c,$$

and we can write

$$\left| \int\int \ldots \int \sum_{i=1}^{N} \left[\frac{1}{2} |\nabla \psi|^2 + \sum_{j<i} \frac{\psi^* \psi}{|\mathbf{r}_i - \mathbf{r}_j|} + \psi^* \left[V(\mathbf{r}_i) + c \right] \psi \right] d\mathbf{r}_1 d\mathbf{r}_2 \ldots d\mathbf{r}_N \right| = |E + c|,$$
$$\int\int \ldots \int \left| \sum_{i=1}^{N} \left[\frac{1}{2} |\nabla \psi|^2 + \sum_{j<i} \frac{\psi^* \psi}{|\mathbf{r}_i - \mathbf{r}_j|} + \psi^* \left[V(\mathbf{r}_i) + c \right] \psi \right] \right| d\mathbf{r}_1 d\mathbf{r}_2 \ldots d\mathbf{r}_N = |E + c|,$$
$$\int\int \ldots \int \left| \hat{H}' \right| d\mathbf{r}_1 d\mathbf{r}_2 \ldots d\mathbf{r}_N = \left| E' \right|, \tag{2.40}$$

where $E' = E + c$. Hence, we derive the following metric,

$$D_V = \int\int \ldots \int \left| \hat{H}'_1 - \hat{H}'_2 \right| d\mathbf{r}_1 d\mathbf{r}_2 \ldots d\mathbf{r}_N \tag{2.41}$$

with spheres of radii E' for the "onion-shell" geometry. It can be seen that this metric can be applied to the potential, rather than the whole Hamiltonian, by considering each of the terms in H'. All of the terms contain the many body wavefunction, $\psi(\mathbf{r}, \mathbf{r}_2, \ldots, \mathbf{r}_N)$; from the Schrödinger equation, the many body wavefunction can be seen to be defined uniquely by the external potential $V(\mathbf{r})$. Hence, we can write,

$$\psi = \psi[V(\mathbf{r})]. \tag{2.42}$$

In DFT, it is sometimes stated that T and U are *universal* functionals of the density. This is because, assuming the nature of the interaction between the electrons is fixed, T and U are identical for all systems - where a system is prescribed by the external potential [3]. Applying a similar argument to the potential metric allows us to write Eq. (2.40) as

$$\int\int \ldots \int \left| \sum_{i=1}^{N} \left[F[V] + \psi^* \left[V(\mathbf{r}_i) + c \right] \psi \right] \right| d\mathbf{r}_1 d\mathbf{r}_2 \ldots d\mathbf{r}_N = |E + c|, \tag{2.43}$$

where $F[V]$ is a functional of the potential analogous to the DFT universal functional $F[\rho]$.

2.3.4.4 A Note on Coulomb Potentials

An important class of systems studied in quantum mechanics are atomic-like systems, where the external potential is of the form of $-\frac{1}{r_i}$ for each particle. At first glance, this causes a problem with the argument in Sec. 2.3.4.2, because if $V(0) = -\infty$ and $\psi(0) \neq 0$, then it is impossible for a gauge transformation to enable the integrand of the potential norm, given by Eq. (2.40), to be positive everywhere.

However, in two dimensions, $d\mathbf{r}_i = r_i dr_i$, and in three dimensions, $d\mathbf{r}_i = r_i^2 \sin\theta dr_i$. Hence, the factors of r_i in the Jacobean determinant cancel with the factor of r_i in the potential, resulting in the potential energy term being finite and, therefore, amenable to a gauge transformation provided we study the system in at least two dimensions. In one-dimensional modelling of quantum systems, Coulomb potentials are typically replaced by softened potentials that are finite at $r_i = 0$ [70, 71].

2.4 Gauge Theory

In this thesis, we will consider systems subject to magnetic fields. When dealing with electromagnetic fields, it is important to consider the choice of gauge. The scalar and vector potentials in the Hamiltonian (1.5) are not unique, as a change of gauge transforms the potentials according to:

$$V'(\mathbf{r}) = V(\mathbf{r}) + c, \quad \mathbf{A}'(\mathbf{r}) = \mathbf{A}(\mathbf{r}) - \nabla\chi, \tag{2.44}$$

where c is a constant and $\chi(\mathbf{r})$ is a scalar field [39]. These transformations preserve the electromagnetic fields and all physical observables.

With regard to the quantities we have considered in this chapter, the particle density is gauge invariant, but the wavefunction, paramagnetic current density and scalar potential are not. After a change of gauge, the wavefunction undergoes a unitary transformation, which is given by [72]

$$\psi'(\mathbf{r}) = e^{[i\chi(\mathbf{r})]}\psi(\mathbf{r}). \tag{2.45}$$

The paramagnetic current density transforms according to [39]

$$\mathbf{j}'_p(\mathbf{r}) = \mathbf{j}_p(\mathbf{r}) + \rho(\mathbf{r})\nabla\chi. \tag{2.46}$$

Thus, when considering changes in the vector potential, we must be aware of the effect of gauge transformations on the physical quantities we are considering. Our metrics are constructed to provide non-trivial information that is physically relevant, since they are based on conservation laws. It is paramount then that they are also gauge invariant.

For wavefunctions, a gauge transformation introduces a global phase factor. In Sec. 2.3.2, we defined all wavefunctions differing only by a constant global phase as equivalent and wrote the wavefunction metric in the form of Eq. (2.18). This has ensured that the wavefunction metric is gauge invariant. We now

consider the effect of gauge theory for the paramagnetic current density metric [63].

2.4.1 Gauge Invariance for the Paramagnetic Current Density Metric

In Ref. [63], we analysed the paramagnetic current density metric in different gauges. In order to consider the gauge properties of $D_{\mathbf{j}_{p_\perp}}(\mathbf{j}_{p_1},\mathbf{j}_{p_2})$, first of all we require that $\mathbf{j}_{p_1}$ and $\mathbf{j}_{p_2}$ are within the same gauge. Then, applying the gauge transformation in Eq. (2.46) we obtain

$$\begin{aligned} D_{\mathbf{j}_{p_\perp}}\left(\mathbf{j}'_{p_1},\mathbf{j}'_{p_2}\right) &= \int \left| \left\{ \mathbf{r} \times \left[\mathbf{j}'_{p_1}(\mathbf{r}) - \mathbf{j}'_{p_2}(\mathbf{r}) \right] \right\}_z \right| d\mathbf{r}, \\ &= \int \left| \left(\mathbf{r} \times \left\{ \mathbf{j}_{p_1}(\mathbf{r}) - \mathbf{j}_{p_2}(\mathbf{r}) + \left[\rho_1(\mathbf{r}) - \rho_2(\mathbf{r}) \right] \nabla\chi \right\} \right)_z \right| d\mathbf{r}. \end{aligned} \tag{2.47}$$

Equation (2.47) states that, in general, the paramagnetic current density distance defined by Eq. (2.28) is modified by a gauge transformation. This seems to contradict the fact that we base our metrics on conservation laws, which must be gauge invariant. In order to reconcile this apparent contradiction let us explore more closely which quantities are gauge variant and which are the ones that *must* be conserved.

With reference to Eq. (2.25), the measurable physical quantity which must be conserved by gauge transformations is m, which, in the gauge chosen, corresponds to the component $\hat{L}_z$ of the angular momentum. However it is crucial to note that $\hat{L}_z$ is not (nor need be) gauge invariant.

The operator $\hat{L}_z$ is defined in Eq. (1.20) as the cross product of $\mathbf{r}$ and the *canonical* linear momentum, $\hat{\mathbf{p}}$. Although $\mathbf{r}$ is gauge invariant, $\hat{\mathbf{p}}$ is gauge variant, and therefore, so is $\hat{L}_z$. In the following we wish to extend Eq. (2.28) so that the metric associated to the conservation of m is indeed gauge invariant.

We consider a system for which there exists at least one gauge such that $[\hat{L}_z,\hat{H}] = 0$, with $\hat{H}$ the system Hamiltonian. We name this the *reference gauge* and refer to its vector potential as $\mathbf{A}_{ref}(\mathbf{r})$ and to its paramagnetic current density as $\mathbf{j}_{p_{ref}}(\mathbf{r})$. In this reference gauge the set $\{m\}$ corresponds to the eigenvalues of $\hat{L}_z$ and both equalities in the relation (2.25) hold. The set $\{m\}$ are then constants of motion, and in this gauge they represent the z-component of the angular momentum, $\hat{L}_z$.

We now focus on the generic gauge corresponding to a generic vector potential $\mathbf{A}(\mathbf{r})$. In this generic gauge, the first equality of Eq. (2.25) holds, but the second equality holds only if $\hat{L}_z$ is a constant of motion in this gauge.

We will now consider the quantity

$$\widetilde{\mathbf{j}}_p(\mathbf{r}) \equiv \mathbf{j}_p(\mathbf{r}) - \rho(\mathbf{r}) \nabla \chi_{ref} \tag{2.48}$$

and the operator

$$\widetilde{\mathbf{L}}_z \equiv \sum_{i=1}^{N} \left[\mathbf{r} \times \left(\hat{\mathbf{p}} - \nabla \chi_{ref}\right)\right]_z, \tag{2.49}$$

where $\nabla \chi_{ref}$ is defined by $\mathbf{A} = \mathbf{A}_{ref} - \nabla \chi_{ref}$. We note that $\widetilde{\mathbf{j}}_p(\mathbf{r})$ is gauge invariant, as, from equation (2.46),

$$\widetilde{\mathbf{j}}_p(\mathbf{r}) \equiv \mathbf{j}_{p_{ref}}(\mathbf{r}) \tag{2.50}$$

always. It follows that

$$\int \left[\mathbf{r} \times \widetilde{\mathbf{j}}_p(\mathbf{r})\right]_z d\mathbf{r} = m, \tag{2.51}$$

independently of the gauge. Furthermore, by using the definition (2.48), and the first equality of Eq. (2.25), which holds regardless of whether or not $\hat{L}_z$ is a constant of motion, we obtain

$$\begin{aligned} \int \left[\mathbf{r} \times \widetilde{\mathbf{j}}_p(\mathbf{r})\right]_z d\mathbf{r} &= \langle \psi | \hat{L}_z | \psi \rangle - \int \left[\mathbf{r} \times \rho(\mathbf{r}) \nabla \chi_{ref}\right]_z d\mathbf{r}, \\ &= \langle \psi | \hat{L}_z | \psi \rangle - \langle \psi | \left(\mathbf{r} \times \nabla \chi_{ref}\right)_z | \psi \rangle, \\ &= \langle \psi | \widetilde{L}_z | \psi \rangle. \end{aligned} \tag{2.52}$$

This demonstrates that equation (2.49) defines the operator associated to the conservation law (2.51), independently of the gauge. In particular, comparison of Eq. (2.51) and Eq. (2.52) shows that indeed $\widetilde{L}_z$ is the operator whose eigenvalues are $\{m\}$ independently of the gauge.[1]

$\widetilde{L}_z$ reduces to $\hat{L}_z$ in the reference gauge, and in all gauges where $\hat{L}_z$ is a constant of motion, as should be expected. This is because the limited set of gauges for which $\left[\hat{L}_z, \hat{H}\right] = 0$ holds, is the same within which both $\hat{L}_z$ and $\left[\mathbf{r} \times \mathbf{j}_p(\mathbf{r})\right]_z$ are unaffected by gauge transformations. These gauges correspond to vector potentials of the form of Eq. (1.22). These vector potentials are linked by gauge transformations of the form $\chi\left(x^2 + y^2, z\right)$. The proofs of these statements are given in Appendices A and B respectively.

[1] We note that $\tilde{L}_z$ is related to the gauge invariant z component of the moment of mechanical momentum $\hat{K}_z = \hat{L}_z + [\mathbf{r} \times \mathbf{A}(\mathbf{r})]_z$ as $\tilde{L}_z = \hat{K}_z - \left(\mathbf{r} \times \mathbf{A}_{ref}\right)_z$, but that $\hat{K}_z$ would not be a constant of motion in all gauges, that is, its eigenvalues are generally different from $\{m\}$. Likewise $\tilde{\mathbf{j}}_p(\mathbf{r})$ does not coincide with the gauge invariant total current density $\mathbf{j}(\mathbf{r}) = \mathbf{j}_p(\mathbf{r}) + \rho(\mathbf{r}) \mathbf{A}(\mathbf{r})$.

Chapter 3

Applying the Metric Space Approach to Current Density Functional Theory

For systems subject to a vector potential with a Hamiltonian of the form of Eq. (1.5), CDFT states that the ground state wavefunction obtained from the Schrödinger equation is uniquely defined by the particle density and the paramagnetic current density taken together, and vice versa [39, 40]. Equations (1.18) and (1.54) clearly demonstrate how each of the densities are obtained from the wavefunction. However, no suggestion on the details of the map from the basic densities to the wavefunction is offered by either Hohenberg and Kohn with regards to standard DFT, or Vignale and Rasolt for CDFT.

The metric space approach to quantum mechanics allows us to explore this unique relationship, comparing the distances between wavefunctions to the distances between their corresponding particle densities and their corresponding paramagnetic current densities. Building on the analysis for standard DFT in Ref. [58], we will consider model systems, for which we can generate highly accurate solutions, and calculate the wavefunctions, particle densities and paramagnetic current densities for a range of Hamiltonians. Comparing the distances between corresponding quantities will enable us to build up a picture of the unique relationship at the core of CDFT. The results in this chapter that relate to varying the confinement potential were published in Ref. [62].

3.1 Model Systems

In this Chapter, and the next, we will consider two model systems: the magnetic Hooke's Atom, and the Inverse Square Interaction System. Both of these are two-dimensional systems, immersed in a magnetic field that is applied perpendicular to the plane of confinement.

3.1.1 Magnetic Hooke's Atom

Hooke's Atom is a system consisting of two electrons confined in a harmonic oscillator potential. It is particularly notable as one of few examples of quantum many-body systems for which exact solutions exist [73, 74]. Analytical solutions also exist when the system is subject to a magnetic field. The Hamiltonian in this case, in atomic units, is given by [42, 75]

$$\hat{H} = \sum_{i=1}^{2} \left\{ \frac{1}{2} \left[\mathbf{p}_i + \frac{1}{c} \mathbf{A}(\mathbf{r}_i) \right]^2 + \frac{1}{2} \omega_0^2 r_i^2 \right\} + \frac{1}{|\mathbf{r}_2 - \mathbf{r}_1|} \tag{3.1}$$

where ω_0 is the harmonic confinement frequency and c is the speed of light. We introduce centre of mass and relative motion coordinates, defined as,

$$\mathbf{R} = \frac{1}{2}(\mathbf{r}_1 + \mathbf{r}_2), \qquad \mathbf{r} = \mathbf{r}_2 - \mathbf{r}_1. \tag{3.2}$$

This allows us to define the momentum operators,

$$\mathbf{p}_R = \mathbf{p}_1 + \mathbf{p}_2, \qquad \mathbf{p}_r = \frac{1}{2}(\mathbf{p}_2 - \mathbf{p}_1), \tag{3.3}$$

and the vector potentials,

$$\mathbf{A}_R(\mathbf{R}) = \frac{1}{2}[\mathbf{A}(\mathbf{r}_1) + \mathbf{A}(\mathbf{r}_2)], \qquad \mathbf{A}_r(\mathbf{r}) = \mathbf{A}(\mathbf{r}_2) - \mathbf{A}(\mathbf{r}_1). \tag{3.4}$$

We will study the system in two dimensions, and work in cylindrical coordinates with the magnetic field applied perpendicular to the plane such that $\mathbf{B} = B\hat{z}$ [42, 75].

In centre of mass and relative motion coordinates, we have

$$\hat{H} = 2\left[\frac{1}{2} \left(\mathbf{p}_r + \frac{1}{2c} \mathbf{A}_r(\mathbf{r}) \right)^2 + \frac{1}{8} \omega_0^2 r^2 + \frac{1}{2r} \right] + \frac{1}{2} \left[\frac{1}{2} \left(\mathbf{p}_R + \frac{2}{c} \mathbf{A}_R(\mathbf{R}) \right)^2 + 2\omega_0^2 R^2 \right]. \tag{3.5}$$

It can be seen that the Hamiltonian is separable into relative motion and centre of mass components. The centre of mass Hamiltonian is simply that of a

single particle harmonic oscillator subject to a magnetic field, which is treated in Refs. [76–78]. Writing the centre of mass wavefunction as $\xi(\mathbf{R}) = e^{iM\theta}U(R)$, the Schrödinger equation reduces to [77]

$$\frac{d^2U}{dR^2} + \frac{1}{R}\frac{dU}{dR} - \frac{M^2}{R^2}U(R) - \widetilde{\omega}^2 r^2 U(R) = 2\left(\eta - \frac{m\omega_c}{4}\right)U(R), \tag{3.6}$$

where η is the centre of mass energy and M is the angular momentum quantum number for the centre of mass. The frequency $\widetilde{\omega}$ is the effective frequency of the harmonic oscillator, which we define using Taut's convention [42, 75] as,

$$\widetilde{\omega} = \sqrt{\omega_0^2 + \left(\frac{\omega_c}{2}\right)^2}, \tag{3.7}$$

where $\omega_c = \frac{B}{c}$ is the cyclotron frequency. The solution for the centre of mass is [75],

$$\xi(\mathbf{R}) = (2\widetilde{\omega}R)^{|M|} e^{iM\theta} L_N^{|M|}\left(2\widetilde{\omega}R^2\right) e^{-\widetilde{\omega}R^2}, \tag{3.8}$$

where $L_N^{|M|}$ are associated Laguerre polynomials [20, 79], $N = 0, 1, 2, \ldots$ and $M = 0, \pm 1, \pm 2, \ldots, \pm N$.

The centre of mass energy is given by [75],

$$\eta = (2N + 1 + |M|)\,\widetilde{\omega} + \frac{M\omega_c}{2}. \tag{3.9}$$

For the ground state, $N = M = 0$, so $\eta = \widetilde{\omega}$ and the normalised ground state wavefunction is

$$\xi_0(\mathbf{R}) = \sqrt{\frac{2\widetilde{\omega}}{\pi}} e^{-\widetilde{\omega}R^2}. \tag{3.10}$$

Turning our attention to the relative motion, we expand the Hamiltonian and choose the symmetric gauge, $\mathbf{A}_r(\mathbf{r}) = \frac{1}{2}\mathbf{B} \times \mathbf{r} = \frac{1}{2}Br\hat{\theta}$, which is of the form of Eq. (1.22). The time-independent Schrödinger equation reads,

$$\left[\frac{1}{2}\left(-i\nabla_r + \frac{1}{2c}\mathbf{A}_r(\mathbf{r})\right)^2 + \frac{1}{8}\omega_0^2 r^2 + \frac{1}{2r}\right]\phi(\mathbf{r}) = \frac{\varepsilon}{2}\phi(\mathbf{r}), \tag{3.11}$$

which can be expanded as,

$$\frac{1}{2}\left[-\nabla_r^2\phi - \frac{i}{2c}\left(\phi\nabla\cdot\mathbf{A}_r(\mathbf{r}) + 2\mathbf{A}_r(\mathbf{r})\cdot\nabla\phi\right) + \frac{A_r^2}{4c^2}\phi\right] + \frac{1}{8}\omega_0^2 r^2\phi + \frac{1}{2r}\phi = \frac{\varepsilon}{2}\phi,$$

From our choice of gauge, we know that $\nabla\cdot\mathbf{A}_r(\mathbf{r}) = 0$. Expanding the remain-

ing vector operations gives,

$$\begin{aligned}\frac{1}{2}\left[-\frac{\partial^2\phi}{\partial r^2}-\frac{1}{r}\frac{\partial\phi}{\partial r}-\frac{1}{r^2}\frac{\partial^2\phi}{\partial\theta^2}-\frac{i\omega_c}{2}\frac{\partial\phi}{\partial\theta}+\frac{1}{16}\omega_c^2r^2\phi\right]+\frac{1}{8}\omega_0^2r^2\phi+\frac{1}{2r}\phi=\frac{\varepsilon}{2}\phi,\\ \frac{1}{2}\left[-\frac{1}{\sqrt{r}}\frac{\partial^2}{\partial r^2}\left(\sqrt{r}\phi\right)-\frac{1}{4r^2}\phi-\frac{1}{r^2}\frac{\partial^2\phi}{\partial\theta^2}-\frac{i\omega_c}{2}\frac{\partial\phi}{\partial\theta}+\frac{1}{16}\omega_c^2r^2\phi\right]+\frac{1}{8}\omega_0^2r^2\phi+\frac{1}{2r}\phi=\frac{\varepsilon}{2}\phi.\end{aligned} \tag{3.12}$$

At this point, Taut writes the ansatz [42, 75],

$$\phi(\mathbf{r})=\frac{e^{im\theta}}{\sqrt{2\pi}}\frac{u(r)}{\sqrt{r}}\qquad m=0,\pm1,\pm2,\ldots, \tag{3.13}$$

where m is the quantum number corresponding to the z-component of the angular momentum for the relative motion. This ansatz reduces Eq. (3.12) to

$$\begin{aligned}&-\frac{1}{2}\left[\frac{d^2}{dr^2}u(r)+\frac{1}{4r^2}u(r)-\frac{m^2}{r^2}u(r)-\frac{1}{2}m\omega_cu(r)-\frac{1}{16}\omega_c^2r^2u(r)\right]+\frac{1}{8}\omega_0^2r^2u(r)+\frac{1}{2r}u(r)=\frac{\varepsilon}{2}u(r),\\ &-\frac{1}{2}\frac{d^2}{dr^2}u(r)+\frac{1}{2r^2}\left(m^2-\frac{1}{4}\right)u(r)+\frac{1}{8}\widetilde{\omega}^2r^2u(r)+\frac{1}{2r}u(r)=\left(\frac{\varepsilon}{2}-\frac{1}{4}m\omega_c\right)u(r).\end{aligned} \tag{3.14}$$

As $r\to\infty$, the system will tend towards that of two isolated single-particle harmonic oscillators. Therefore, we write

$$u(r)=e^{-\frac{\widetilde{\omega}r^2}{4}}t(r), \tag{3.15}$$

so that the solution for the single-particle harmonic oscillator dominates at large r. This reduces Eq. (3.14) to

$$-\frac{1}{2}\frac{d^2t}{dr^2}+\frac{1}{8}\widetilde{\omega}r^2\frac{dt}{dr}+\left[-\frac{1}{32}\widetilde{\omega}^2r^4+\frac{1}{2r^2}\left(m^2+\frac{1}{4}\right)+\frac{1}{8}\widetilde{\omega}^2r^2+\frac{1}{2r}\right]t(r)=\left(\frac{\varepsilon}{2}-\frac{1}{4}m\omega_c\right)t(r). \tag{3.16}$$

At this point, we note that Eq. (3.16) is amenable to solution via the Frobenius method.

The Frobenius method [80, 81] states that any differential equation of the form

$$x^2\frac{d^2y}{dx^2}+xb(x)\frac{dy}{dx}+c(x)y=0 \tag{3.17}$$

has at least one solution that can be written as

$$y(x)=x^j\sum_{i=0}^{\infty}a_ix^i. \tag{3.18}$$

By expanding $b(x)$ and $c(x)$ as polynomials, and differentiating Eq. (3.18), we can write Eq. (3.17) as,

$$x^2\sum_{i=0}^{\infty}(i+j)(i+j-1)a_i x^{i+j-2}+x\sum_{i=0}^{\infty}b_i x^i\sum_{i=0}^{\infty}(i+j)a_i x^{i+j-1}+\sum_{i=0}^{\infty}c_i x^i\sum_{i=0}^{\infty}a_i x^i=0. \tag{3.19}$$

Equation (3.19) yields a system of equations for each coefficient a_i by comparing the coefficients of each power $x^j, x^{j+1}\ldots$ The coefficients of x_j yield,

$$\begin{aligned}[j(j-1)+b_0 j+c_0]a_0&=0,\\ j(j-1)+b_0 j+c_0&=0,\end{aligned}$$

which allows us to determine j.

For Eq. (3.16) the Frobenius method yields the solution [75]

$$t(r)=\left(\sqrt{\frac{\widetilde{\omega}}{2}}r\right)^{|m|+\frac{1}{2}}\sum_{i=0}^{\infty}a_i\left(\sqrt{\frac{\widetilde{\omega}}{2}}r\right)^i, \tag{3.20}$$

with coefficients,

$$a_0\neq 0, \tag{3.21}$$

$$a_1=\frac{1}{2\left(|m|+\frac{1}{2}\right)}\sqrt{\frac{2}{\widetilde{\omega}}}a_0, \tag{3.22}$$

$$a_v=\frac{1}{v(v+2|m|)}\left\{\sqrt{\frac{2}{\widetilde{\omega}}}a_{v-1}+\left[2(v+|m|-1)-\varepsilon''\right]a_{v-2}\right\}, \tag{3.23}$$

where $v\geqslant 2$ and

$$\varepsilon''=\frac{2}{\widetilde{\omega}}\left(\varepsilon-\frac{1}{2}m\omega_c\right).$$

Although the polynomial in Eq. (3.20) has an infinite number of terms in general, for each $v=n$ there are particular values of m and $\widetilde{\omega}$ for which the polynomial consists of only n terms. In these cases, $\varepsilon''=2(|m|+n)$. Hence we have a discrete, infinite series of exact solutions. For frequencies where an exact solution does not exist, we construct an approximate solution by building on the method of Coe *et al.* [82] by taking as many terms of the polynomial such that its value converges within an acceptable tolerance.

The wavefunction for the magnetic Hooke's Atom is hence given by,

$$\psi(\mathbf{r},\mathbf{R})=R^{|M|}e^{iM\theta}L_N^{|M|}\left(2\widetilde{\omega}R^2\right)e^{-\widetilde{\omega}R^2}\frac{e^{im\theta}}{\sqrt{2\pi r}}e^{-\frac{\widetilde{\omega}r^2}{4}}\left(\sqrt{\frac{\widetilde{\omega}}{2}}r\right)^{|m|+\frac{1}{2}}\sum_{i=0}^{\infty}a_i\left(\sqrt{\frac{\widetilde{\omega}}{2}}r\right)^i. \tag{3.24}$$

In order to be in the ground state, $N = M = 0$ for the centre of mass, so the ground state wavefunction for the magnetic Hooke's Atom is given by,

$$\begin{aligned}\psi(\mathbf{r},\mathbf{R}) &= \frac{1}{\pi}\sqrt{\frac{\widetilde{\omega}}{r}}e^{im\theta}e^{-\widetilde{\omega}R^2}e^{-\frac{\widetilde{\omega}r^2}{4}}\left(\sqrt{\frac{\widetilde{\omega}}{2}}r\right)^{|m|+\frac{1}{2}}\sum_{i=0}^{\infty}a_i\left(\sqrt{\frac{\widetilde{\omega}}{2}}r\right)^{i}, \\ &= \frac{1}{\pi}\sqrt{\frac{\widetilde{\omega}}{r}}e^{im\theta}e^{-\widetilde{\omega}R^2}u(r). \end{aligned} \tag{3.25}$$

The particle density for the magnetic Hooke's Atom is given by [42],

$$\rho(\mathbf{r}_1) = \frac{4\widetilde{\omega}}{\pi}e^{-2\widetilde{\omega}r_1^2}\int_0^{\infty}e^{-\frac{\widetilde{\omega}}{2}r^2}I_0(2\widetilde{\omega}r_1 r)\left[u(r)\right]^2 dr, \tag{3.26}$$

where $I_n(x)$ is a modified Bessel function. The paramagnetic current density is given by [42],

$$\mathbf{j}_p(\mathbf{r}_1) = \hat{\theta}_1\frac{4m\widetilde{\omega}}{\pi}e^{-2\widetilde{\omega}r_1^2}\int_0^{\infty}e^{-\frac{\widetilde{\omega}}{2}r^2}I_1(2\widetilde{\omega}r_1 r)\frac{\left[u(r)\right]^2}{r}dr. \tag{3.27}$$

These expressions are proved in Appendix C.

3.1.2 Inverse Square Interaction System

Our second system also consists of two electrons confined in a harmonic oscillator potential, but the Coulomb repulsion between the electrons is replaced by an $\frac{\alpha}{r^2}$ potential [83]. This has the significant advantage that the Schrödinger equation is now exactly solvable for arbitrarily strong confinement potentials, many-body interactions and magnetic fields. We again focus on the two dimensional case with the field applied perpendicular to the plane of confinement. The Hamiltonian for the Inverse Square Interaction (ISI) system is:

$$\hat{H} = \sum_{i=1}^{2}\left[\frac{1}{2}\left(\mathbf{p}_i + \frac{1}{c}\mathbf{A}(\mathbf{r}_i)\right)^2 + \frac{1}{2}\omega_0^2 r_i^2\right] + \frac{\alpha}{(\mathbf{r}_2 - \mathbf{r}_1)^2}, \tag{3.28}$$

which can be decoupled into centre of mass and relative motion coordinates as,

$$\hat{H} = 2\left\{\frac{1}{2}\left[\mathbf{p}_r + \frac{1}{2c}\mathbf{A}_r(\mathbf{r})\right]^2 + \frac{1}{8}\omega_0^2 r^2 + \frac{\alpha}{2r^2}\right\} + \frac{1}{2}\left\{\frac{1}{2}\left[\mathbf{p}_R + \frac{2}{c}\mathbf{A}_R(\mathbf{R})\right]^2 + 2\omega_0^2 R^2\right\}. \tag{3.29}$$

The centre of mass Hamiltonian is the same as that for Hooke's Atom, and the solution is therefore given by Eq. (3.8). For the relative motion, we again work in the symmetric gauge, which, following Sec. 3.1.1 allows the Schrödinger

equation for the relative motion to be written as

$$-\frac{\partial^2\phi}{\partial r^2}-\frac{1}{r}\frac{\partial\phi}{\partial r}-\frac{1}{r^2}\frac{\partial^2\phi}{\partial\theta^2}-\frac{i\omega_c}{2}\frac{\partial\phi}{\partial\theta}+\frac{1}{16}\omega_c^2r^2\phi+\frac{1}{4}\omega_0^2r^2\phi+\frac{\alpha}{2r^2}\phi=\varepsilon\phi, \tag{3.30}$$

Using the substitution $\phi(\mathbf{r})=e^{im\theta}u(r)$, we can write

$$\begin{aligned}-\frac{d^2}{dr^2}u(r)-\frac{1}{r}\frac{du}{dr}+\frac{m^2}{r^2}u(r)+\frac{1}{2}m\omega_c u(r)+\frac{1}{16}\omega_c^2r^2u(r)+\frac{1}{4}\omega_0^2r^2u(r)+\frac{\alpha}{2r^2}u(r)=\varepsilon u(r),\\ \frac{d^2}{dr^2}u(r)+\frac{\mu^2}{r^2}u(r)+\frac{1}{4}\widetilde{\omega}^2r^2u(r)+\frac{1}{2}m\omega_c u(r)=\varepsilon u(r),\end{aligned} \tag{3.31}$$

where we have defined $\mu=\sqrt{m^2+\alpha}$. It can now be seen that Eq. (3.31) is identical to Eq. (3.6), the corresponding equation for the centre of mass with modified parameters. Consequently, we can obtain the solution to Eq. (3.31) by substituting the appropriate parameters into the solution of Eq. (3.6), which is given by Eq. (3.8). The relative motion wavefunction is therefore,

$$\phi(\mathbf{r})=\left(\sqrt{\frac{\widetilde{\omega}}{2}}r\right)^{\mu}e^{im\theta}L_n^{\mu}\left(\frac{\widetilde{\omega}r^2}{2}\right)e^{-\frac{\widetilde{\omega}r^2}{4}}. \tag{3.32}$$

The full wavefunction for the ISI system is given by,

$$\psi(\mathbf{r},\mathbf{R})=(2\widetilde{\omega}R)^{|M|}e^{iM\theta}L_N^{|M|}\left(2\widetilde{\omega}R^2\right)e^{-\widetilde{\omega}R^2}\left(\sqrt{\frac{\widetilde{\omega}}{2}}r\right)^{\mu}e^{im\theta}L_n^{\mu}\left(\frac{\widetilde{\omega}r^2}{2}\right)e^{-\frac{\widetilde{\omega}r^2}{4}}. \tag{3.33}$$

and the normalised ground state, with the centre of mass parameters M and N set to zero, is,

$$\psi(\mathbf{r},\mathbf{R})=\frac{\widetilde{\omega}}{\pi}\sqrt{\frac{1}{\Gamma(\mu+1)}}\left(\sqrt{\frac{\widetilde{\omega}}{2}}r\right)^{\mu}e^{im\theta}L_n^{\mu}\left(\frac{\widetilde{\omega}r^2}{2}\right)e^{-\frac{\widetilde{\omega}r^2}{4}}e^{-\widetilde{\omega}R^2}. \tag{3.34}$$

The energy of the ISI system is given by,

$$E=2\widetilde{\omega}\left[N+1-\frac{1}{2}\left(1-\frac{\omega_c}{2\widetilde{\omega}}\right)M+n+\frac{\omega_c}{4\widetilde{\omega}}m+\frac{1}{2}\mu\right]. \tag{3.35}$$

The particle density for the ISI system is written as

$$\rho(\mathbf{r}_1)=\frac{2\widetilde{\omega}^2}{\pi}\frac{1}{\Gamma(\mu+1)}\left(\frac{\widetilde{\omega}}{2}\right)^{\mu}e^{-2\widetilde{\omega}r_1^2}\int_0^{\infty}e^{-\widetilde{\omega}r^2}I_0(2\widetilde{\omega}r_1r)\,r^{(2\mu+1)}dr, \tag{3.36}$$

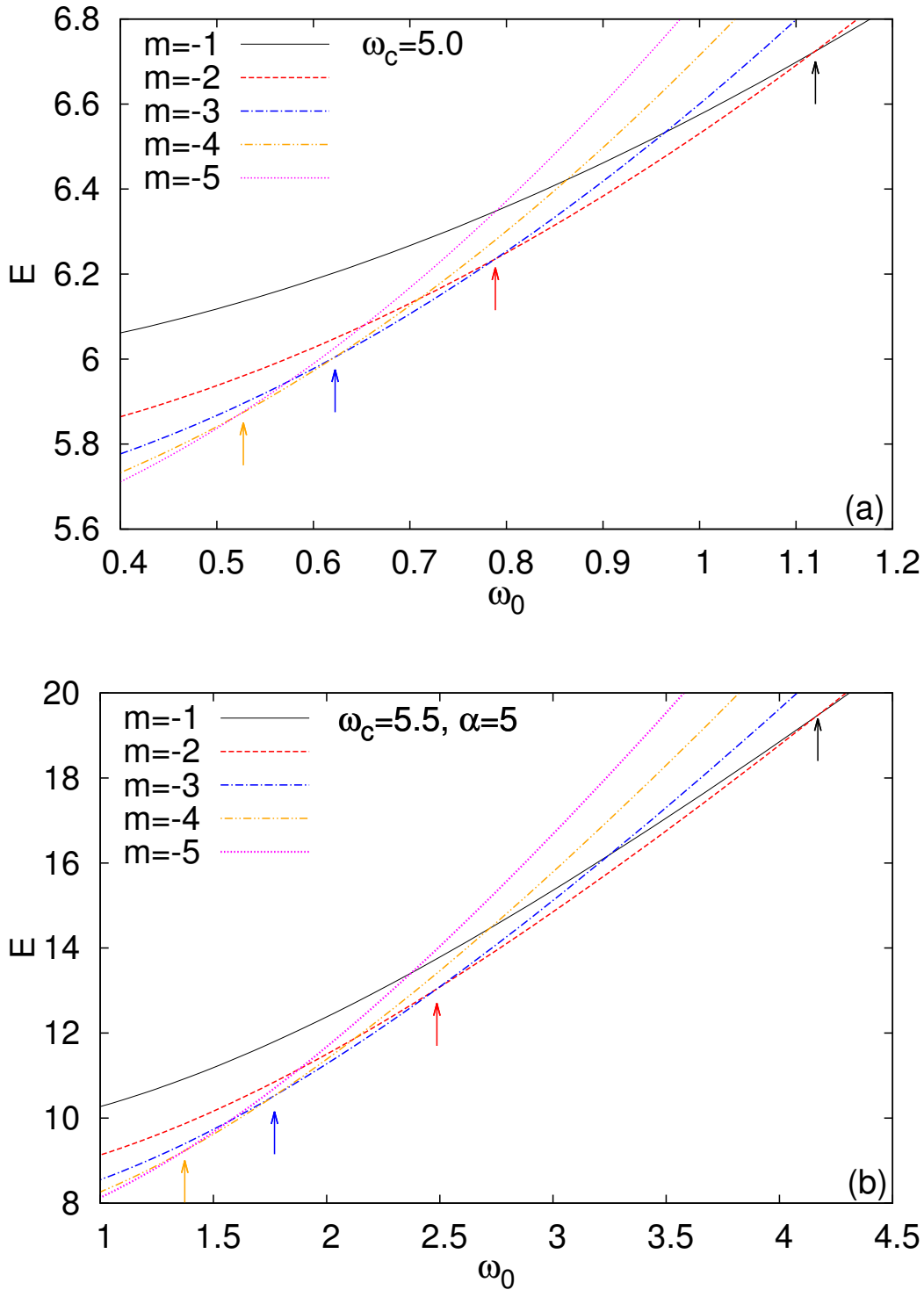

Figure 3.1: Energy is plotted against the confinement frequency for (a) Magnetic Hooke's Atom and (b) the ISI system. The energy is plotted for several values of the angular momentum quantum number m (as labelled), and with constant cyclotron frequency and interaction strength. Arrows indicate where the value of m for the ground state changes.

and the paramagnetic current density is

$$\mathbf{j}_p(\mathbf{r}_1) = \hat{\theta}_1 \frac{2m\widetilde{\omega}^2}{\pi} \frac{1}{\Gamma(\mu+1)} \left(\frac{\widetilde{\omega}}{2}\right)^{\mu} e^{-2\widetilde{\omega}r_1^2} \int_0^{\infty} e^{-\widetilde{\omega}r^2} I_1(2\widetilde{\omega}r_1 r)\, r^{2\mu} dr. \tag{3.37}$$

The derivation of the densities is demonstrated in Appendix C.

3.1.3 Ground States

The unique relationship between the wavefunction, and the particle density and the paramagnetic current density in CDFT applies only to ground states. Therefore, we must ensure that when we select a particular state for analysis, that state is a ground state. From Eq. (3.9) we can clearly see that for ground states, $N = M = 0$ for both systems. Similarly, Eq. (3.35) states that, for the ISI system, $n = 0$ in the ground state. However, the value of the angular momentum quantum number, m, is not so easy to determine. Figure 3.1 shows for both systems how the energy varies with the confinement frequency for several values of m. For any particular value of ω_0, the lowest-lying curve represents the ground state. For both systems, it can be seen that the curve, and therefore the value of m, corresponding to the ground state changes through the range of frequencies plotted. This change in m is an abrupt change between two consecutive values at particular "transition frequencies", where the values of the energy for m and $m+1$ are equal. When sweeping values of ω_0, with all other parameters constant, crossing a "transition frequency" means that the ground state value of m switches from one value of m to another, such that large values of $|m|$ are ground states at small confinement frequencies, and small values of $|m|$ are ground states at large confinement frequencies.

Since the ISI system can be solved analytically for all values of ω_0 (and ω_c), we can derive an expression for the points of intersection in Fig. 3.1(b) by considering the ground state energy, which is given by [83]

$$E_m = 2\widetilde{\omega}\left(1 + \frac{\omega_c}{4\widetilde{\omega}}m + \frac{1}{2}\sqrt{m^2+\alpha}\right). \tag{3.38}$$

The values of ω_0, or ω_c, at the points of intersection can be found by determin-

ing the frequencies where $E_m = E_{m+1}$,

$$
\begin{aligned}
2\widetilde{\omega}\left(1+\frac{\omega_c}{4\widetilde{\omega}}m+\frac{1}{2}\sqrt{m^2+\alpha}\right) &= 2\widetilde{\omega}\left(1+\frac{\omega_c}{4\widetilde{\omega}}(m+1)+\frac{1}{2}\sqrt{(m+1)^2+\alpha}\right), \\
\frac{\omega_c}{2\widetilde{\omega}}m+\sqrt{m^2+\alpha} &= \frac{\omega_c}{2\widetilde{\omega}}(m+1)+\sqrt{(m+1)^2+\alpha}, \\
\sqrt{m^2+\alpha} &= \frac{\omega_c}{2\widetilde{\omega}}+\sqrt{(m+1)^2+\alpha}, \\
\frac{\omega_c}{2\widetilde{\omega}} &= \left(\sqrt{m^2+\alpha}-\sqrt{(m+1)^2+\alpha}\right).
\end{aligned}
$$

By writing

$$
\Omega_{m,\alpha} = \sqrt{m^2+\alpha}-\sqrt{(m+1)^2+\alpha}, \tag{3.39}
$$

and using the definition of $\widetilde{\omega}$ from Eq. (3.7), we have

$$
\begin{aligned}
\frac{\omega_c^2}{\omega_c^2+4\omega_0^2} &= \Omega_{m,\alpha}^2, \\
\omega_c^2 &= \Omega_{m,\alpha}^2\omega_c^2+\Omega_{m,\alpha}^2 4\omega_0^2, \\
1 &= \Omega_{m,\alpha}^2+4\Omega_{m,\alpha}^2\frac{\omega_0^2}{\omega_c^2}.
\end{aligned}
$$

This gives the following expression for the relationship between ω_0 and ω_c when $E_m = E_{m+1}$,

$$
\left(\frac{\omega_0}{\omega_c}\right)^2 = \frac{1-\Omega_{m,\alpha}^2}{4\Omega_{m,\alpha}^2}. \tag{3.40}
$$

3.2 Varying the Confinement Potential

In Ref. [62], we concentrated on the sets of ground state wavefunctions, related particle densities, and related paramagnetic current densities to study the relationship between them at the core of CDFT. Since ground states are non-empty subsets of all states, ground-state-related functions form metric spaces with the metrics (2.18), (2.10), and (2.28). To produce families of ground states, for each system we systematically vary the value of ω_0 (while keeping all other parameters constant), and for each value we calculate the ground state wavefunction, particle density, and paramagnetic current density. A reference state is determined by choosing a specific ω_0 value, and the appropriate metric is then used to calculate the distances between it and each member of the family. To ensure that we select ground states, varying ω_0 may require varying the quantum number m [42, 83]. In Fig. 3.1, we see that as ω_0 increases, we must decrease the value of $|m|$ in order to remain in the ground state. As a result of this property, within each family of ground states, paramagnetic current den-

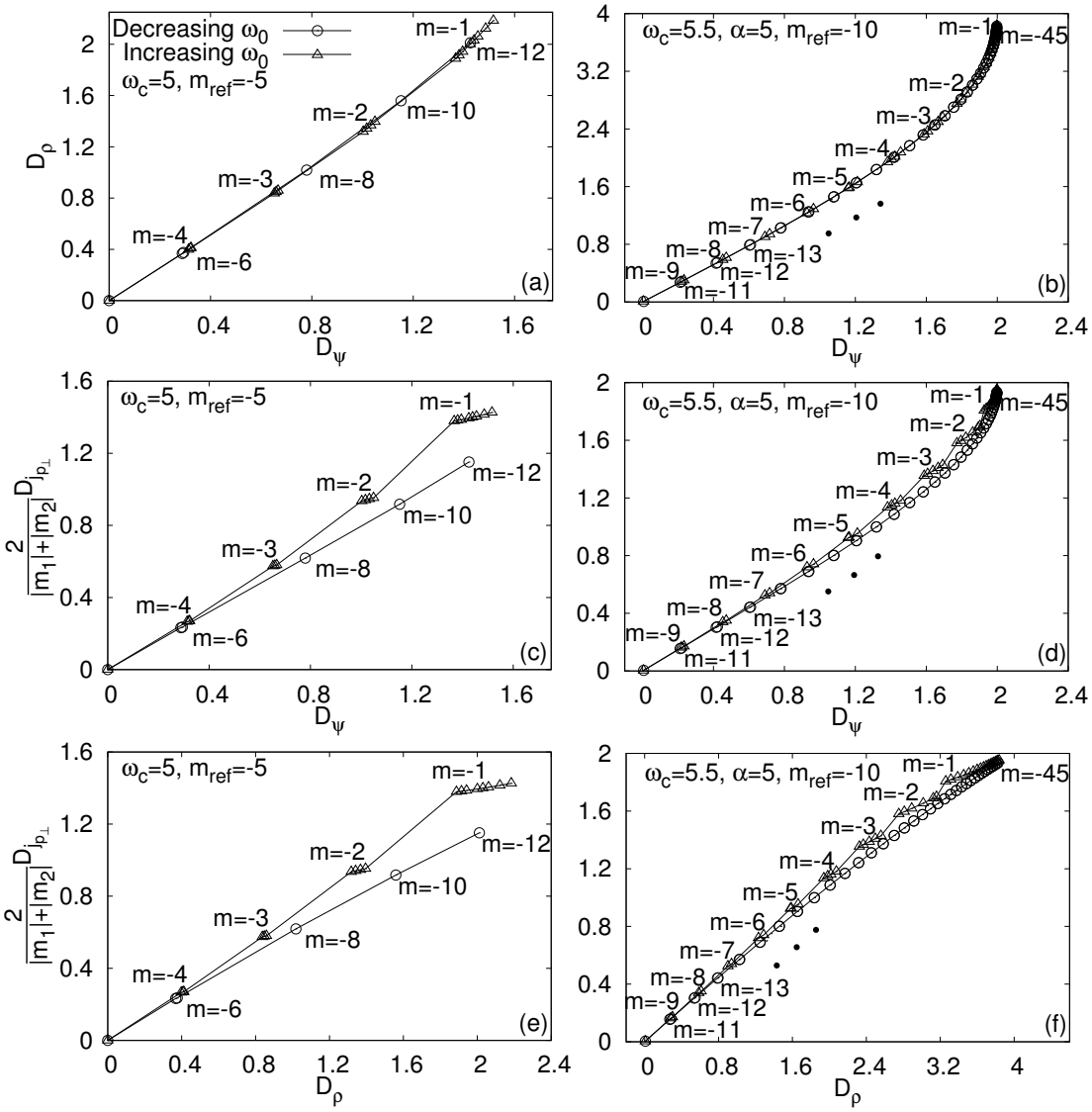

Figure 3.2: Results for ground states. Left: Hooke's atom (reference state $\omega_0 = 0.5, \omega_c = 5, m_{ref} = -5$). Right: ISI system (reference state $\omega_0 = 0.62, \omega_c = 5.5, \alpha = 5, m_{ref} = -10$). Panels (a) and (b): D_ρ vs D_ψ; (c) and (d): rescaled $D_{\mathbf{j}_{p_\perp}}$ vs D_ψ; (e) and (f): rescaled $D_{\mathbf{j}_{p_\perp}}$ vs D_ρ. Frequencies smaller than the reference are labelled with circles, larger with triangles.

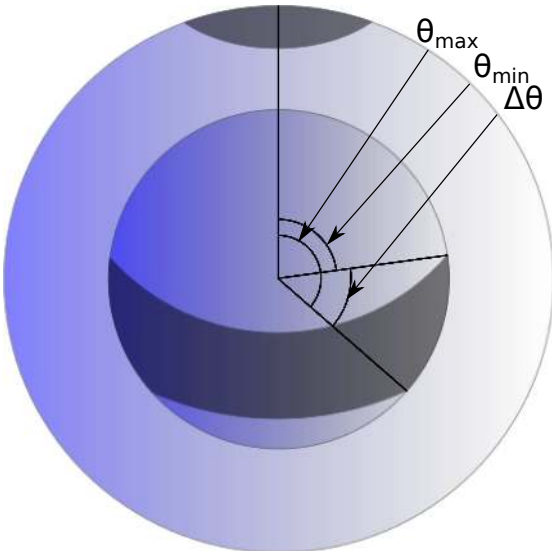

Figure 3.3: With reference to the "onion-shell" geometry of our metric spaces, we define the maximum and minimum angles between paramagnetic current densities on each sphere and the reference. We also define the difference between these angles as $\Delta\theta$.

sities will "jump" from one sphere of the onion-shell geometry to another (see Fig. 2.1, where the reference state is the "north pole" of its sphere). To obtain ground states with non-zero paramagnetic current densities, we must use ω_0 values corresponding to $m < 0$ [42, 83].

In Fig. 3.2, we plot the relationship between each pair of distances for the two systems. The reference states have been chosen so that most of the available distance range can be explored both for the case of increasing and for the case of decreasing values of ω_0. When considering the relationship between ground state wavefunctions and related particle densities, Figs. 3.2(a) and 3.2(b), our results confirm the findings in Ref. [58] (shown in Fig 1.1): a monotonic mapping, linear for low to intermediate distances, where nearby wavefunctions are mapped onto nearby particle densities, and distant wavefunctions are mapped onto distant particle densities, and the curves for increasing and decreasing ω_0 collapse onto each other. However closer inspection reveals a fundamental difference with Ref. [58], the presence of a "band structure." By this we mean regions of allowed ("bands") and forbidden ("gaps") distances, whose widths depend on the value of $|m|$, at least for the systems considered here. This structure is due to the changes in the value of the quantum number m, which result in a substantial modification of the ground state wavefunction (and therefore particle density) and a subsequent large increase in the related distances.

When we focus on the plots of paramagnetic current densities' against wavefunctions' distances, shown in Figs. 3.2(c) and 3.2(d), we find that the "band structure" dominates the behaviour. Here the change in $|m|$ has an even stronger

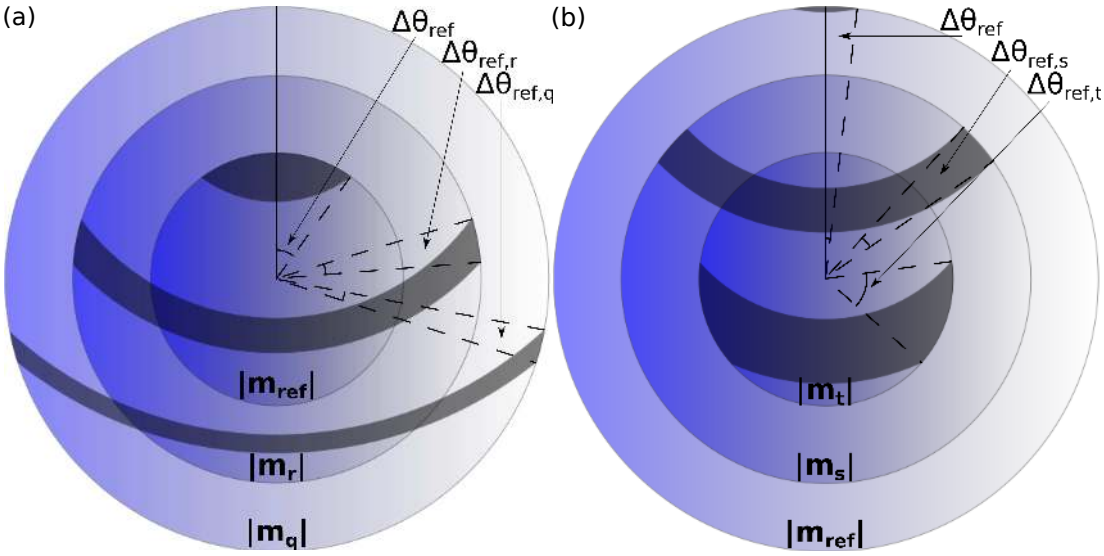

Figure 3.4: Sketch of the "onion-shell" geometry of the metric space for paramagnetic current densities, where: (a) $|m_q| > |m_r| > |m_{ref}|$ and (b) $|m_{ref}| > |m_s| > |m_t|$. The reference state is at the north pole on the reference sphere. The dark grey areas denote the regions where ground state currents are located ("bands"), with dashed lines indicating their widths. $m_{q,r,s,t}$ are arbitrary values of the quantum number m, such that $|m_q| > |m_r| > |m_{ref}| > |m_s| > |m_t|$.

effect, in that the gradient $dD_{\mathbf{j}_{p_\perp}}/dD_\psi$ is noticeably discontinuous when moving from one sphere to the next in $\mathbf{j}_p$ metric space. This discontinuity is more pronounced for the path $|m| < |m_{ref}|$ than for the path $|m| > |m_{ref}|$. Similarly to Figs. 3.2(a) and 3.2(b), the mapping of D_ψ onto $D_{\mathbf{j}_{p_\perp}}$ maps vicinities onto vicinities and remains monotonic, but for small and intermediate distances it is only piecewise linear. In contrast with D_ρ vs D_ψ, curves corresponding to increasing and decreasing ω_0 do not collapse onto each other.

Figures 3.2(e) and 3.2(f) show the mapping between particle and paramagnetic current density distances: this has characteristics similar to the one between D_ψ and $D_{\mathbf{j}_{p_\perp}}$, but remains piecewise linear even at large distances.

We will now concentrate on the $\mathbf{j}_p$ metric space to characterize the "band structure" observed in Fig. 3.2. Within the metric space geometry, we consider the polar angle θ between the reference $\mathbf{j}_{p_{ref}}$ and the paramagnetic current density $\mathbf{j}_p$ of angular momentum $|m|$. Using the law of cosines, θ is given by

$$\cos\theta = \frac{m_{ref}^2 + m^2 - D^2_{\mathbf{j}_{p_\perp}}(\mathbf{j}_{p_{ref}}, \mathbf{j}_p)}{2\,|m_{ref}|\,|m|}. \tag{3.41}$$

We define the polar angles corresponding to the two extremes of a given band as θ_{min} and θ_{max}, shown in Fig. 3.3. The width of each band is then $\Delta\theta = \theta_{max} - \theta_{min}$, and its position defined by θ_{min}. We will now calculate the widths and positions of the bands by sweeping the values of ω_0 corresponding to ground

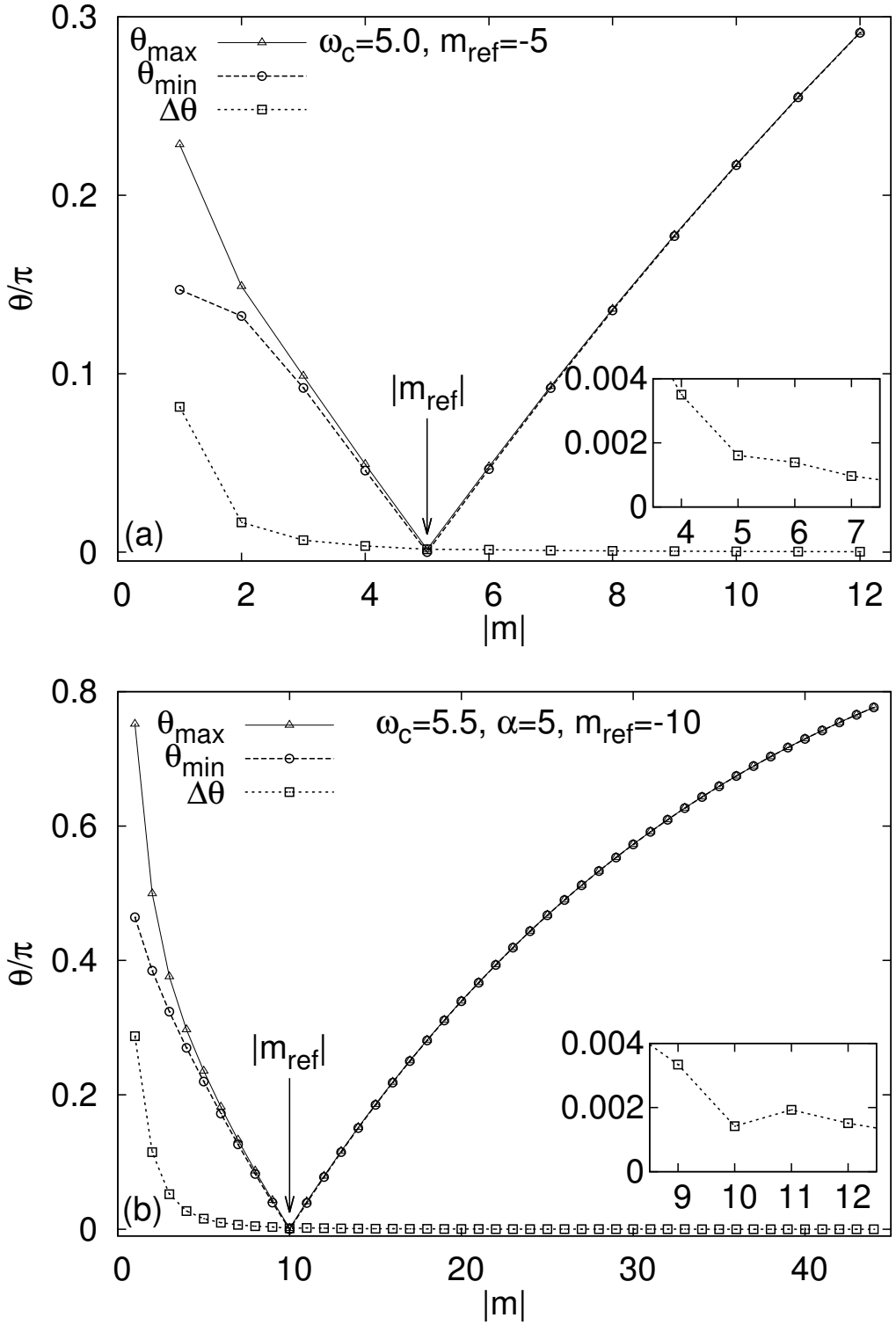

Figure 3.5: Results of the angular displacement of ground state currents for (a) Hooke's Atom and (b) the ISI system with the behaviour of $\Delta\theta$ close to the origin shown in the inset. Lines are a guide to the eye.

states for each value of $|m|$.

For both systems under study, we find that as $|m|$ increases from $|m_{ref}|$, both θ_{max} and θ_{min} increase. This has the effect of the bands moving from the north pole to the south pole as we move away from the reference. Additionally, we find that the bandwidth $\Delta\theta$ decreases as $|m|$ increases [sketched in Fig. 3.4(a)]. As $|m|$ decreases from $|m_{ref}|$, we again find that both θ_{max} and θ_{min} increase, with the bands moving from the north pole to the south pole. However, this time, as $|m|$ decreases, $\Delta\theta$ increases, meaning that the bands get wider as we move away from the reference [sketched in Fig. 3.4(b)].

Quantitative results for Hooke's Atom and the ISI system are shown in Fig. 3.5. The band on the surface of each sphere indicates where all ground state paramagnetic current densities lie within that sphere. In contrast with particle densities or wavefunctions, we find that, at least for the systems at hand, ground state currents populate a well-defined, limited region of each sphere, whose size and position display monotonic behaviour with respect to the quantum number m. This regular behaviour is not at all expected, as the CDFT-HK theorem does not guarantee monotonicity in metric space, and not even that the mapping of D_ψ to $D_{\mathbf{j}_{p_\perp}}$ is single valued. In the CDFT-HK theorem ground state wavefunctions are uniquely determined only by particle and paramagnetic current densities *together*. In this sense we can look at the panels in Fig. 3.2 as projections on the axis planes of a 3-dimensional $D_\psi D_\rho D_{\mathbf{j}_{p_\perp}}$ relation. The complexity of the mapping due to the application of a magnetic field – the changes in quantum number m – is fully captured by $D_{\mathbf{j}_{p_\perp}}$ only, as this is related to the relevant conservation law. However the mapping from D_ρ to D_ψ inherits the "band structure," showing that the two mappings $D_{\mathbf{j}_{p_\perp}}$ to D_ψ and D_ρ to D_ψ are not independent.

3.3 Varying the Electron Interaction

As well as the confining potential, the interaction between the electrons also contributes to the potential energy of our model systems. For the ISI system, the parameter α allows us to vary the strength of the electronic interaction, hence we can repeat the analysis of the CDFT-HK theorem in Sec. 3.2 for the case of varying α. Additionally, $|m|$ for the ground state increases as α increases, in contrast to the decrease in the ground state value of $|m|$ shown in Fig. 3.1 for ω_0.

Figure 3.6 shows plots of each pair of distances. As was the case for Fig 3.2, all of the plots show a "band structure" corresponding to the value of the angu-

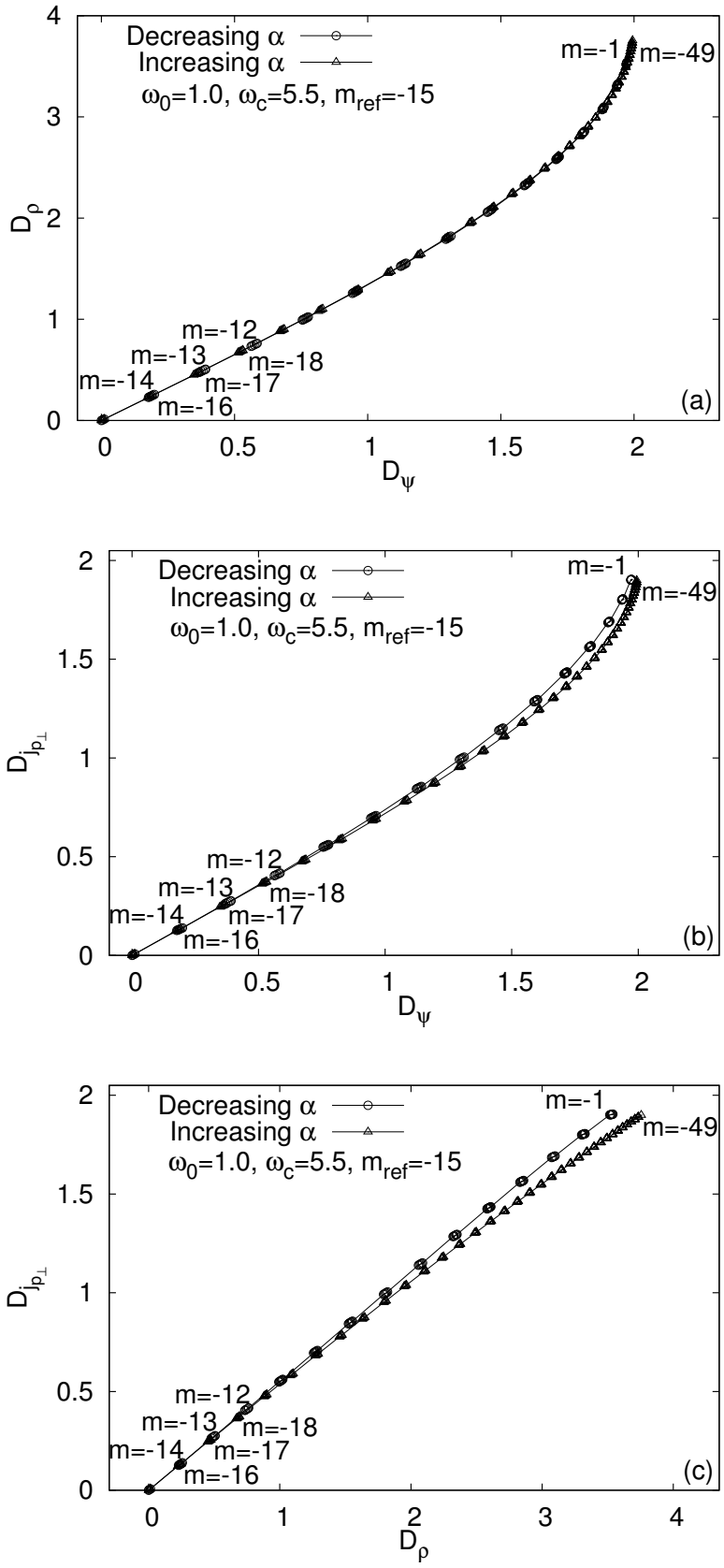

Figure 3.6: Results for ground states for the ISI system when varying α (reference state $\omega_0 = 1.0, \omega_c = 5.5, \alpha = 29.756, m_{ref} = -15$). The reference value of α is taken halfway between the two "transition frequencies" related to m_{ref}. Panel (a): D_ρ vs D_ψ; (b): rescaled $D_{\mathbf{j}_{p_\perp}}$ vs D_ψ; (c): rescaled $D_{\mathbf{j}_{p_\perp}}$ vs D_ρ. Values of α smaller than the reference are labeled with circles, larger with triangles.

lar momentum quantum number m, that consists of "bands" of distances for each particular value of m separated by "gaps" of forbidden distances. When considering D_ρ against D_ψ [Fig. 3.6(a)], the path traced out by the curve is almost identical to that in Fig. 3.2, and again depicts a monotonic relationship between D_ρ and D_ψ which is almost linear for small to intermediate distances and follows the same curve for the cases of increasing α and decreasing α. Figures 3.6(b) and 3.6(c) show that, as before, the "band structure" causes discontinuities in the gradient when we introduce the paramagnetic current density. However, in contrast to Fig. 3.2, the discontinuity in the gradient between "bands" is considerably less pronounced, and also as $|m|$ decreases, the bands cover a smaller range of distances. Comparison of the results for both systems in Fig. 3.2 and Fig. 3.6 suggests that as the reference value of $|m|$ becomes larger, the discontinuity in the gradient between bands is reduced. A consequence of the less pronounced discontinuity is that the curves for increasing and decreasing α are more similar than those for increasing and decreasing ω_0.

Figure 3.7 shows the angular displacement of the bands on each of their metric space spheres for the paramagnetic current density. As for the case of varying ω_0, we observe that the bands move from the north pole to the south pole as we depart from m_{ref}, and that the bands get narrower as $|m|$ increases. However, we note that the width of the bands, particularly for small values of $|m|$, are considerably smaller compared to those in Fig. 3.5. Consequently, the bandwidth is plotted in Fig. 3.7(b), in which we observe that the width of the band for m_{ref} is considerably smaller than the bands corresponding to all nearby values of m. We suggest that this is an artifact of the arbitrary choice of our reference, especially given that the shape of the reference band is different from all of the others, as depicted in Fig. 3.4. Comparing with the case of varying ω_0, the insets of Fig. 3.5 show a similar decrease in the bandwidth for the ISI system, but not for Hooke's Atom (albeit we do observe a discontinuity in the gradient of the overall decrease in $\Delta\theta$).

In conclusion, we find that the metric space approach to quantum mechanics offers considerable insight into the mapping at the core of CDFT. The mapping between the fundamental quantities in CDFT inherits the features observed for standard DFT. However, varying the potential energy through either the confinement potential or the strength of the electronic interaction introduces a "band structure" into the ground state metric spaces for wavefunctions, particle densities and paramagnetic current densities; a feature that is entirely absent when a magnetic field is not present. The origin of the "band structures" is changes in the value of the quantum number for the angular momentum, m, and the value of $|m|$ is shown to control the shape of the "bands".

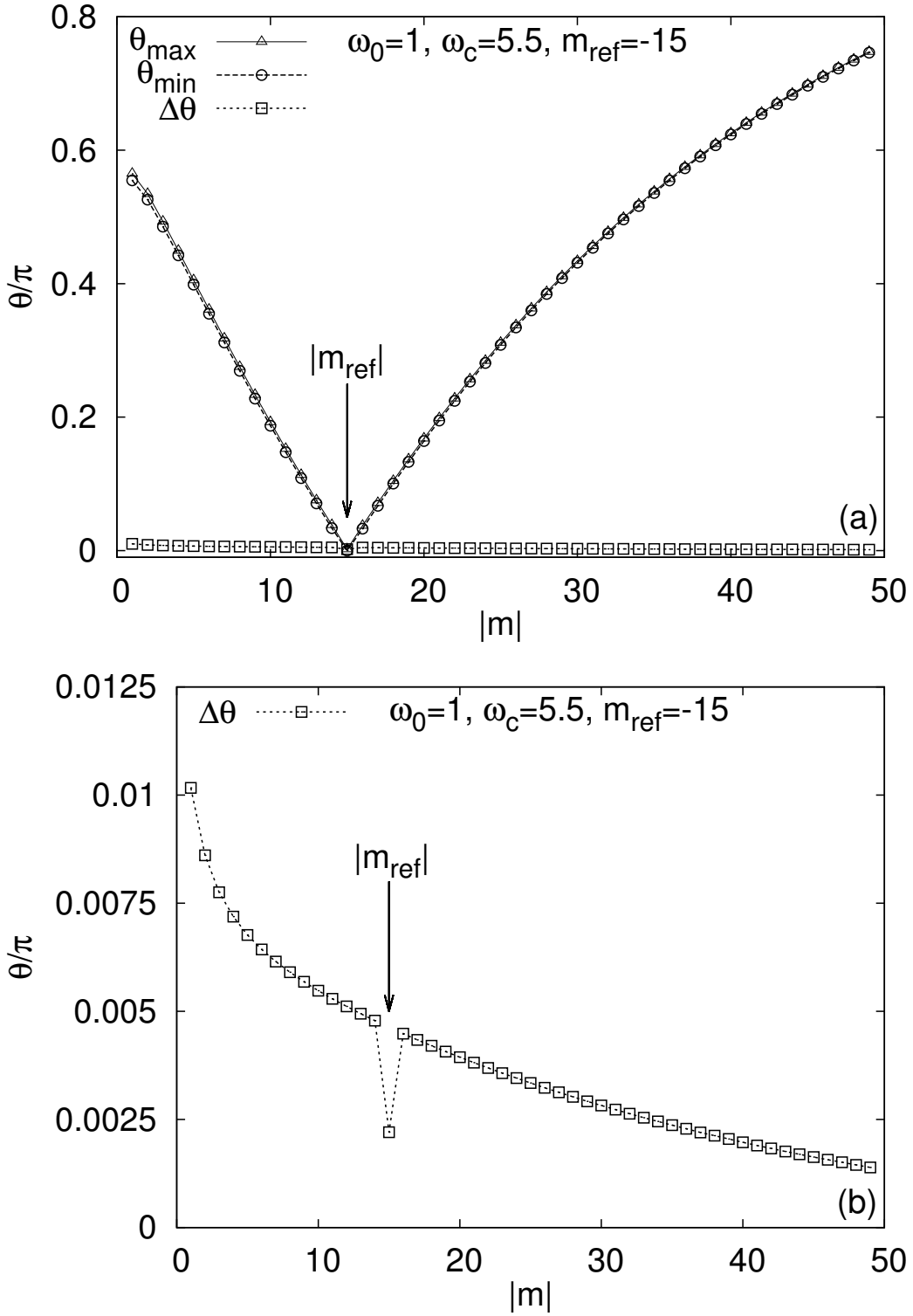

Figure 3.7: Results of the angular displacement of ground state currents when varying α for the ISI system. Panel (a) shows θ_{max}, θ_{min} and $\Delta\theta$, and we focus on $\Delta\theta$ in panel (b). Lines are a guide to the eye.

Chapter 4

Exploring the Effects of Varying Magnetic Fields With the Metric Space Approach

In Chapter 3, we have shown the effect of changes in the scalar and electronic interaction potentials on the wavefunction, particle density and paramagnetic current density, and their unique relationship for ground states, as defined in CDFT. However, a quantity far more amenable to varying experimentally is the strength of the magnetic field itself. Systems immersed in magnetic fields are subject to a vector potential, $\mathbf{A}(\mathbf{r})$, which represents the magnetic field in the Hamiltonian (1.5). Hence, by exploring changes in this vector potential, we can use the metric space approach to quantum mechanics to study systems subject to a magnetic field as the field changes.

Systems immersed in magnetic fields are a fundamental research topic, for example, atoms immersed in strong fields [84, 85], and phenomena such as nuclear magnetic resonance [86] and the quantum hall effect [87]; and are also an integral part of emerging quantum technologies such as quantum computation which utilise quantum systems controlled or otherwise affected by magnetic fields. For example the inhomogeneous magnetic field generated by the nuclei's spins decreases quantum coherence of electron spin qubits in III-V quantum dots [88], while full polarisation of the spin bath through an applied magnetic field suppresses electron-spin decoherence in nitrogen-vacancy centres and nitrogen impurities in diamond [89]. Understanding systems immersed in a magnetic field at a quantum level is therefore both of fundamental and technological importance.

Varying the strength of the magnetic field for ground state systems will allow us to enhance the insights into the fundamental relationship between the ba-

sic variables of CDFT provided by the results in Chapter 3. In particular, in the presence of a magnetic field, the metric spaces for ground state wavefunctions, particle densities and paramagnetic current densities are characterised by a "band structure" [62]. In paramagnetic current density metric space, when considering variations in the scalar potential [62], the "band structure" is formed by spherical segments of *allowed* and *forbidden* distances on the concentric spheres, at least for the systems analysed. The specific arc length of these segments varies depending on the radius $|m|$ of the sphere. The "band structure" of allowed and forbidden distances also presents itself in the metric spaces for wavefunctions and particle densities, but only on a single sphere in these cases. We will investigate how this "band structure" responds to changes in the magnetic field.

One of the key strengths of the metric space approach to quantum mechanics is that it can easily be applied to excited states as well as ground states, which makes the approach a widely applicable tool for the study of many-body systems. We will then study the relationship between the wavefunction, particle density and paramagnetic current density for excited states when varying the magnetic field, and compare and contrast the results with those for ground states.

The results in this chapter were published in Ref. [63].

4.1 Ground States

4.1.1 Ground States of Model Systems

We again focus on the model systems employed in Chapter 3: the magnetic Hooke's Atom and the Inverse Square Interaction (ISI) system [42, 75, 83]. We vary the strength of the magnetic field via the cyclotron frequency, ω_c. Once again, we must ensure that the value of the angular momentum quantum number m is such that we are in the ground state for all values of ω_c.

Figure 4.1 shows how the energy varies with the cyclotron frequency for several values of m, with the lowest-lying curve representing the ground state, as in Fig. 3.1. As was the case for the confinement frequency, Fig. 4.1 shows that the ground state value of m changes as we sweep through the values of ω_c, with abrupt changes in the ground state value of m at "transition frequencies". However, there is one significant difference which is that when varying ω_c, the value of $|m|$ for the ground state *increases* as ω_c increases. This difference indicates that the relationship between the basic variables in CDFT may differ as

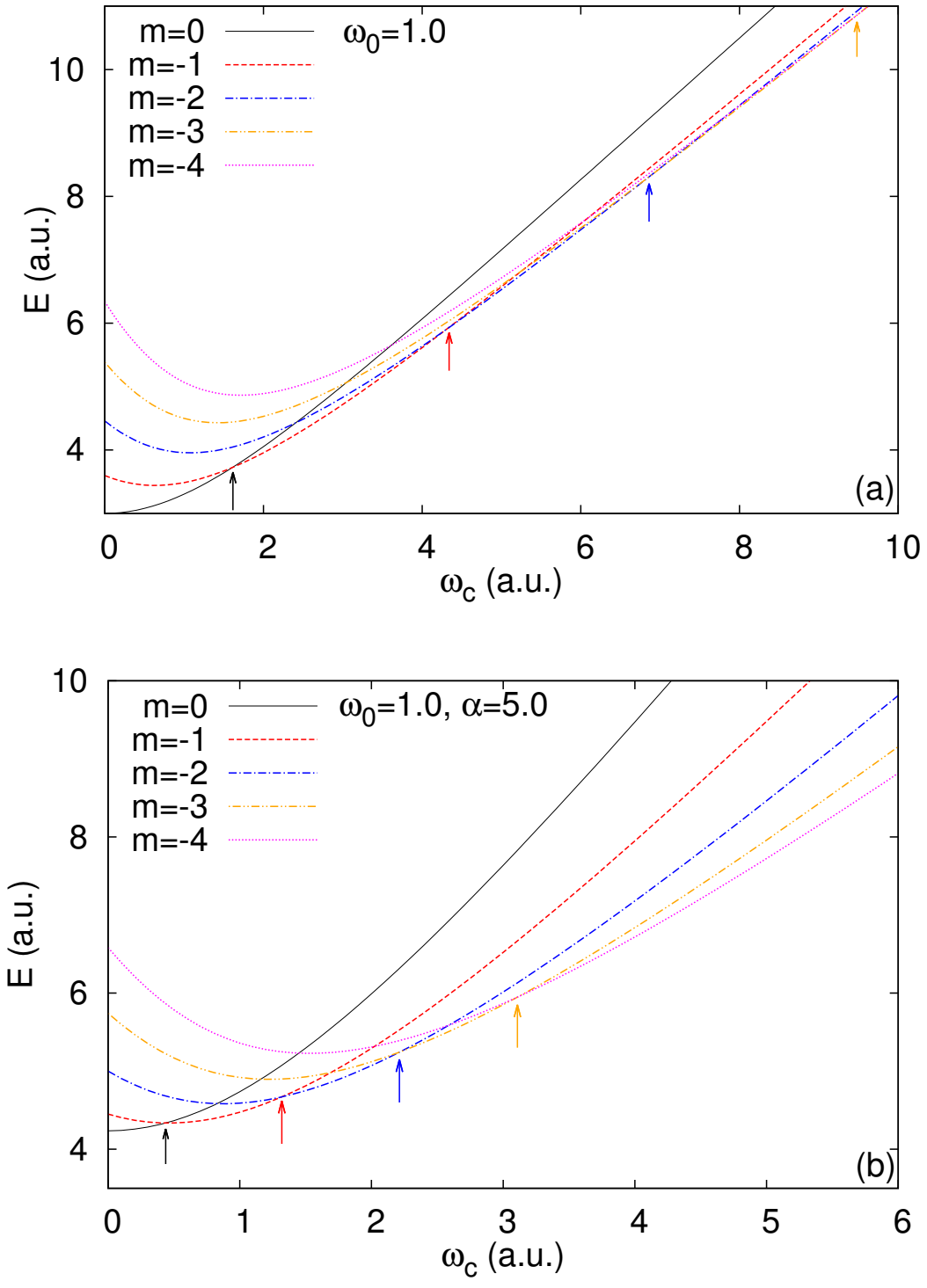

Figure 4.1: Energy is plotted against the cyclotron frequency for several values of m for (a) Magnetic Hooke's Atom and (b) the ISI system. The confinement frequency and interaction strength are held constant. Arrows indicate where the value of m for the ground state changes.

we vary the vector potential compared to varying the scalar potential.

As in Chapter 3, we generate families of states, this time by varying the magnetic field via the cyclotron frequency ω_c, whilst holding the confinement frequency, ω_0, and all other parameters in the Hamiltonian constant. Within each family, one value of ω_c (and hence m) is selected as a reference ($\omega_{c_{ref}}, m_{ref}$ respectively), with the appropriate metrics used to find the distance between the physical functions at the reference and all of the others in the family.

4.1.2 Band Structure of Metric Spaces

We will start by comparing the distances between wavefunctions, their related particle densities and their related paramagnetic current densities. Figure 4.2 shows plots of the relationships between the various distances considered, with each point referring to a particular value of ω_c. Let us consider first the plots of particle density distance against wavefunction distance [Figs. 4.2(a) - 4.2(d)]. As observed in Chapter 3, metric space regions corresponding to ground states present a "band structure", where points associated to the same value of $|m|$ are grouped into distinct segments, i.e., bands. However, in contrast to the band structure observed in Chapter 3 [sketched in Fig. 4.3(a)], when varying the vector potential we obtain a series of "overlapping bands", where the minimum wavefunction and minimum particle density distances for one value of $|m|$ are smaller than the maximum distances for the previous value of $|m|$. This implies that there is now an overlap between the projections of the bands on the metric space sphere representing the densities, as sketched in Fig. 4.3(b) (similarly for the projection on the sphere representing the wavefunctions). Though overlapping, this band structure still results in discontinuities in the relationship between D_ρ and D_ψ when the value of m changes. Unlike when varying ω_0 [62], by varying the magnetic field we do not observe any forbidden distances, so we cannot identify forbidden regions for ground states by considering the density and wavefunction metric spaces alone. In the range of distances explored here, nearby wavefunctions are mapped onto nearby particle densities and distant wavefunctions are mapped onto distant particle densities. However, in contrast to Chapter 3, the mapping is only piecewise linear; when acting on the vector potential, as ω_c is swept through each "transition" frequency, ground states and their densities abruptly revert to be closer to the reference state, while a (almost) linear mapping is maintained within two consecutive "transition" frequencies. Also, in contrast with the results in Chapter 3, the two families of ground states corresponding to $|m| < |m_{ref}|$ and $|m| > |m_{ref}|$ describe distinct paths in metric space [e.g., com-

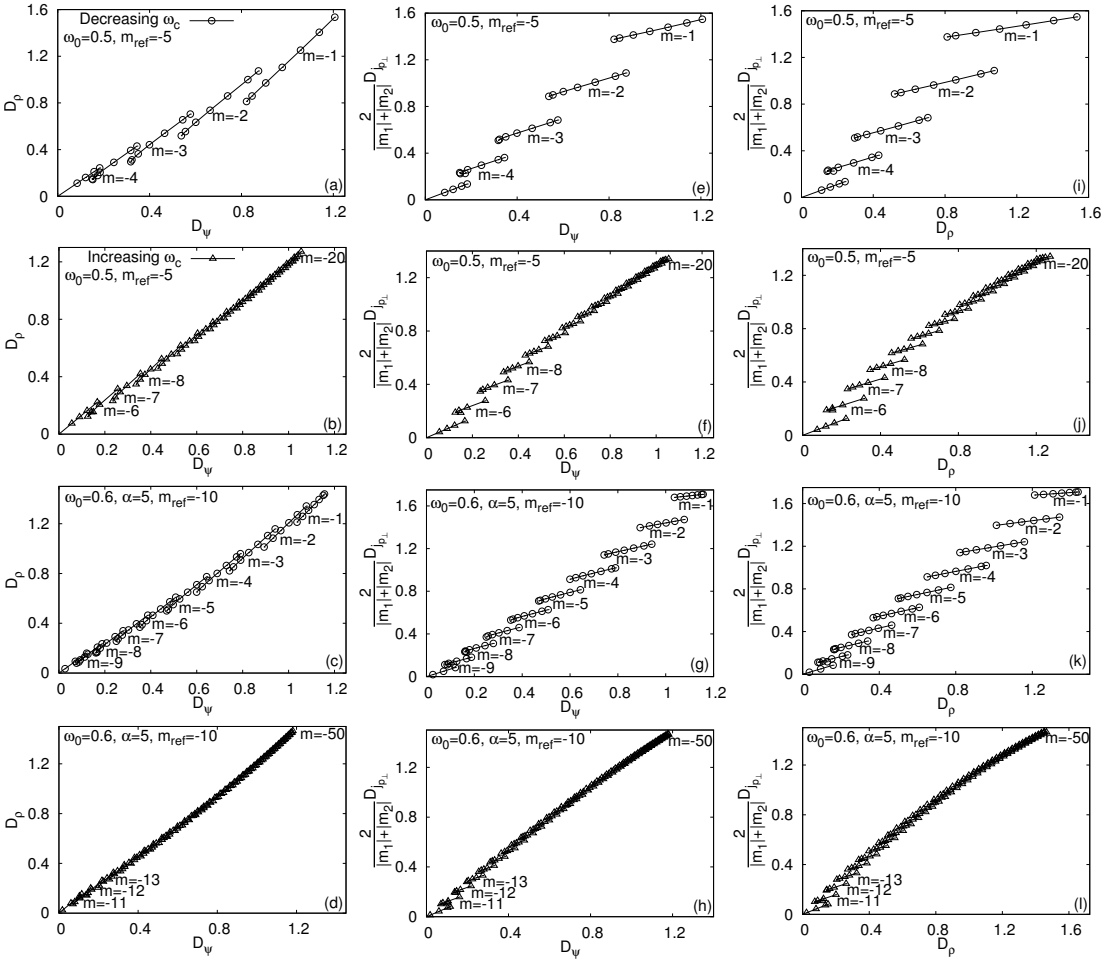

Figure 4.2: Plots of distances for Hooke's Atom with reference state $\omega_0 = 0.5, \omega_c = 5.238, m_{ref} = -5$ (top two rows) and for the ISI system with reference state $\omega_0 = 0.6, \omega_c = 5.36, \alpha = 5, m_{ref} = -10$ (bottom two rows). (a) - (d) show particle density distance against wavefunction distance, (e) - (h) show paramagnetic current density distance against wavefunction distance and (i) - (l) show paramagnetic current density distance against particle density distance. The reference frequency is taken halfway between the two "transition frequencies" related to m_{ref}.

pare Figs. 4.2(a) and 4.2(b)], with the size of the bands greater for $|m| < |m_{ref}|$ compared to $|m| > |m_{ref}|$. For all of these reasons the CDFT-HK mapping between wavefunctions and related densities acquires added complexity when varying the vector potential compared to varying the scalar potential [compare Figs. 3.2(a) and 3.2(b) with Figs. 4.2(a) - 4.2(d)].

In Figs. 4.2(e) - 4.2(h) we consider paramagnetic current density distance against wavefunction distance. Here we find once more an overlapping band structure for wavefunction distances, however a band structure with regions of allowed ("bands") and forbidden ("gaps") distances is observed for paramagnetic current density distances. In contrast with the one sketched in Fig. 4.3(a), in this case each band resides on a different sphere according to the value of $|m|$ (the

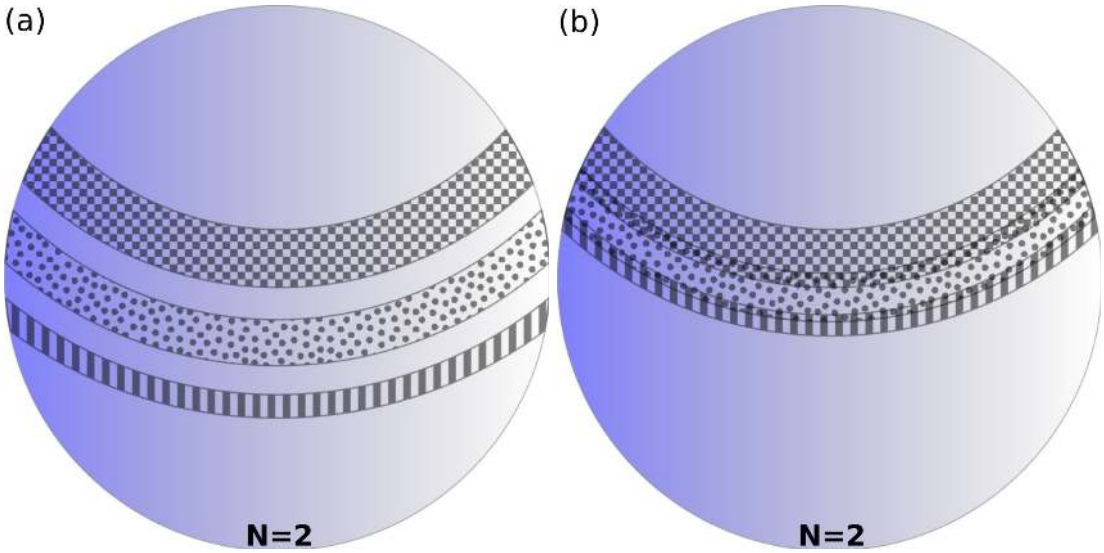

Figure 4.3: Sketches of "band structures" consisting of (a) "bands" and "gaps" and (b) "overlapping bands" in particle density metric space for three consecutive bands, where a different patterning corresponds to a different value of m. The reference state is at the north pole.

radius of the sphere). For both wavefunction and paramagnetic current density distances, there are discontinuities between the bands. As for Figs. 4.2(a) - 4.2(d), the curves for increasing and decreasing ω_c (and hence $|m|$) do not overlap, with larger bands for small values of $|m|$. Finally Figs. 4.2(i) - 4.2(l) present the plots of paramagnetic current density distance against particle density distance. These exhibit similar behaviour to Figs. 4.2(e) - 4.2(h).

The overlapping band structures observed in Fig. 4.2 demonstrate that mappings between some of the distances considered here are multivalued. This multivalued mapping does *not* represent a contradiction of the CDFT-HK theorem as it is entirely possible to have distinct functions at the same distance away from a reference. In particular, in terms of the "onion-shell" geometry, all states situated at the same polar angle and on the same sphere will have the same distance from the reference state.

In Fig. 4.4 the wavefunction and paramagnetic current density distances are plotted against ω_c for both systems, enabling the band structures for individual functions to be analysed. We firstly note that, as observed in Fig. 4.2, there is a decrease in the wavefunction distance at transitions [Figs. 4.4(a) and 4.4(b)], but an increase in the paramagnetic current density distance [Figs. 4.4(c) and 4.4(d)]. These features give rise to "overlapping bands" and "bands and gaps" band structures respectively. The other major feature is that, when varying ω_c, there is non-monotonic behaviour within bands corresponding to values of m close to m_{ref} (see insets). For both wavefunctions and paramagnetic cur-

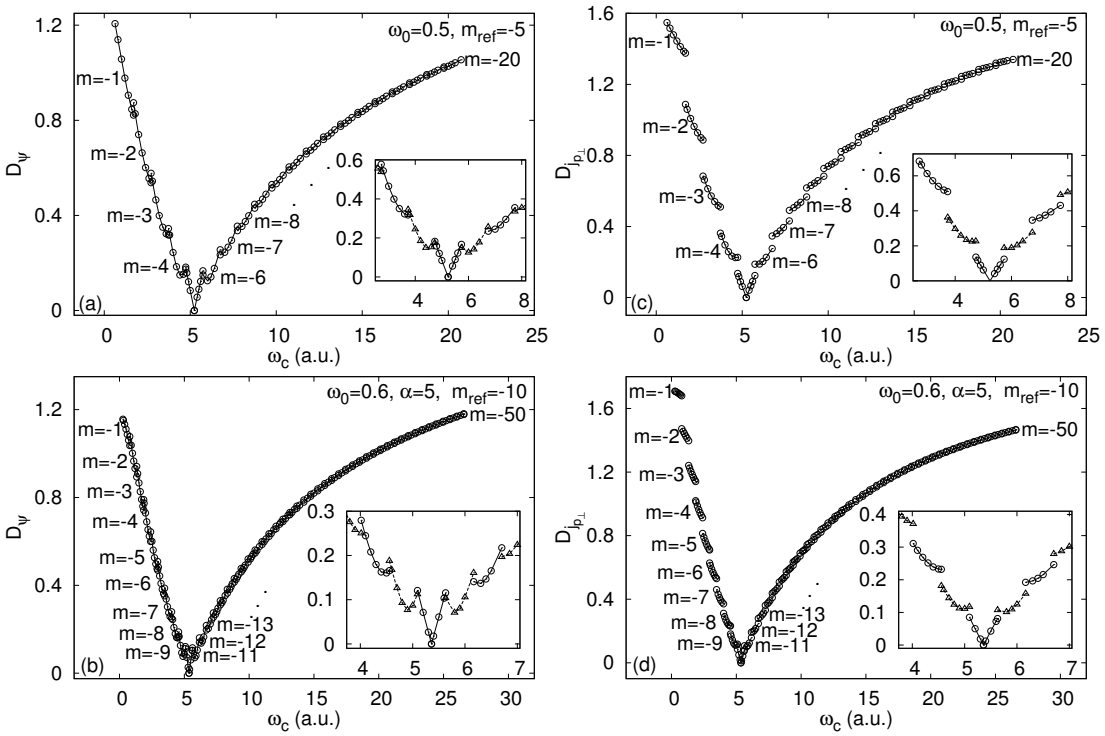

Figure 4.4: For Hooke's Atom (top) and the ISI system (bottom), wavefunction distance [(a) and (b)] and paramagnetic current density distance [(c) and (d)] are plotted against ω_c. The behaviour around the reference frequency is shown in each inset. The reference states are $\omega_0 = 0.5, \omega_{c_{ref}} = 5.238, m_{ref} = -5$ for the Magnetic Hooke's Atom and $\omega_0 = 0.6, \omega_{c_{ref}} = 5.36, \alpha = 5, m_{ref} = -10$ for the ISI system.

rent densities, we observe that immediately after each transition frequency, the distances initially decrease to a minimum for that particular band, before increasing to the maximum for the band. This occurs at the transition frequency to the next band. This behaviour is more pronounced for wavefunctions than for paramagnetic current densities. As stated, the non-monotonicity is not in contradiction with the Hohenberg-Kohn theorem of CDFT, but shows a richer behaviour with respect to what was observed in Chapter 3 when varying the scalar potential.

We point out that the band structure in metric space for paramagnetic current density is fundamentally different from the ones for particle density and wavefunction, as the first develops on different spheres, one band for each sphere, while the latter are within a single sphere where they may display "distinct" or "overlapping" bands, see Fig. 4.3. All these band structures originate from the conservation law characterising the paramagnetic current density, and the features of the metric spaces for wavefunctions and particle densities are a direct consequence of the mapping of $\mathbf{j}_p(\mathbf{r})$ onto $\psi(\mathbf{r})$ and onto $\rho(\mathbf{r})$. In this sense the band structure features of the metric spaces for wavefunctions and particle

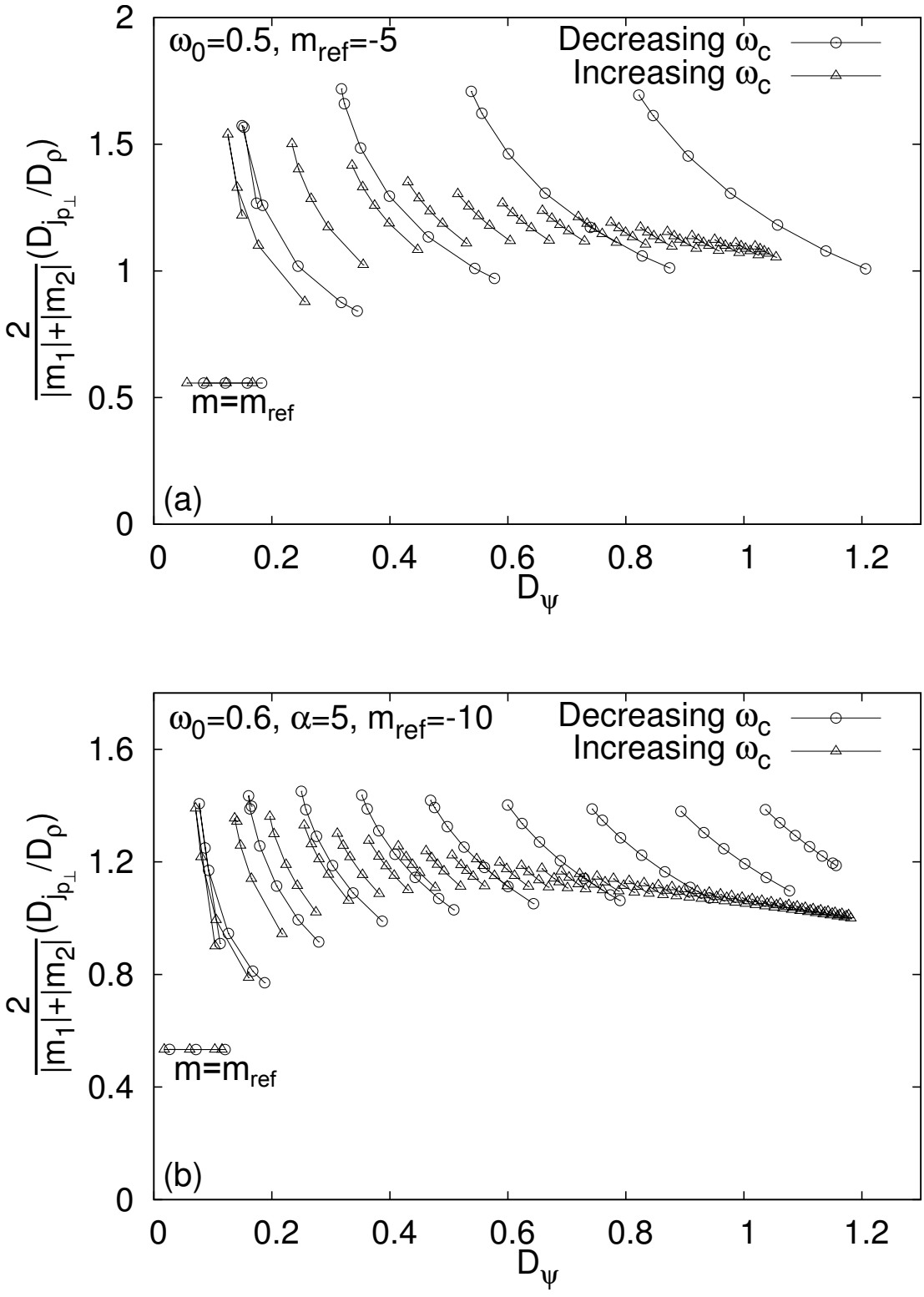

Figure 4.5: Plots of the ratio of paramagnetic current density distance to particle density distance against wavefunction distance for (a) Magnetic Hooke's Atom with reference state $\omega_0 = 0.5, \omega_{c_{ref}} = 5.238, m_{ref} = -5$, and (b) the ISI system with reference state $\omega_0 = 0.6, \omega_{c_{ref}} = 5.36, \alpha = 5, m_{ref} = -10$.

densities could be seen merely as the "projections" of the band structure characterising the paramagnetic current density, that result from these mappings.

Finally, we wish to concentrate on the implications of our findings for CDFT. CDFT requires that both $\rho(\mathbf{r})$ and $\mathbf{j}_p(\mathbf{r})$ are taken together to ensure a one-to-one mapping to the wavefunction. The metric analysis allows us to provide evidence for an important aspect of this mapping, that is to understand the relative contributions of $\rho(\mathbf{r})$ and $\mathbf{j}_p(\mathbf{r})$ when mapping to the wavefunction, which may provide insight as to when the inclusion of $\mathbf{j}_p(\mathbf{r})$ in the mapping becomes really crucial for the one-to-one correspondence to hold.

We present in Fig. 4.5 the ratio $D_{\mathbf{j}_{p_\perp}}/D_\rho$ against D_ψ for both the Magnetic Hooke's atom and the ISI system. From the data it is immediately clear that, in metric space, to a good level of approximation, $D_{\mathbf{j}_{p_\perp}} = const \times D_\rho$ as long as $m = m_{ref}$. This constant is the same for $\omega_c > \omega_{c_{ref}}$ and $\omega_c < \omega_{c_{ref}}$. These findings suggest that, at least for the systems at hand, as long as we remain on the *same sphere* in the paramagnetic current density metric space, $\mathbf{j}_p(\mathbf{r})$ and $\rho(\mathbf{r})$ carry very similar information and the role of $\mathbf{j}_p(\mathbf{r})$ in the core mapping of CDFT is secondary. The situation becomes very different for ground states with $m \neq m_{ref}$. In this case the ratio $D_{\mathbf{j}_{p_\perp}}/D_\rho$ is far from constant and Fig. 4.5 clearly shows that the information contents of $\mathbf{j}_p(\mathbf{r})$ and $\rho(\mathbf{r})$ are both necessary to define the state.

To support these results, we will analyse in the next section the behaviour of states where m is kept equal to m_{ref} at all values of ω_c.

4.2 Excited States

Although an understanding of the ground state is important, for studying systems subject to magnetic fields it is often necessary to go beyond ground states, for example, when studying rapidly varying fields or spintronic devices that operate with excited states. With the metrics at hand, we investigate for the first time excited states, and consider distances between families of states corresponding to fixed values of m.[1] For each value of m, we will construct a family of states by varying ω_c (with ω_0 and α kept constant), and calculating the corresponding wavefunctions, particle densities and paramagnetic current densities. As for ground states, we choose $m < 0$. With respect to Fig. 4.1, this corresponds to following individual energy curves smoothly, i.e., without switching to a different curve at crossings, as done for the ground state case. Each family of states will then lie on a particular sphere in the paramag-

[1] The centre of mass quantum number, M, is held constant at zero throughout this analysis.

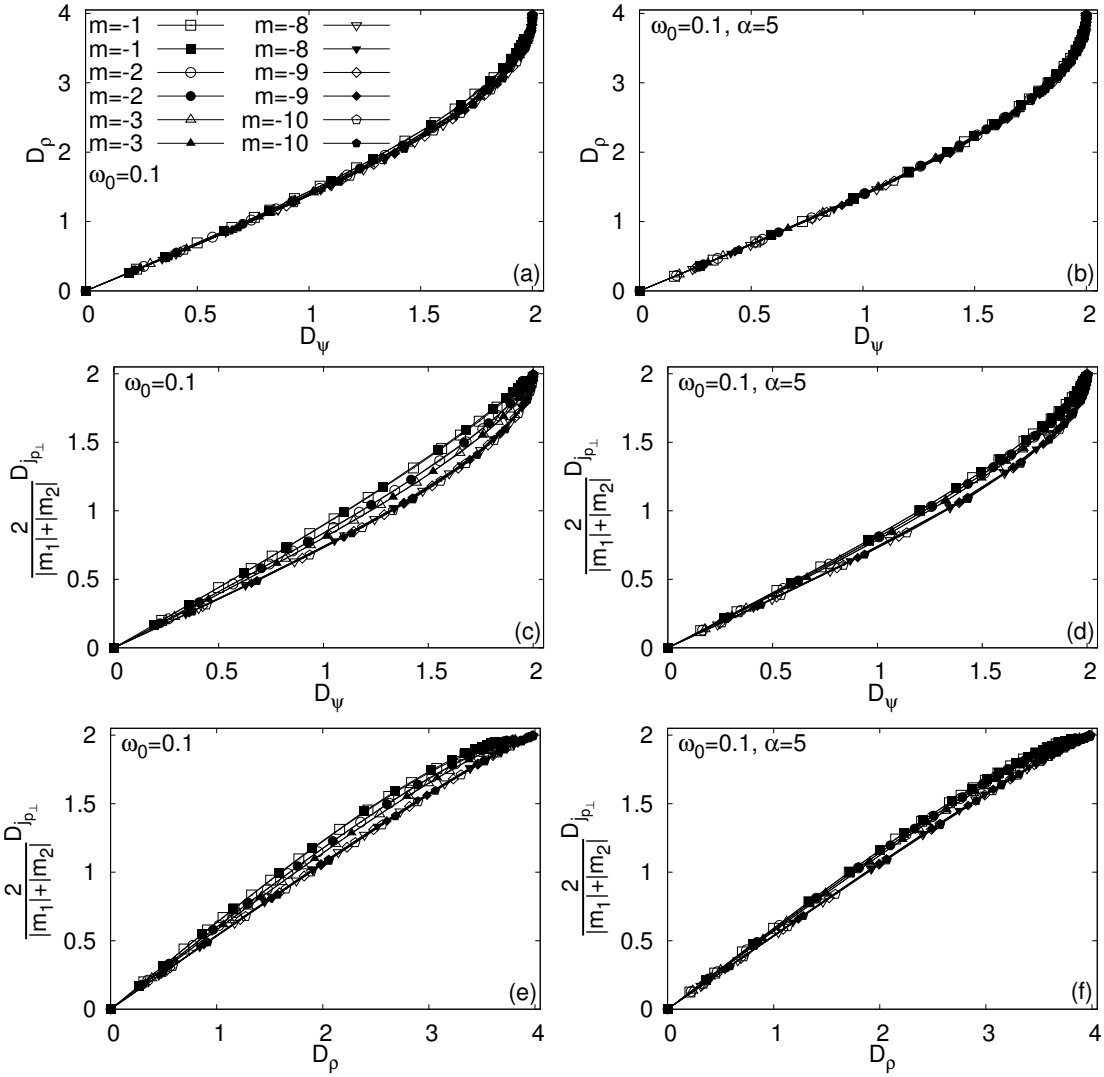

Figure 4.6: Plots of: (a) and (b) particle density distance against wavefunction distance, (c) and (d) paramagnetic current density distance against wavefunction distance, (e) and (f) paramagnetic current density distance against particle density distance for $m = -1, -2, -3, -8, -9, -10$. The reference states, for each value of m, are: For Hooke's Atom (left) $\omega_0 = 0.1, \omega_{c_{ref}} = 30.0$, and for the ISI system (right), $\omega_0 = 0.1, \omega_{c_{ref}} = 5.0, \alpha = 5$. Closed symbols represent decreasing ω_c and open symbols represent increasing ω_c.

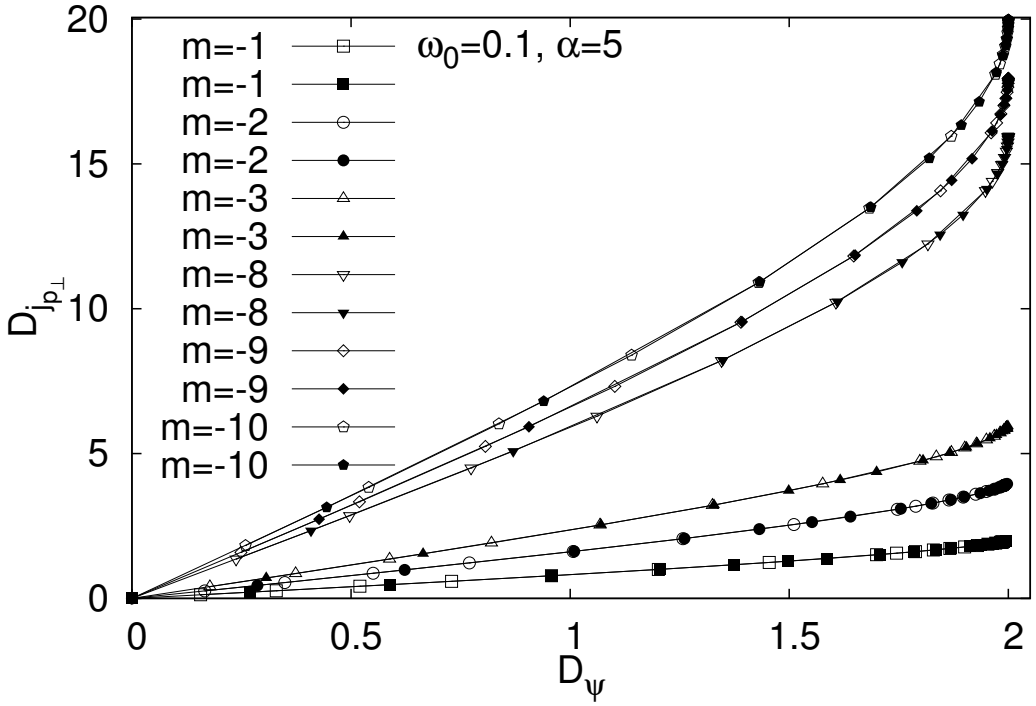

Figure 4.7: Plot of paramagnetic current density distance against wavefunction distance for $m = -1, -2, -3, -8, -9, -10$ for the ISI system. We take the state with $\omega_0 = 0.1, \omega_{c_{ref}} = 5.0, \alpha = 5$ as a reference for each value of m and consider distances across the surface of each individual sphere.

netic current density metric space. As the states considered are not necessarily ground states, there is no one-to-one mapping between the wavefunction and particle and paramagnetic current densities, but, these being fundamental quantities that characterise the system, we will still explore their relationships. Additionally, the study of these quantities allows us to corroborate the findings related to Fig. 4.5.

Fig. 4.6 shows the relationship between each pair of distances for six different values of m. For each pair of distances discussed, we find a monotonic relationship that is linear in the low to intermediate distance regime, before one of the two functions rises more sharply to its maximum (see also Fig. 4.7). The mapping between the each of the three physical functions considered is such that nearby functions are mapped onto nearby functions and distant functions are mapped onto distant functions for each function set. Crucially, as opposed to ground states, the distances do not form any kind of metric space "band structure" – confirming that the origin of band structures is changes in m.

Looking at wavefunction distances against particle density distances, Figs. 4.6(a) and 4.6(b), and contrasting with Figs. 4.2(a)-4.2(d), we observe that the curves

for increasing and decreasing ω_c and all values of $|m|$ collapse onto one another. This hints to a universal behaviour of the mapping between particle density and wavefunction when all the physical quantities describing the system remain on the same sphere in the related metric space whilst a physical parameter is smoothly changed.

When considering paramagnetic current density distance against wavefunction distance in Figs. 4.6(c) and 4.6(d), although the curves for increasing and decreasing ω_c collapse onto one another, the curves for different values of m are *distinct*, particularly when $|m|$ is low. For lower values of $|m|$ the linear region extends across a larger range of distances. There is also a relatively small increase in the gradient at greater distances for low $|m|$. The curves in Figs. 4.6(c) and 4.6(d) all start and end at the same points. With the rescaling for $D_{\mathbf{j}_{p_\perp}}$ used in Fig. 4.6, the curves tend to a limiting curve with increasing value of $|m|$. In Fig. 4.7, we show the relationship between wavefunction distance and paramagnetic current density distance for the ISI system without rescaling $D_{\mathbf{j}_{p_\perp}}$. Here, the curves for each value of $|m|$ intersect only at the origin, and each has a unique maximum of $2|m|$ for the paramagnetic current density distance. We observe that the gradient of the initial linear region increases with $|m|$. Figure 4.8 shows, for both systems, that the gradient in this region increases linearly with $|m|$, $D_{\mathbf{j}_{p_\perp}} \approx k|m| D_\psi$, with $k \approx 0.69$ for Hooke's Atom and $k \approx 0.68$ for the ISI system, and is approximately equal for both decreasing and increasing ω_c. These results imply that when rescaled as in Fig. 4.6, the initial slope of the curves will always be below 45°, a result also observed in Ref. [58] for the case in which different spheres in the wavefunction metric space geometry were considered.

When considering paramagnetic current density distance against particle density distance [Figs. 4.6(e) and 4.6(f)] we see that, as for $D_{\mathbf{j}_{p_\perp}}$ vs D_ψ, with the rescaling of Fig. 4.6 there are distinct curves for each value of m which converge onto a single curve as $|m|$ increases. As opposed to $D_{\mathbf{j}_{p_\perp}}$ vs D_ψ, the extent of the linear behaviour of these curves is increasing as $|m|$ increases.

The behaviour of the curves observed in Fig. 4.6 reflects the "onion-shell" geometry of the metric spaces. For wavefunctions and particle densities the sphere radius is associated to the number of particles in the system, which is fixed for the systems considered. Thus, regardless of the value of $|m|$, wavefunctions and particle densities always lie on the same sphere in their respective metric spaces. The fact that the related curves still superimpose for different values of $|m|$ seems to imply that the value of $|m|$ has no significant effect on the curves that represent the relative change of ψ and ρ for changing parameters. In paramagnetic current density metric space, the sphere radius is related

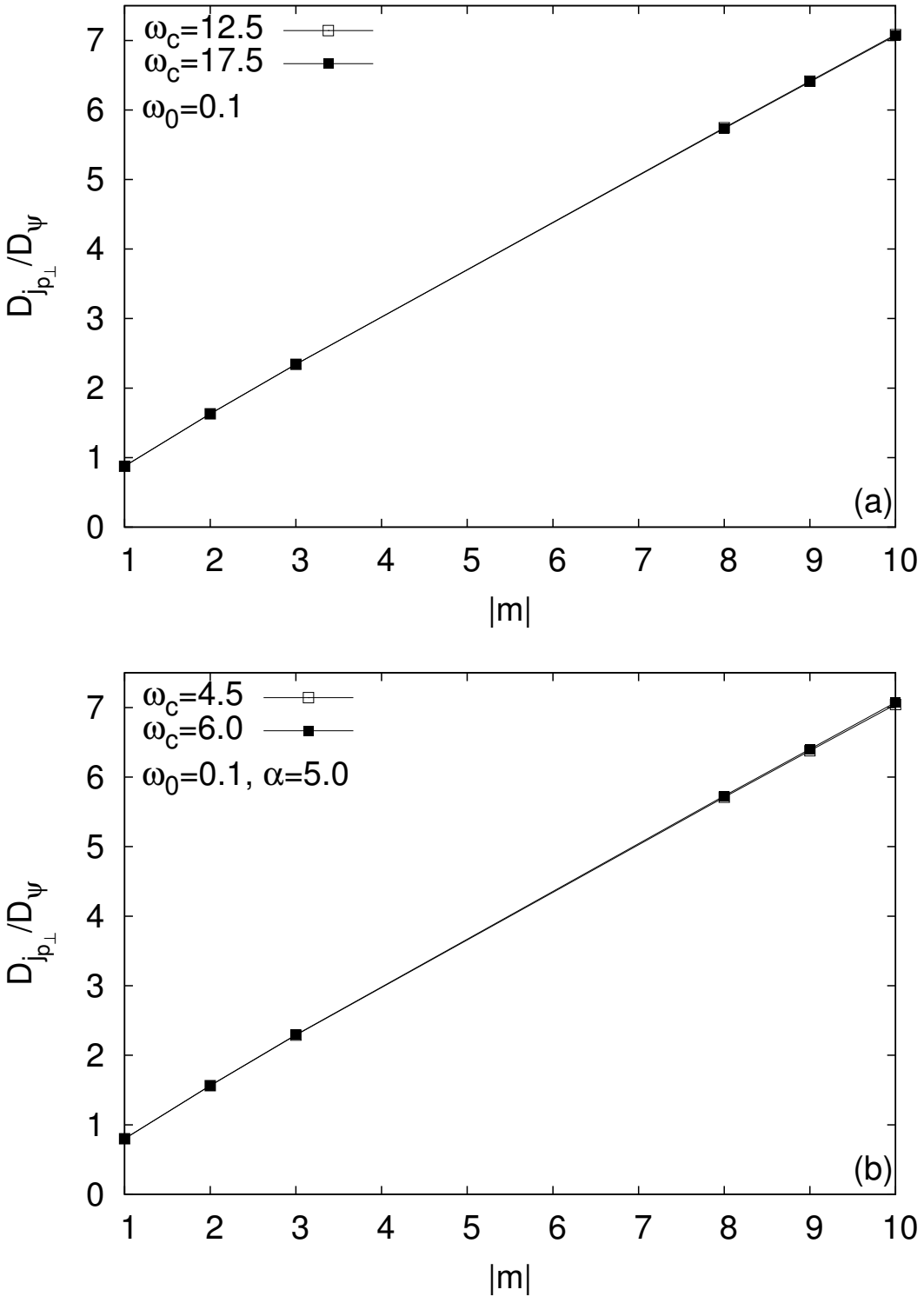

Figure 4.8: Plot of the ratio of paramagnetic current density distance to wavefunction distance against $|m|$ for (a) Magnetic Hooke's Atom, with reference $\omega_0 = 0.1, \omega_{c_{ref}} = 30.0$, and (b) the ISI system, with reference $\omega_0 = 0.1, \omega_{c_{ref}} = 5.0, \alpha = 5$. The gradient is taken at the frequencies corresponding to the closest points to $\omega_{c_{ref}}$ for both decreasing and increasing ω_c in Fig. 4.7, which for Hooke's Atom are $\omega_c = 12.5$ for decreasing frequencies and $\omega_c = 17.5$ for increasing frequencies, and for the ISI system are $\omega_c = 4.5$ for decreasing frequencies and $\omega_c = 6.0$ for increasing frequencies.

to $|m|$, so paramagnetic current densities are on the surface of different spheres each time we consider a different value of $|m|$. As a result we see that the shape each of the curves is affected and they do not collapse onto each other. A similar "universal" behaviour within each sphere and, by contrast, the breaking of this universality when different spheres were considered was also observed in Ref. [58], where different values of N, and hence different spheres, for both wavefunctions and particle densities were considered. This seems to suggest that different behaviour for the mappings should be expected when curves on different spheres in the metric spaces are involved.

Finally Fig. 4.9 combines all distances for each system in a single plot. Importantly this figure shows that for small to medium wavefunction distances $D_{\mathbf{j}_{p_\perp}}/D_\rho \sim const$, where the constant depends on $|m|$, so that this ratio is independent over variations of the wavefunction for relatively close wavefunctions. In this respect, for relatively close wavefunctions this suggests that the mappings between paramagnetic current densities and wavefunctions, and between particle densities and wavefunctions, are very similar, as long as the family of states follows the evolution of the same energy curve as driven by the varying parameter (see Fig. 4.1).

In conclusion we have shown that varying the magnetic field has a profound effect on the "band structure" in ground state metric spaces, illustrating the important role played by the vector potential in such systems, and providing additional insight into the CDFT-HK theorem. Changes in the magnetic field generate a "band structure" that consists of overlapping bands for the wavefunction and particle density, whilst the gaps of forbidden distances observed when varying quantities related to the scalar potential in Chapter 3 were not observed for the wavefunction or particle density. Combining the metrics for the particle and paramagnetic current densities and comparing with wavefunction distances, we find that the nature of the ratio of the paramagnetic current density distance to the particle density distance has a strong dependence on whether or not the values of m are the same for the two functions considered to calculate each distance. When $m = m_{ref}$, the ratio is a constant depending on m, but when $m \neq m_{ref}$, the value of the ratio fluctuates considerably. We also gain additional insight into the geometry of our metric spaces by exploring excited states, where we observe that the value of m studied affects the relationships involving the metric for the paramagnetic current density, the geometry of which is characterised by the angular momentum quantum number. When considering the ratios of paramagnetic current density to particle density distances, the constant relationship found for ground states is shown to persist up to fairly large values of the wavefunction distance.

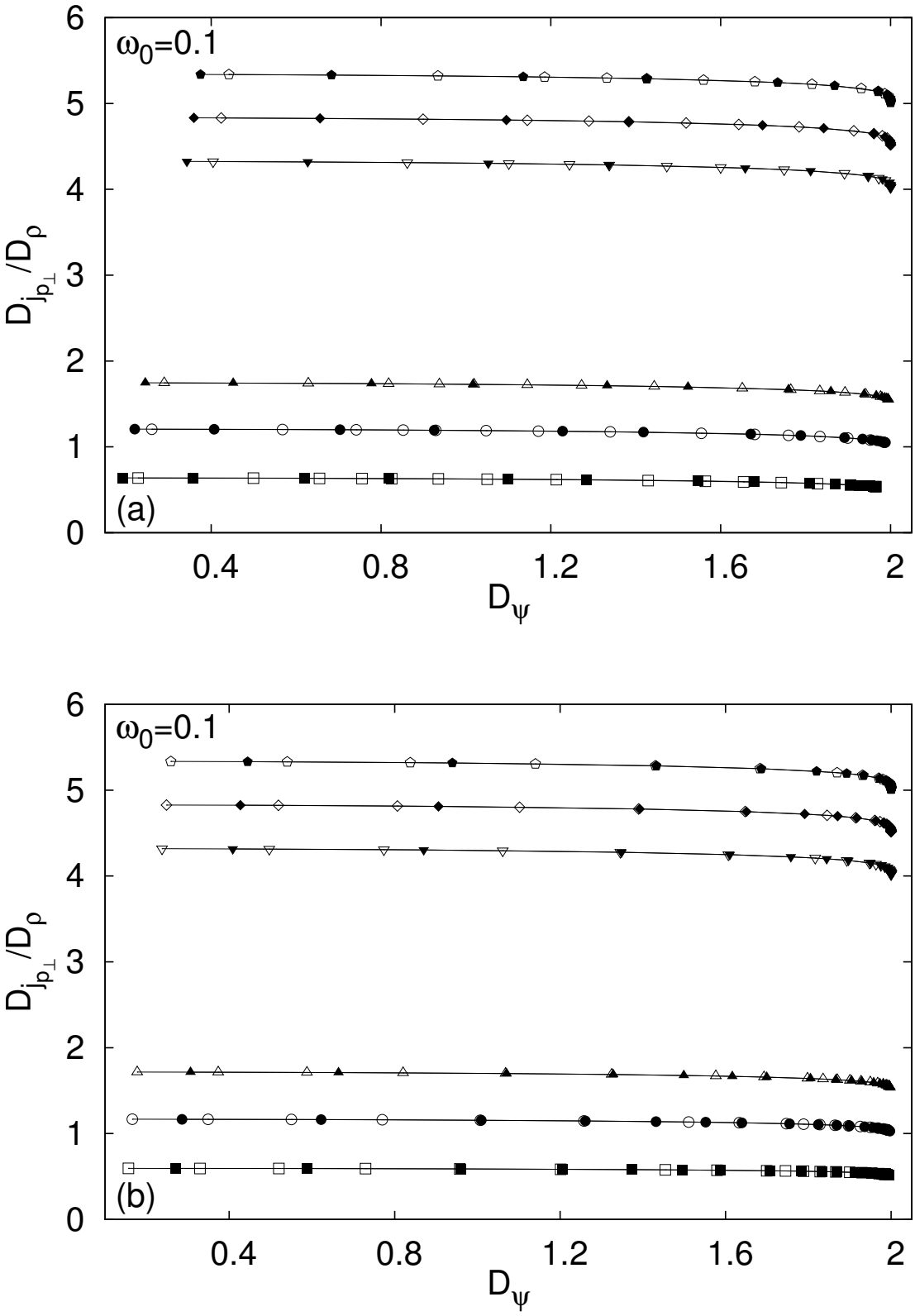

Figure 4.9: Plots of the ratio of paramagnetic current density distance to particle density distance against wavefunction distance for (a) Magnetic Hooke's Atom, with reference state $\omega_0 = 0.1, \omega_{c_{ref}} = 30.0$, and (b) the ISI system, with reference state $\omega_0 = 0.1, \omega_{c_{ref}} = 5.0, \alpha = 5$. Closed symbols represent decreasing ω_c and open symbols represent increasing ω_c.

Chapter 5

Comparing Many-Body and Kohn-Sham Systems Using the Metric Space Approach

The vast majority of practical implementations of DFT make use of the Kohn-Sham scheme, where the system of interacting electrons confined within a particular potential is replaced with an auxiliary system of non-interacting electrons confined by a different potential. The particle density of this auxiliary system is identical to that generated by the original many-body interacting system. The principle reason for the success of the Kohn-Sham scheme is that the majority of the Kohn-Sham potential is known, and the unknown part of the Kohn-Sham potential, the exchange-correlation potential, V_{xc}, can be effectively approximated. Indeed, even relatively crude approximations to V_{xc} can yield good results [24].

So far, the metric space approach to quantum mechanics has been used to explore the relationships between wavefunctions and densities for DFT and CDFT. In order to further our understanding of the fundamentals of DFT we will now investigate the Kohn-Sham scheme with the metric space approach, which has already been attempted [90]. In this chapter we will apply our metrics to the wavefunctions and potentials used to describe systems in the many-body picture, alongside the wavefunctions and potentials used in the Kohn-Sham description. We will compare the distances between many-body and Kohn-Sham quantities as we vary a particular parameter for model quantum systems. We will also use our metrics to determine distances between the many-body and Kohn-Sham quantities that describe the same system, providing a quantitative analysis of how the effective quantities employed in the Kohn-Sham picture differ from those of the many-body picture.

In addition, our metric for potentials allows us to expand on the analysis of the HK theorem in Ref. [58], by considering the unique relationship between potentials and wavefunctions and, consequently, potentials and densities, defined in standard DFT. We will also compare and contrast the information given by each of the three metrics in order to assess the relative merits of each of our three metrics for quantitative comparisons of many-body systems.

The results in this chapter are ongoing research [64].

5.1 Model Systems

In this chapter, we require model systems from which we can obtain both the many-body and Kohn-Sham quantities with high accuracy. Since it is possible to reverse engineer the Kohn-Sham equations exactly for systems of two electrons [91–93], we will study two-electron model systems: Hooke's Atom and Helium-like atoms.

5.1.1 Hooke's Atom

The Hamiltonian for the three-dimensional Hooke's Atom is [73]

$$\hat{H} = \frac{1}{2}\left(\mathbf{p}_1^2 + \omega_0^2 r_1^2 + \mathbf{p}_2^2 + \omega_0^2 r_2^2\right) + \frac{1}{|\mathbf{r}_1 - \mathbf{r}_2|}. \tag{5.1}$$

We solve this system using the method in Ref. [73], which is exactly analagous to the method used for solving the Magnetic Hooke's Atom in Sec. 3.1.1 [75].

In centre of mass and relative motion coordinates, the Hamiltonian is

$$\hat{H} = \frac{1}{4}\mathbf{p}_R^2 + \omega_0^2 R^2 + \mathbf{p}_r^2 + \frac{1}{4}\omega_0^2 r^2 + \frac{1}{r}. \tag{5.2}$$

The Hamiltonian for the centre of mass is simply that of a one-particle harmonic oscillator, hence the solution is given by [1, 10]

$$\xi(\mathbf{R}) = H_{n_1}\left(\sqrt{2\omega_0}R\sin\theta\cos\phi\right) H_{n_2}\left(\sqrt{2\omega_0}R\sin\theta\sin\phi\right) H_{n_3}\left(\sqrt{2\omega_0}R\cos\theta\right) e^{-\omega_0 R^2}, \tag{5.3}$$

and the normalised, ground-state wavefunction is

$$\xi_0(\mathbf{R}) = \left(\frac{2\omega_0}{\pi}\right)^{\frac{3}{4}} e^{-\omega_0 R^2}. \tag{5.4}$$

For the relative motion, we write the ansatz [73]

$$\phi(\mathbf{r}) = \frac{u(r)}{r} Y_{lm}(\hat{r}), \tag{5.5}$$

where Y_{lm} are the spherical harmonics and $\hat{r}$ is the unit vector in the direction of the relative motion.

This ansatz reduces the Schrödinger equation for the relative motion to

$$\left[-\frac{d^2}{dr^2} + \frac{1}{4}\omega_0^2 r^2 + \frac{1}{r} + \frac{l(l+1)}{r^2}\right] u(r) = \varepsilon u(r), \tag{5.6}$$

where ε is the energy related to the relative motion. For large values of r, the relative motion should correspond to two isolated harmonic oscillators, which allows us to write,

$$u(r) = e^{-\frac{\omega_0 r^2}{4}} t(r). \tag{5.7}$$

Substituting Eq. (5.7) into Eq. (5.6) and performing the Frobenius method gives,

$$t(r) = \left(\sqrt{\frac{\omega_0}{2}} r\right)^{l+1} \sum_{v=0}^{\infty} a_v \left(\sqrt{\frac{\omega_0}{2}} r\right)^{v}, \tag{5.8}$$

with coefficients that obey a three-term recursion relation:

$$\begin{aligned}
&a_0 \neq 0, \\
&a_1 = \frac{1}{2(l+1)\sqrt{\frac{\omega_0}{2}}} a_0, \\
&a_v = \frac{1}{v(v+2l+1)} \left\{ \frac{1}{\sqrt{\frac{\omega_0}{2}}} a_{v-1} + \left[2(l+v) - 1 - \frac{2\varepsilon}{\omega_0}\right] a_{v-2} \right\},
\end{aligned}$$

for $v \geqslant 2$.

The ground-state wavefunction (i.e., $l = m = 0$) for Hooke's Atom is

$$\begin{aligned}
\psi(\mathbf{r}, \mathbf{R}) &= \frac{1}{2\sqrt{\pi} r} \left(\frac{2\omega_0}{\pi}\right)^{\frac{3}{4}} e^{-\omega_0 R^2} e^{-\frac{\omega_0 r^2}{4}} \sqrt{\frac{\omega_0}{8\pi}} \sum_{i=0}^{\infty} a_i \left(\sqrt{\frac{\omega_0}{2}} r\right)^{i}, \\
&= \frac{1}{2\sqrt{\pi} r} \left(\frac{2\omega_0}{\pi}\right)^{\frac{3}{4}} e^{-\omega_0 R^2} u(r),
\end{aligned} \tag{5.9}$$

and the density is given by,

$$\rho(\mathbf{r}_1) = \left(\frac{2\omega_0}{\pi}\right)^{\frac{3}{2}} e^{-2\omega_0 r_1^2} \int \frac{u(r)^2 e^{-\frac{\omega_0 r^2}{2}} \sinh(2\omega r_1 r)}{\omega r_1 r} dr, \tag{5.10}$$

which is shown in appendix C.

As was the case for the magnetic Hooke's Atom in Chapter 3, there are certain values of the confinement frequency for which the polynomial terminates after a finite number of terms, n. In these cases, the relative motion energy is given by $\varepsilon = \omega_0 \left(l + n + \frac{1}{2}\right)$. We therefore have two types of solution of Hooke's Atom: the discrete, infinite set of exact solutions; and the approximate solutions constructed by taking a sufficiently large number of terms in order to converge the value of the polynomial [82].

5.1.2 Helium-like Atoms

The Helium atom consists of two electrons orbiting a nucleus of charge $Z = 2$. We will study the Helium isoelectronic series, i.e., two electrons orbiting a nucleus of any charge Z. The Hamiltonian for these Helium-like atoms is given by,

$$\hat{H} = \frac{1}{2}\mathbf{p}_1^2 + \frac{Z}{r_1} + \frac{1}{2}\mathbf{p}_2^2 + \frac{Z}{r_2} + \frac{1}{|\mathbf{r}_1 - \mathbf{r}_2|}, \tag{5.11}$$

where we have neglected the nuclear degrees of freedom by applying the Born-Oppenheimer approximation [94].

We solve the Helium atom quantum mechanically using the Rayleigh-Ritz variational method [1, 8]. At the core of this method is the Rayleigh-Ritz variational principle [16], which states,

$$E_0 \leqslant E[\psi], \tag{5.12}$$

where E_0 is the ground state energy, and the equality applies only if ψ is the ground state wavefunction. Therefore, if we evaluate $E[\psi]$ for a set of wavefunctions, the wavefunction that minimises $E[\psi]$ provides an approximation to the ground state. The Rayleigh-Ritz method involves the use of a trial function of the form [8]

$$\psi(\mathbf{r}) = \sum_{i=1}^{n} c_i \chi_i(\mathbf{r}), \tag{5.13}$$

where the coefficients c_i are referred to as variational parameters. It can be seen that Eq. (5.13) represents a vector in an n-dimensional Hilbert space spanned by the basis $\chi_i(\mathbf{r})$. By optimising the coefficients c_i with the objective of minimising $E[\psi]$, we obtain the best approximation to the ground state within the n-dimensional Hilbert space explored, the energy of which will be an upper bound on the true ground state energy.

The choice of basis for the Helium atom is a very well studied problem, first

considered by Kellner [95] and shortly followed by the seminal work of Hylleraas [96, 97]. This research has led to the development of highly sophisticated basis functions capable of modelling ground and excited states of the Helium atom and the Helium isoelectronic series to very high precision [98–101]. It has been shown that the minimum nuclear charge required for a bound state containing two electrons is $Z \approx 0.911$ [102], hence, we will restrict our study to atoms with $Z \geqslant 1$.

For our purposes, we need a basis set that will allow us to obtain the ground state for any entry in the Helium isoelectronic series, i.e., two-electron ions with any nuclear charge, Z. The basis set chosen is

$$\psi(\mathbf{r}_1, \mathbf{r}_2) = \frac{1}{\sqrt{8}\pi} e^{-Z(r_1+r_2)} \sum_{i,j,k}^{i+j+k \leqslant \Omega} c_{ijk} N_{ijk} L_i^{(2)}(2Zr_1) L_j^{(2)}(2Zr_2) P_k(\cos\theta), \quad (5.14)$$

with,

$$N_{ijk} = \sqrt{\frac{1}{(i+1)(i+2)}} \sqrt{\frac{1}{(j+1)(j+2)}} \sqrt{\frac{2k+1}{2}}, \quad (5.15)$$

where $L_n^{(2)}$ are the generalised Laguerre polynomials, P_n are Legendre polynomials and θ is the angle between r_1 and r_2. This choice combines the approaches taken by Accad *et al.* [103] and Coe *et al.* [104]. It has the important advantages that, with the constants N_{ijk}, each basis function is orthonormal, and separable in the three coordinates $(2Zr_1, 2Zr_2, \cos\theta)$. These coordinates are chosen so that the basis function with $i, j, k = 0$ corresponds to the ground state of a Hydrogen-like atom of charge Z. This basis function always makes the largest contribution to the ground state (i.e., $c_{000} >> c_{ijk}$), particularly for large Z, and hence enables the ground state to converge more rapidly with respect to the number of basis functions.

For the wavefunction given by Eq. (5.14), the density is,

$$\rho(\mathbf{r}_1) = \frac{1}{2\pi} e^{-2Zr_1} \sum_{\substack{i,j,k,\\ i',j',k'}}^{\substack{i+j+k \leqslant \Omega,\\ i'+j'+k' \leqslant \Omega}} \delta_{j,j'} \delta_{k,k'} c_{ijk} c_{i'j'k'} \sqrt{\frac{1}{(i+1)(i+2)(i'+1)(i'+2)}} L_i^{(2)}(2Zr_1) L_{i'}^{(2)}(2Zr_1), \quad (5.16)$$

which is demonstrated in Appendix C.

5.2 Solving the Kohn-Sham Equations for the Model Systems

In order to be able to apply our metrics to quantities in the exact Kohn-Sham picture, we must be able to exactly solve the Kohn-Sham equations, Eqs. (1.52)-(1.53). This is a formidable task in general as it is usually impossible to determine the Kohn-Sham potential *a priori*. However, since the exact Kohn-Sham equations must reproduce the density from the many-body picture, we can use the exact density to reverse engineer the Kohn-Sham equations.

The density is given in terms of Kohn-Sham orbitals by Eq. (1.53). For our model systems, the two electrons have opposite spins in the ground state. Therefore, in the Kohn-Sham picture, both electrons are described by the same Kohn-Sham orbital and, thus, are expressed in terms of the exact density as [93],

$$\phi_{KS} = \sqrt{\frac{\rho(\mathbf{r})}{2}}. \tag{5.17}$$

Now we have the Kohn-Sham orbitals, we can reverse engineer Eq. (1.52) in order to obtain the Kohn-Sham potential [93],

$$V_{KS}(\mathbf{r}) = \varepsilon_{KS} + \frac{1}{2}\frac{\nabla^2\phi_{KS}}{\phi_{KS}}. \tag{5.18}$$

In order to obtain $V_{KS}(\mathbf{r})$ from Eq. (5.18), we require the value of the Kohn-Sham eigenvalue, ε_{KS}. In general, Kohn-Sham eigenvalues do not possess any physical meaning (but are of semiquantitative value [105]), however, the work of Perdew *et al.* [91] demonstrated that, provided $V_{KS}(\mathbf{r}) \to 0$ as $\mathbf{r} \to \infty$, the eigenvalue of the highest occupied Kohn-Sham state is equal to the ionisation energy of the system.

For our model systems, only one Kohn-Sham state is occupied, and thus both eigenvalues are equal to the ionisation energy. For Hooke's Atom, the centre of mass energy is identical to that of a one-electron harmonic oscillator, so the ionisation energy is clearly equal to the relative motion energy [92, 93]. Ionising an electron from any entry in the Helium isoelectronic series results in a Hydrogenic atom with energy $-Z^2/2$ Hartrees. Therefore the ionisation energy is found from the difference between the Helium and Hydrogen ground state energies.

In order to make a direct comparison with the many-body picture, we will form the two-electron Kohn-Sham wavefunction from the product of the or-

bitals,

$$\psi_{KS}(\mathbf{r}_1, \mathbf{r}_2) = \phi_{KS}(\mathbf{r}_1)\,\phi_{KS}(\mathbf{r}_2)\,, \tag{5.19}$$

and the two-electron potential from the sum of the single-particle Kohn-Sham potentials,

$$V_{KS}(\mathbf{r}_1, \mathbf{r}_2) = V_{KS}(\mathbf{r}_1) + V_{KS}(\mathbf{r}_2)\,. \tag{5.20}$$

We will apply our metrics to these two-electron Kohn-Sham quantities.

5.3 Extending the Hohenberg-Kohn Theorem Analysis

We will first revisit the Hohenberg-Kohn theorem of standard DFT, which was first studied with the metric space approach to quantum mechanics in Ref. [58]. Previously only the second part of Eq. (1.45), concerning ground state wavefunctions and densities, has been studied. The results of this, previously published in Ref. [58], have been reproduced in Fig. 1.1. Now, with the external potential metric, we will extend the study to incorporate the first part of Eq. (1.45), which establishes a unique map between the external potential and the wavefunction.

Following directly from the methods in Chapters 3 and 4, we will generate families of states by varying a parameter in the Hamiltonians of our systems. For Hooke's Atom, we vary the strength of the harmonic confinement via the frequency ω_0, and for the Helium-like atoms we will vary the nuclear charge, Z. After choosing a reference state we will use our metrics to determine the distance between the wavefunctions, densities and potentials at the reference and all of the other physical functions in each family of states.

Figure 5.1 shows plots of the potential metric against the wavefunction and density metrics for both systems. Considering firstly the plots of wavefunction distance against potential distance [Figs. 5.1(a) and 5.1(b)], we observe many features in common with Fig. 1.1. The relationship between the wavefunction and potential is again monotonic, with nearby wavefunctions mapped onto nearby potentials, and distant wavefunctions mapped onto distant potentials. The curves for increasing parameters and decreasing parameters are also seen to overlap, or almost overlap, with one another. Finally, both curves have a region where the relationship between the two distances is linear. Interestingly, when considering the potential, we observe that this linear region covers a greater extent of the distance range for Helium-like atoms compared to Hooke's Atom, and that the curves for Helium-like atoms overlap more closely

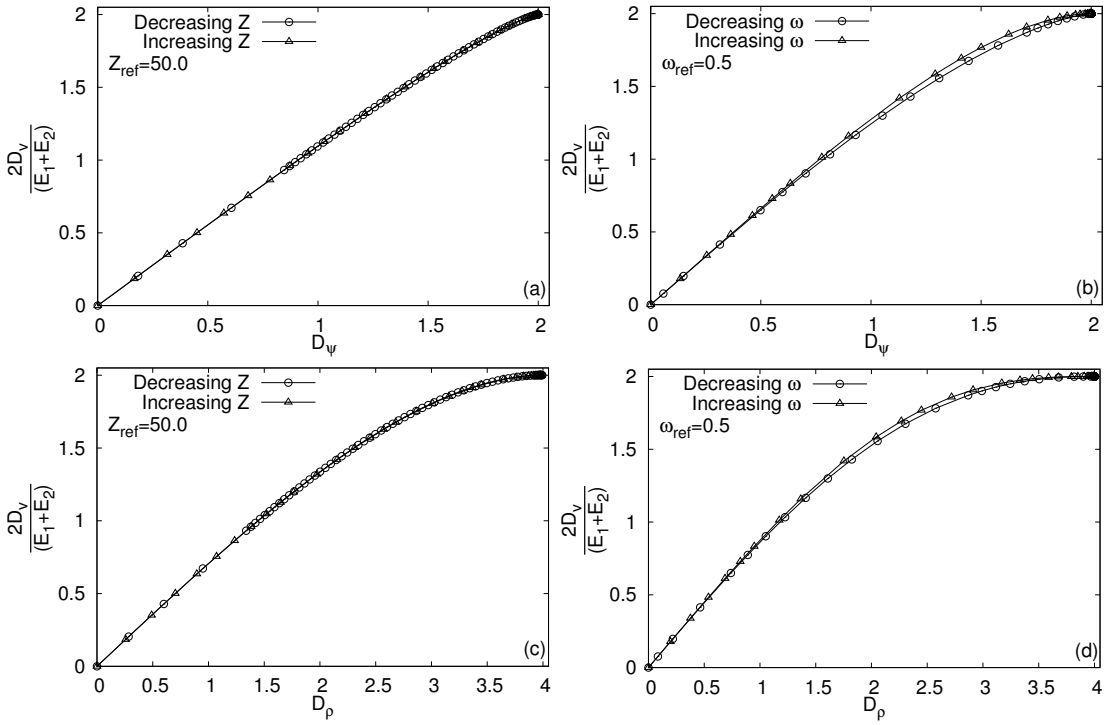

Figure 5.1: Plots of rescaled potential distance against: wavefunction distance [(a) and (b)], and density distance [(c) and (d)]. The Helium-like atoms are shown on the left, with Hooke's Atom on the right.

than the curves for Hooke's Atom.

In Figs. 5.1(c) and 5.1(d) we plot the potential metric against the density metric. Again we observe a monotonic mapping with a linear region at small distances. We observe that, for both systems, the linear region covers a smaller range of distances in this plot compared to Fig. 1.1 and Figs. 5.1(a) and 5.1(b). As was the case for the previous plots, the relationship between the potential and density metrics is monotonic, with curves for increasing and decreasing parameters overlapping or almost overlapping one another.

5.4 Comparison of Metrics for Characterising Quantum Systems

The metric space approach to quantum mechanics allows us to generate various metrics which we can use in order to study changes in physical quantities associated with quantum systems. The metrics for wavefunctions, particle densities and potentials are equally appropriate for characterising systems subject only to scalar potentials, therefore it is worthwhile to make a comparison between the information given by each of these metrics when used in

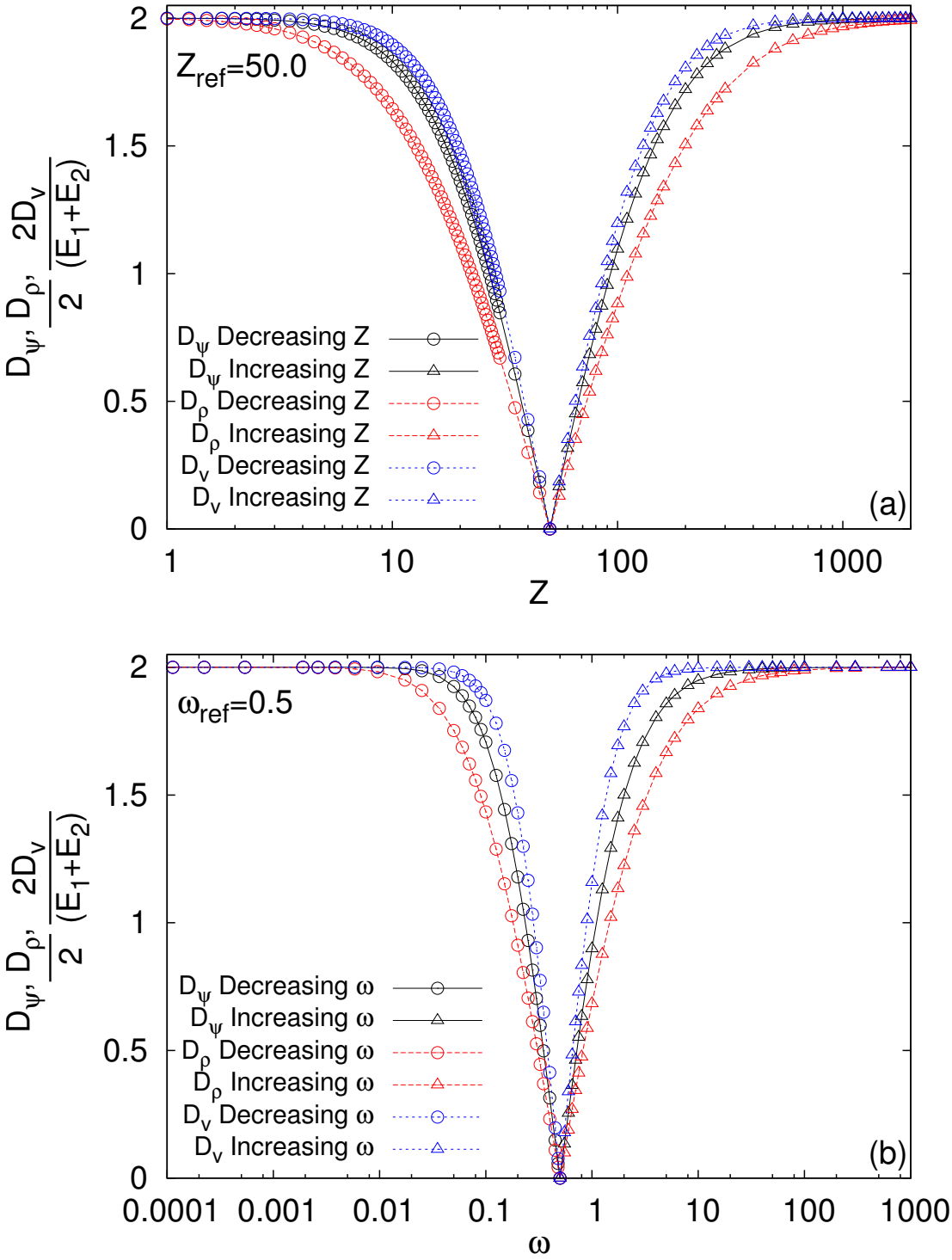

Figure 5.2: The wavefunction, density, and potential distances for the many-body systems are plotted (a) against the nuclear charge for Helium-like atoms, and (b) against the confinement frequency for Hooke's Atom. All of the metrics are scaled such that their maximum value is 2.

practical calculations. This analysis will also shed light on the results found for the HK theorem.

Figure 5.2 shows the values of the wavefunction, particle density and potential metrics plotted against the parameter values for both of our model systems. The metrics are all scaled to have a maximum value of 2 for ease of comparison. We can immediately observe that all of the metrics follow broadly the same trend, increasing monotonically from the reference and converging on the maximum value. The curves for increasing and decreasing values of the parameters are mirror images about the reference in all cases, and incorporate a linear region of increasing distance for parameter values close to the reference, a region where the distance asymptotically approaches its maximum for parameter values far from the reference, along with a transition region in between. The crucial difference between the three metrics however, is how the metrics converge to the maximum value. Figure 5.2 shows that, as we depart from the reference, the potential metric is the first to converge to its maximum, followed by the wavefunction metric, with the density metric being the slowest to converge. This means that when comparing systems that are significantly different from one another, the density metric is the most useful tool for analysis, as it is capable of providing non-trivial information over a wider range of parameter space than the metrics for wavefunctions and potentials. When comparing systems that are relatively similar to one another, all three metrics provide useful information to quantitatively characterise the differences between the systems.

In Fig. 5.3, we again plot the values of our three metrics across parameter space, this time comparing Kohn-Sham quantities. We observe a clear similarity to the many-body picture for both systems, with the density metric again providing non-trivial information across the largest extent of parameter space.

With regard to practical calculations, the density metric confers another significant advantage in that, in general, it is considerably easier to calculate than the metrics for wavefunctions and potentials. This is because the density metric need only be integrated over three degrees of freedom, compared to $3N$ degrees of freedom for the other two metrics. The same value of the density metric can also be obtained from both the many-body and Kohn-Sham systems, since, unlike for wavefunctions and potentials, the densities must be identical in these cases.

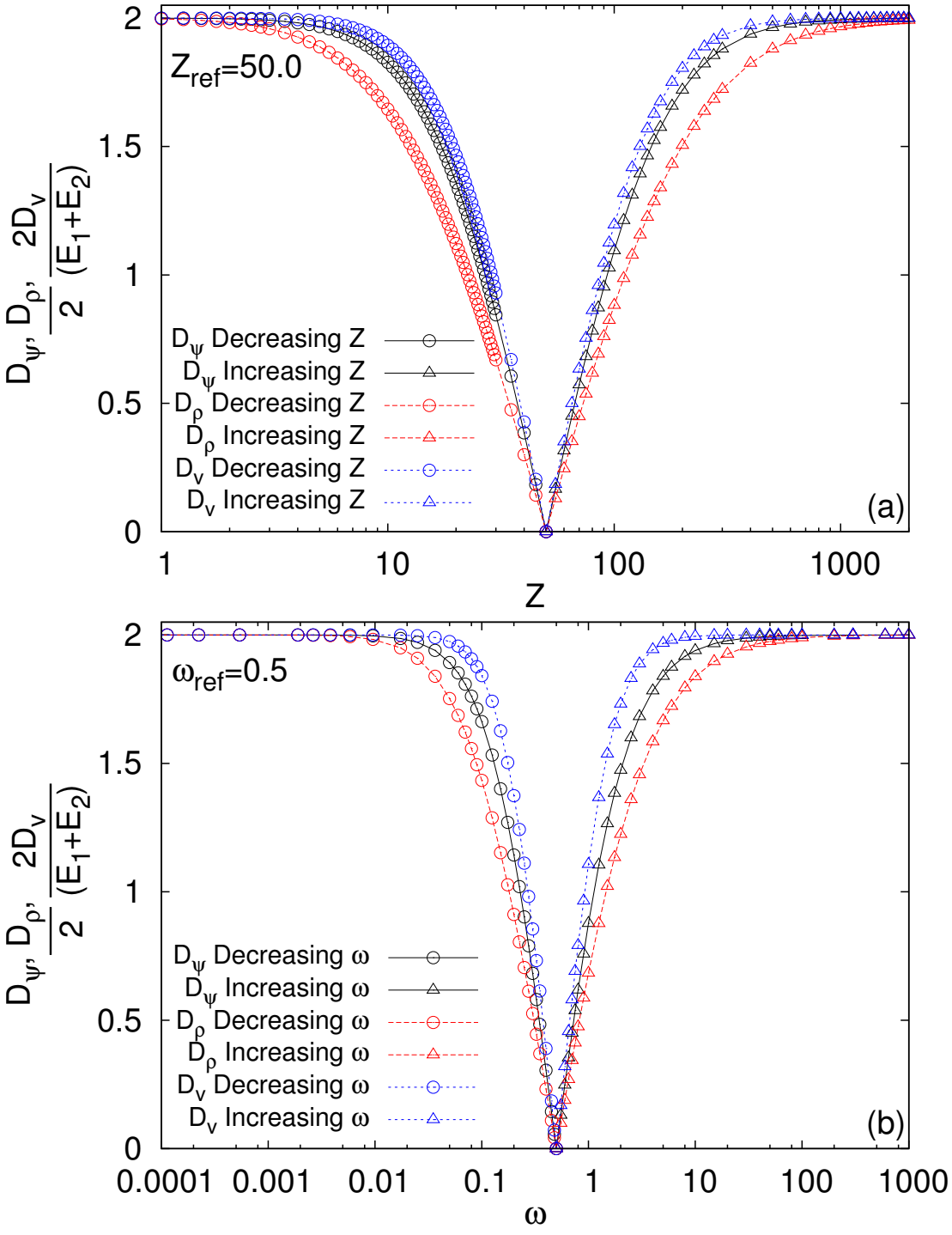

Figure 5.3: The wavefunction, density, and potential distances for Kohn-Sham systems are plotted (a) against the nuclear charge for Helium-like atoms, and (b) against the confinement frequency for Hooke's Atom. All of the metrics are scaled such that their maximum value is 2.

5.5 Determining the Distances between Corresponding Many-Body and Kohn-Sham Quantities

Finally, we will use our metrics to determine the distance between the wavefunctions and potentials used in the many-body picture, and those used to describe the same system in the Kohn-Sham picture.[1] For the first time, we are able to provide a quantitative description of the differences between the many-body and exact Kohn-Sham descriptions of quantum systems.

In Fig. 5.4, the distances between many-body and Kohn-Sham wavefunctions and potentials are plotted for a range of parameter values. We firstly observe that the wavefunction and potential distances always take approximately the same value throughout the parameter range explored for both systems. This demonstrates that the two metrics provide a consistent measure of how the many-body description differs from the Kohn-Sham description of our systems. For both systems we have also plotted the ratio of the expectation value of the Coulomb operator to the expectation value of the external potential operator. This ratio can be seen to follow broadly the the same trend as the metrics. This is an important observation as it provides further confirmation that the metrics derived from the metric space approach to quantum mechanics provide a physically relevant comparison of quantum mechanical functions. It also shows that, alongside the two metrics, this ratio is a useful measure of how much the many-body and Kohn-Sham descriptions of the system differ from one another.

For Helium-like atoms, we observe that the many-body and Kohn-Sham descriptions of the system are always relatively similar across the parameter range studied, with the distances between the quantities decreasing monotonically as Z increases. For this system, the external potential always dominates over the Coulomb interaction between the electrons. We also observe that the distance between the potentials is always larger than the distance between the wavefunctions.

For Hooke's atom, we consider three regimes: large values of ω_0, where the external potential dominates over the Coulomb interaction; intermediate values of ω_0, where the external potential and Coulomb interaction make comparable contributions; and small values of ω_0, where the Coulomb interaction dominates over the external potential. For small and large values of ω_0, we observe that the value of the potential metric is greater than that of the wavefunction metric. However, in the region where the ratio is approximately unity, the

[1] For densities, it is required that $D_\rho(\rho_{MB}, \rho_{KS}) \equiv 0$.

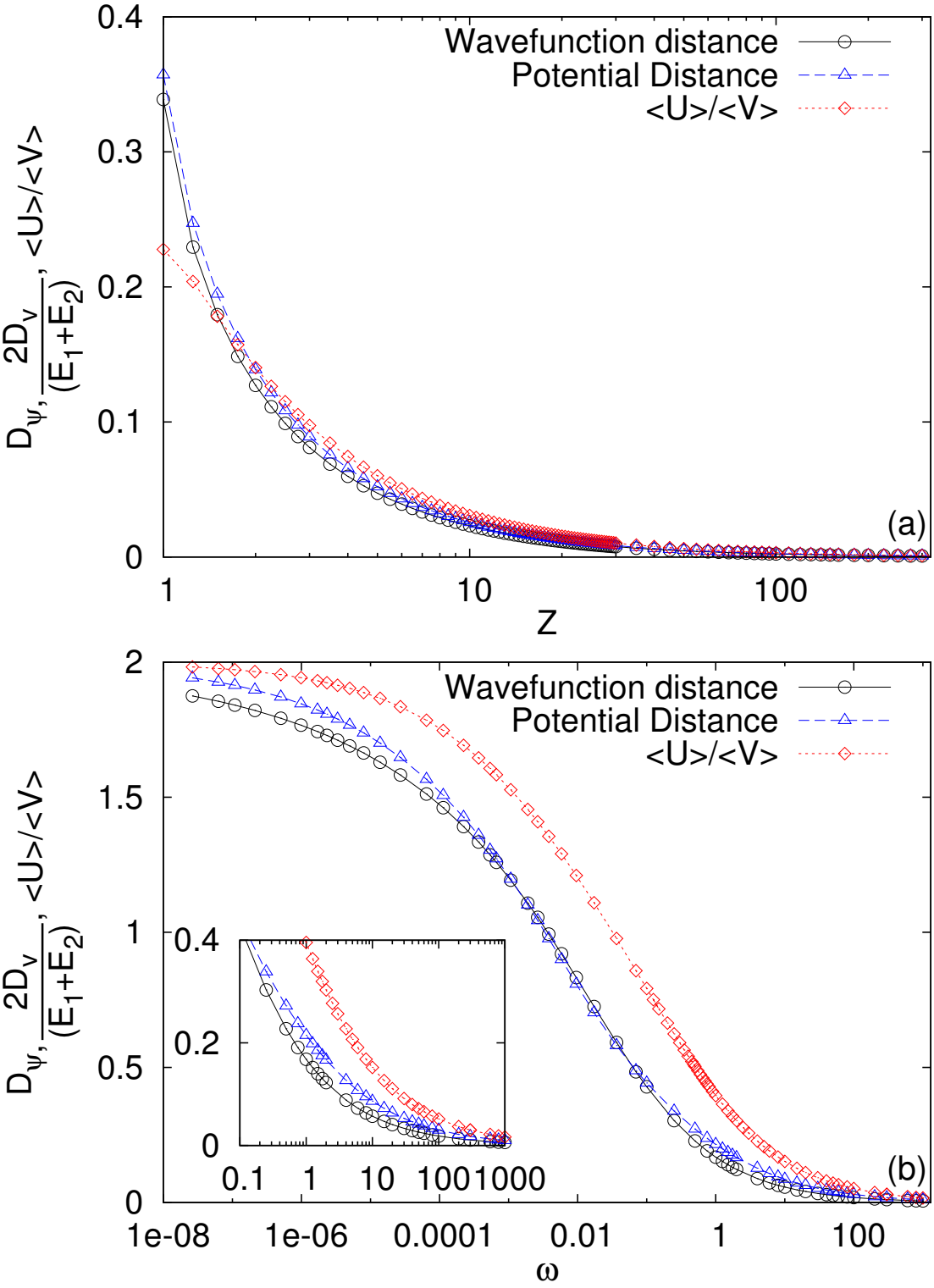

Figure 5.4: For (a) Helium-like atoms and (b) Hooke's Atom, the distances between many-body and Kohn-Sham wavefunctions, and between many-body and Kohn-Sham potentials, are plotted against the parameter values. In addition, the ratio of the expectation of the electron-electron interaction to the many-body external potential energy is plotted and shown to follow a similar trend to the metrics. In the inset, we focus on Hooke's Atom in the regime of distances covered by the Helium-like atoms.

wavefunction metric takes a larger value than the potential metric.

Physically, the values of the wavefunction and potential metrics for the distances between many-body and Kohn-Sham systems can be interpreted as a measure of the electron-electron interaction effects. Specifically, the Kohn-Sham wavefunction is the product of single particle states, hence the wavefunction distance can be interpreted as a measure of the features present in the many-body wavefunction that go beyond single particle approximations. For potentials, the Kohn-Sham potential is composed of three components: the external potential used for the many-body description, the Hartree potential and the exchange-correlation potential. Therefore, the value of the metric $D_V\left(V_{ext}, V_{KS}\right)$ can be interpreted as measuring the contribution of the Hartree and exchange-correlation potentials to the Kohn-Sham potential.

The results in this Chapter provide us with a new perspective on Kohn-Sham DFT. Previous studies comparing many-body and Kohn-Sham (either exact or approximated) quantities have either made qualitative statements [82, 106, 107], or identified features of Kohn-Sham quantities [71, 108, 109]. With our metrics, we have a well-defined numerical value that gives a simple description of how different the many-body and Kohn-Sham descriptions of a quantum system are. This measure is an important addition to the range of tools used to explore the Kohn-Sham picture. When developing functionals and approximations for DFT, our metrics can be used in order to quantify how closely they reproduce the exact KS quantities, and how they compare to other approximations. In addition, the fact that, for the systems studied, the ratio of the Coulomb interaction between the electrons to the external potential closely mirrors the values of the metrics is a significant result. Although further analysis is required to see if this result holds for more complex systems, this ratio, which is relatively simple to approximate for many systems, could potentially give users of DFT an indication of the significance of Hartree-exchange-correlation effects, and, consequently, could act as a guide as to which approximation to V_{xc} is most appropriate for the system studied.

Chapter 6

Conclusions

In this thesis, we have developed and applied the metric space approach to quantum mechanics, which is a new method to derive physically relevant metrics for quantum mechanical functions. We have applied the approach to study many-body quantum mechanics, specifically by considering Density Functional Theory (DFT) and Current Density Functional Theory (CDFT), and in doing so have gained additional insight into the fundamental nature of these theories.

In Chapter 1, we introduced the theory of quantum mechanics, drew attention to the significance of conservation laws in developing theoretical physics, and proved various conservation laws in quantum mechanics. We then outlined the many-body problem in quantum mechanics and introduced one of the main approaches employed in order to tackle it, namely DFT. We discussed the Hohenberg-Kohn theorem and the Kohn-Sham scheme, highlighting that both of these fundamental elements of DFT draw connections between different quantum mechanical functions, and are therefore amenable to studies involving comparisons between these functions. We then introduced the concept of a metric space, and showed the connection between vector spaces and quantum mechanics. Finally, we examined previous work in the literature that applied metric spaces to quantum mechanical functions.

The fundamental theory behind the metric space approach to quantum mechanics was set out in Chapter 2. We argued that the best choice of metric for studying quantum mechanical functions is one that captures fundamental physics at its core, and for this reason we chose to base our metrics on conservation laws. Another highly significant advantage of developing metrics from conservation laws is that we demonstrated a straightforward, general method to derive metrics from integral, or sum, conservation laws. These metrics were shown to possess an "onion-shell" geometry consisting of concentric

spheres, that allows us to visualise the metric spaces. We then applied the metric space approach to generate metrics for specific quantum mechanical functions: wavefunctions, particle densities, paramagnetic current densities, and scalar potentials. All of these quantities can be linked to quantum mechanical conservation laws, and are fundamentally important for DFT and CDFT.

We also demonstrated the extensions to the metric space approach that enable the theory to be applied to a wider range of functions. For wavefunctions, we showed how equivalence classes can be defined in order to restrict the derived metric to wavefunctions that correspond to different physical situations, ensuring that wavefunctions that differ by a trivial phase factor are assigned zero distance. Equivalence classes were also utilised in order to associate the metric derived from the z-component of angular momentum to the transverse component of the paramagnetic current density. In this case the equivalence classes were directly induced by the conservation law. In addition, we showed that the gauge variant paramagnetic current density can be associated with a gauge invariant current density. This enables the paramagnetic current density metric to be used in all gauges. All of these measures have ensured that the metrics we define are gauge invariant.

Having established the physical and mathematical framework of the metric space approach to quantum mechanics, the approach was then used to gain a deeper insight into CDFT. Specifically, we calculated the wavefunctions, particle densities and paramagnetic current densities of two different model systems, generating a family of states by varying a single parameter in the Hamiltonian. Applying our metrics to each of these quantities allowed us to compare the distances between ground-state wavefunctions, and their corresponding particle densities and paramagnetic current densities; and to study the unique relationship between these three variables defined in CDFT. In Chapter 3, we considered variations in the potential energy, firstly by changing the strength of the harmonic confining potential for the Magnetic Hooke's Atom and the Inverse Square Interaction (ISI) system and then the strength of the electron-electron interaction for the ISI system. We considered the relationships between each of the three metrics; the relationship between the wavefunction and particle density metrics was found to bear a close resemblence to that found for systems without magnetic fields in Ref. [58]. Specifically, we once again observe a monotonic relationship, which is linear for low to intermediate distances, and the curves for increasing and decreasing confinement strength overlapping one another. However, the application of a magnetic field caused a significant feature to emerge for ground state metric spaces – the "band structure" of allowed ("bands") and forbidden ("gaps") distances, caused by

changes in the angular momentum quantum number, m. When considering the "onion-shell" geometry of our metric spaces, we observed that paramagnetic current densities "jump" from one sphere to another when the value of m changes, and as such we can determine the angular width of each of the bands in this metric space. It was found that the bands moved from the north pole of the sphere to the south pole as we departed from the reference value of m, and that the width of the bands decreased as m increased.

In Chapter 4, the analysis of the metrics and their interrelationships was extended to encompass variations in the magnetic field, and we examined how the "band structure" arising from the presence of the magnetic field responded to changes in the field. The principal result of this analysis was the emergence of "overlapping bands" in the metric spaces for ground state wavefunctions and particle densities, resulting in a lack of forbidden distances for these quantities. We also used our metrics in order to gain an insight into the unique relationship between wavefunctions, particle densities, and paramagnetic current densities in CDFT by examining the ratio of the metrics for paramagnetic current densities and particle densities, where we found that there was a stark difference between the situations where $m = m_{ref}$, and $m \neq m_{ref}$. When considering functions with the same value of m, the ratio of paramagnetic current density and particle density metrics was seen to be constant, but this was not the case for functions with different values of m. We then extended our analysis beyond CDFT to consider excited states. In this case, when considering different values of m, the curves for wavefunctions and particle densities were seen to collapse on to one another, but this was not the case when paramagnetic current densities were considered. Examining again the ratio of paramagnetic current density and particle density metrics, the constant relationship for equal values of m was seen to persist up to fairly large wavefunction distances. All of these findings indicate that changes in m are very significant when modelling systems subject to magnetic fields.

Chapter 5 was concerned with the Kohn-Sham scheme of ground-state DFT, and extending the analysis of the Hohenberg-Kohn theorem using the metric for potentials. The relationship between the external potential and the wavefunction was seen to share many characteristics with the relationship between wavefunctions and densities, principally the monotonic relationship that incorporates a linear region. We observed that the extent of this linear region was different depending on which two metrics were considered. With three metrics now available for characterising many-body systems, we analysed the performance of each of them, and found that the density metric is more useful for comparing systems at large distances, as this metric will provide non-trivial

information about these systems. Finally, we studied the distances between corresponding many-body and Kohn-Sham systems in order to quantify how different the many-body interacting and Kohn-Sham descriptions of quantum systems are. We found that both wavefunctions and potentials gave complementary results, showing the same qualitative picture and a similar quantitative picture throughout the parameter space explored. For the model systems studied, we also found that the ratio of the expectation of the electronic pairwise Coulomb interaction to that of the potential energy followed the same qualitative trend as the metrics.

Overall, the metric space approach to quantum mechanics has enabled us to examine quantum mechanics beyond the wavefunction. This has been achieved by constructing metric spaces for a range of quantum mechanical functions, allowing all of them to be treated on an equal footing. DFT is a particularly useful illustration of the metric space approach, since the fundamental tenet of DFT is to move from the Hilbert space of wavefunctions to the set of densities, which does not form a vector space. When applied to relationships fundamental to DFT and CDFT, our approach has revealed distinctive signatures such as: monotonicity, (piecewise) linearity, and "band structures", that go beyond what is defined by the theories. Our metrics also provide quantitative, physically meaningful information when comparing quantum systems. Hence, they could enhance the development of approaches to quantum modelling, and provide a physically relevant way to assess the construction of approximations to quantum mechanical functions. The results in this thesis suggest that the metric space approach to quantum mechanics is a powerful tool to study quantum systems governed by conservation laws.

6.1 Future Work

Having established the formalism of the metric space approach to quantum mechanics, there are many possible applications and directions for future research. We have primarily considered DFT and CDFT in this thesis, but our approach is easily applicable to the study of quantum mechanical functions in order to gain insight into quantum phenomena and other approaches used to model quantum systems. Although most of the research in this thesis has been concerned with systems in the ground state, in Chapter 4 we showed that the metric space approach to quantum mechanics can be easily applied to excited states. Given that there are fewer approaches to modelling systems in excited states compared to ground states, the metric space approach could prove useful in improving the understanding of excited state properties.

One example of a theory that provides insight into excited states, and on which a significant amount of research is currently underway, is time-dependent DFT (TDDFT). The metric space approach may also be able to provide insight into this rapidly developing theory. In TDDFT, the Runge-Gross theorem states that the many-body wavefunction and potential at a particular time are uniquely determined by the density at the current time and all previous times, along with the initial wavefunction of the system [37]. TDDFT also defines a version of the Kohn-Sham scheme for time-dependent systems. Our metrics for wavefunctions and densities are immediately applicable in the time-dependent case, and thus the metric space approach to quantum mechanics could be applied to gain insight into the relationships between many-body wavefunctions and densities, as defined by the Runge-Gross theorem, and many-body and Kohn-Sham quantities. These relationships can be studied at particular points in time, and we can also use our metrics to quantify how much wavefunctions and densities evolve in time.

The most significant result from our studies of CDFT is the presence of the "band structure" in ground-state metric spaces. It would be worthwhile to explore a greater range of systems in order to establish how universal this feature is, and whether changes in the value of m continue to carry significance. A metric-space-based analysis of the non-uniqueness problem may provide some interesting insights, particularly since this problem is one of the biggest issues curtailing practical implementation of CDFT. However, there are some challenges; in particular we do not have a metric for the vector potential, and our metric for scalar potentials applies only to systems where $\mathbf{A}(\mathbf{r}) = 0$. If these issues could be overcome, it would be interesting to take a range of potentials that map to the same wavefunction, and compare the distances between them. The values of distances between scalar and vector potentials and the relationship between these distances could both provide a much greater insight into the non-uniqueness problem.

The fact that the ratio of Coulomb interaction energy to external potential energy closely follows the values of the distances between many-body and Kohn-Sham systems is an intriguing result that is worthy of further consideration. It would be interesting to see if this result continues to hold for a wider variety of systems than those studied in this thesis. Also, as it has been indicated that this measure of interaction is not applicable for non-monotonic potentials [110], it would also be interesting to see how other proposed measures compare to the metrics in these cases, and whether or not measures of interaction are a suitable way to estimate how the many-body picture differs from the Kohn-Sham picture for the system under consideration.

A natural, and promising, extension to the calculations of distances between many-body and Kohn-Sham systems in Chapter 5 would be to consider the wavefunctions, densities, and potentials arising from approximations in DFT and TDDFT, and hence use the metric space approach to quantum mechanics in order to quantify the performance of these approximations. For model systems like the ones studied in this thesis, our metrics could be used to measure how much the wavefunctions and potentials corresponding to approximations such as the local density approximation [24] differ from those used in the exact Kohn-Sham description. For more complex systems where the exact Kohn-Sham quantities cannot be obtained, the metrics could still be useful in order to compare approximations with one another, which can help to determine regions of parameter space where certain approximations may perform better than others for the system considered. This analysis could also be performed in order to guide the development of new approximations.

Appendix A

Determining the Gauges where $\hat{L}_z$ is a Constant of Motion

In order to be a constant of motion, the z-component of the angular momentum $\hat{L}_z = -i[\mathbf{r}\times\nabla]_z$ must commute with the Hamiltonian. Given that a vector potential is present, we consider the Pauli Hamiltonian

$$\hat{H} = -\frac{1}{2}\nabla^2 - \frac{i}{2}(\mathbf{A}\cdot\nabla + \nabla\cdot\mathbf{A}) + \frac{1}{2}A^2 + V(\mathbf{r}), \tag{A.1}$$

with $V(\mathbf{r})$ such that $\left[V(\mathbf{r}), \hat{L}_z\right] = 0$. The Hamiltonian Eq. (A.1) does not necessarily commute with $\hat{L}_z$ for a particular $\mathbf{A}(\mathbf{r})$, because $\hat{L}_z$ is gauge variant. For instance, $\hat{L}_z$ commutes with the Hamiltonian Eq. (A.1) in the symmetric gauge $\mathbf{A} = [y, -x, 0]$ and does not commute with it in the Landau gauge $\mathbf{A} = [0, -x, 0]$. We wish to determine the general set of vector potentials where $\left[\hat{H}, \hat{L}_z\right] = 0$.[1]

A.1 Simplifying the Commutator

The commutator we wish to evaluate is:

$$\begin{aligned}\left[\hat{H}, \hat{L}_z\right] = -i\Bigg[&\mathbf{A}\cdot\nabla\left(x\frac{\partial\psi}{\partial y}\right) - \mathbf{A}\cdot\nabla\left(y\frac{\partial\psi}{\partial x}\right) - x\frac{\partial}{\partial y}(\mathbf{A}\cdot\nabla\psi) + y\frac{\partial}{\partial x}(\mathbf{A}\cdot\nabla\psi)\\ &+\nabla\cdot\left(\mathbf{A}x\frac{\partial\psi}{\partial y}\right) - \nabla\cdot\left(\mathbf{A}y\frac{\partial\psi}{\partial x}\right) - x\frac{\partial}{\partial y}\nabla\cdot(\mathbf{A}\psi) + y\frac{\partial}{\partial x}\nabla\cdot(\mathbf{A}\psi)\Bigg]\\ &+A^2x\frac{\partial\psi}{\partial y} - A^2y\frac{\partial\psi}{\partial x} - x\frac{\partial}{\partial y}\left(A^2\psi\right) + y\frac{\partial}{\partial x}\left(A^2\psi\right),\end{aligned} \tag{A.2}$$

[1] In the case where we have many-body interactions, we only consider the case $\left[U(\mathbf{r}_i, \mathbf{r}_j), \hat{L}_z\right] = 0$, as is the case for the Coulomb interaction.

where we have used that $\left[-\frac{1}{2}\nabla^2 + V(\mathbf{r}), \hat{L}_z\right] = 0$. We will impose the condition $\left[\hat{H}, \hat{L}_z\right] = 0$, and then solve the commutator to obtain the vector potential $\mathbf{A}$. Eq. (A.2) reduces to

$$\begin{aligned}\left[\hat{H}, \hat{L}_z\right] = &-i\left[\mathbf{A}\cdot\left(x\nabla\frac{\partial\psi}{\partial y}\right) + \mathbf{A}\cdot\left(\frac{\partial\psi}{\partial y}\nabla x\right) - \mathbf{A}\cdot\left(y\nabla\frac{\partial\psi}{\partial x}\right) - \mathbf{A}\cdot\left(\frac{\partial\psi}{\partial x}\nabla y\right)\right.\\ &-2x\frac{\partial}{\partial y}(\mathbf{A}\cdot\nabla\psi) + 2y\frac{\partial}{\partial x}(\mathbf{A}\cdot\nabla\psi),\\ &\left.+\nabla\cdot\left(\mathbf{A}x\frac{\partial\psi}{\partial y}\right) - \nabla\cdot\left(\mathbf{A}y\frac{\partial\psi}{\partial x}\right) - x\frac{\partial}{\partial y}(\psi\nabla\cdot\mathbf{A}) + y\frac{\partial}{\partial x}(\psi\nabla\cdot\mathbf{A})\right]\\ &-x\psi\frac{\partial A^2}{\partial y} + y\psi\frac{\partial A^2}{\partial x} = 0.\end{aligned}$$

We now perform the vector operations. For compactness, we use a notation $r_i = r_1, r_2, r_3 = x, y, z$, which gives,

$$\begin{aligned}\left[\hat{H}, \hat{L}_z\right] &= \sum_{i=1}^{3}\left\{-i\left[A_i x\frac{\partial}{\partial r_i}\frac{\partial\psi}{\partial y} + A_i\frac{\partial\psi}{\partial y}\frac{\partial x}{\partial r_i} - A_i y\frac{\partial}{\partial r_i}\frac{\partial\psi}{\partial x} - A_i\frac{\partial\psi}{\partial x}\frac{\partial y}{\partial r_i}\right.\right.\\ &\quad -2x\frac{\partial}{\partial y}\left(A_i\frac{\partial\psi}{\partial r_i}\right) + 2y\frac{\partial}{\partial x}\left(A_i\frac{\partial\psi}{\partial r_i}\right)\\ &\quad \left.+\frac{\partial}{\partial r_i}\left(A_i x\frac{\partial\psi}{\partial y}\right) - \frac{\partial}{\partial r_i}\left(A_i y\frac{\partial\psi}{\partial x}\right) - x\frac{\partial}{\partial y}\left(\psi\frac{\partial A_i}{\partial r_i}\right) + y\frac{\partial}{\partial x}\left(\psi\frac{\partial A_i}{\partial r_i}\right)\right]\\ &\quad \left.-x\psi\frac{\partial A^2}{\partial y} + y\psi\frac{\partial A^2}{\partial x}\right\},\\ &= \sum_{i=1}^{3}\left\{-i\left[-xA_i\frac{\partial}{\partial r_i}\frac{\partial\psi}{\partial y} - 2x\frac{\partial\psi}{\partial r_i}\frac{\partial A_i}{\partial y} + 2A_i\frac{\partial\psi}{\partial y}\frac{\partial x}{\partial r_i} + yA_i\frac{\partial}{\partial r_i}\frac{\partial\psi}{\partial x} + 2y\frac{\partial\psi}{\partial r_i}\frac{\partial A_i}{\partial x}\right.\right.\\ &\quad -2A_i\frac{\partial\psi}{\partial x}\frac{\partial y}{\partial r_i} + A_i y\frac{\partial\psi}{\partial y}\frac{\partial x}{\partial r_i} + xA_i\frac{\partial}{\partial r_i}\frac{\partial\psi}{\partial y} + x\frac{\partial\psi}{\partial y}\frac{\partial A_i}{\partial r_i} - A_i\frac{\partial\psi}{\partial x}\frac{\partial y}{\partial r_i} - yA_i\frac{\partial}{\partial r_i}\frac{\partial\psi}{\partial x}\\ &\quad \left.-x\psi\frac{\partial}{\partial y}\frac{\partial A_i}{\partial r_i} - x\frac{\partial A_i}{\partial r_i}\frac{\partial\psi}{\partial y} + y\psi\frac{\partial}{\partial x}\frac{\partial A_i}{\partial r_i} + y\frac{\partial A_i}{\partial r_i}\frac{\partial\psi}{\partial x}\right]\\ &\quad \left.-x\psi\frac{\partial A^2}{\partial y} + y\psi\frac{\partial A^2}{\partial x}\right\},\\ &= \sum_{i=1}^{3}\left\{-i\left[2A_i\left(\frac{\partial\psi}{\partial y}\frac{\partial x}{\partial r_i} - \frac{\partial\psi}{\partial x}\frac{\partial y}{\partial r_i}\right) - 2x\frac{\partial\psi}{\partial r_i}\frac{\partial A_i}{\partial y} + 2y\frac{\partial\psi}{\partial r_i}\frac{\partial A_i}{\partial x} - x\psi\frac{\partial}{\partial y}\frac{\partial A_i}{\partial r_i} + y\psi\frac{\partial}{\partial x}\frac{\partial A_i}{\partial r_i}\right]\right.\\ &\quad \left.-x\psi\frac{\partial A^2}{\partial y} + y\psi\frac{\partial A^2}{\partial x}\right\} = 0.\end{aligned}$$

Writing this out explicitly, we obtain

$$-i\left[\left(2A_x\frac{\partial\psi}{\partial y}-2A_y\frac{\partial\psi}{\partial x}\right)-2x\left(\frac{\partial\psi}{\partial x}\frac{\partial A_x}{\partial y}+\frac{\partial\psi}{\partial y}\frac{\partial A_y}{\partial y}+\frac{\partial\psi}{\partial z}\frac{\partial A_z}{\partial y}\right)\right.$$
$$+2y\left(\frac{\partial\psi}{\partial x}\frac{\partial A_x}{\partial x}+\frac{\partial\psi}{\partial y}\frac{\partial A_y}{\partial x}+\frac{\partial\psi}{\partial z}\frac{\partial A_z}{\partial x}\right)-x\psi\frac{\partial}{\partial y}\left(\frac{\partial A_x}{\partial x}+\frac{\partial A_y}{\partial y}+\frac{\partial A_z}{\partial z}\right)$$
$$\left.+y\psi\frac{\partial}{\partial x}\left(\frac{\partial A_x}{\partial x}+\frac{\partial A_y}{\partial y}+\frac{\partial A_z}{\partial z}\right)\right]-x\psi\frac{\partial A^2}{\partial y}+y\psi\frac{\partial A^2}{\partial x}=0. \tag{A.3}$$

In order to progress with the solution of this equation, we first consider the case where ψ, $\frac{\partial\psi}{\partial x}$, $\frac{\partial\psi}{\partial y}$ and $\frac{\partial\psi}{\partial z}$ are all independent of each other. This choice allows us to decompose Eq. (A.3) into a set of simultaneous equations, which we can then solve. The solution of these equations will provide properties of the general set of vector potentials where $\left[\hat{H},\hat{L}_z\right]=0$. Using these properties, we will then solve Eq. (A.3) for $\mathbf{A}(\mathbf{r})$ using a general wavefunction.

With our choice of trial wavefunction, we write the set of simultaneous equations

$$ix\frac{\partial}{\partial y}\left(\frac{\partial A_x}{\partial x}+\frac{\partial A_y}{\partial y}+\frac{\partial A_z}{\partial z}\right)-x\frac{\partial A^2}{\partial y}-iy\frac{\partial}{\partial x}\left(\frac{\partial A_x}{\partial x}+\frac{\partial A_y}{\partial y}+\frac{\partial A_z}{\partial z}\right)+y\frac{\partial A^2}{\partial x}=0, \tag{A.4}$$

$$A_y+x\frac{\partial A_x}{\partial y}-y\frac{\partial A_x}{\partial x}=0, \tag{A.5}$$

$$A_x-x\frac{\partial A_y}{\partial y}+y\frac{\partial A_y}{\partial x}=0, \tag{A.6}$$

$$y\frac{\partial A_z}{\partial x}-x\frac{\partial A_z}{\partial y}=0. \tag{A.7}$$

We concentrate first on Eqs. (A.5)-(A.7), a set of three equations for the three unknowns A_x, A_y and A_z. Firstly, we consider Eq. (A.7). In order to solve this partial differential equation (PDE), we use the method of characteristics [111].

The method of characteristics requires the visualisation of Eq. (A.7) in 4D coordinates (x,y,z,u). By considering the solution surface $u=A_z(x,y,z)$, we can write

$$A_z(x,y,z)-u=0.$$

For any surface, S, a normal vector to the surface is given by ∇S. Thus, the vector $\left[\frac{\partial A_z}{\partial x},\frac{\partial A_z}{\partial y},\frac{\partial A_z}{\partial z},-1\right]$ is normal to the solution surface. We now write the PDE (A.7) as a scalar product

$$[y,-x,0,0]\cdot\left[\frac{\partial A_z}{\partial x},\frac{\partial A_z}{\partial y},\frac{\partial A_z}{\partial z},-1\right]=0.$$

Since the scalar product of these two vectors is zero, they must be orthogo-

nal. Given also that the vector $\left[\frac{\partial A_z}{\partial x}, \frac{\partial A_z}{\partial y}, \frac{\partial A_z}{\partial z}, -1\right]$ is normal to the surface, this tells us that the vector field $[y, -x, 0, 0]$ is tangent to the surface at every point, providing a geometrical interpretation of the PDE. Thus, any curve within the surface $A_z(x,y,z) - u = 0$ that has the vector $[y, -x, 0, 0]$ as a tangent at every point must lie entirely within the surface. Such curves are called characteristic curves [111]. Any curve can be described by a parameter, t, and the tangent of such a curve, $\mathbf{r}(t)$, is given by the derivative with respect to this parameter $\mathbf{r}'(t)$. Therefore, the tangent of a characteristic curve, $\mathbf{r}(t) = [x(t), y(t), z(t), A_z(t)]$, is given by the vector

$$\mathbf{r}'(t) = \left[\frac{dx}{dt}, \frac{dy}{dt}, \frac{dz}{dt}, \frac{dA_z}{dt}\right].$$

This vector is therefore proportional to the tangent vector $[y, -x, 0, 0]$ for this characteristic curve, allowing us to construct the equations

$$\frac{dx}{dt} = y, \tag{A.8}$$
$$\frac{dy}{dt} = -x, \tag{A.9}$$
$$\frac{dz}{dt} = 0, \tag{A.10}$$
$$\frac{dA_z}{dt} = 0. \tag{A.11}$$

These are the characteristic equations of the PDE (A.7).

Solving this set of ordinary differential equations (ODEs) yields the solution of the original PDE (A.7), since

$$\begin{aligned}\frac{dA_z}{dt} &= \frac{dx}{dt}\frac{\partial A_z}{\partial x} + \frac{dy}{dt}\frac{\partial A_z}{\partial y} + \frac{dz}{dt}\frac{\partial A_z}{\partial z}, \\ &= y\frac{\partial A_z}{\partial x} - x\frac{\partial A_z}{\partial y} = 0.\end{aligned}$$

By eliminating the parameter t in Eqs. (A.8)-(A.11), we can reduce the set of ODEs to three equations

$$\frac{dy}{dx} = -\frac{x}{y}, \tag{A.12}$$
$$\frac{dz}{dx} = 0, \tag{A.13}$$
$$\frac{dA_z}{dx} = 0. \tag{A.14}$$

We now note that the "constant" of integration in Eq. (A.14) has a functional dependence on the solutions to Eqs. (A.12) and (A.13). This is because the

ODEs are solved along characteristic curves; the constants of integration are constant along a particular characteristic, but can vary between characteristics. The solutions to Eqs. (A.12) and (A.13) are

$$x^2+y^2=a, \qquad z=b, \tag{A.15}$$

respectively, where a and b are the constants of integration. Thus, the solution for A_z is

$$A_z=\gamma\left(x^2+y^2,z\right), \tag{A.16}$$

where γ is an arbitrary function.

A.2 Solving the Simultaneous Equations

We will now solve Eqs. (A.5) and (A.6) simultaneously. Firstly, we differentiate Eq. (A.5) with respect to both x and y which gives:

$$\frac{\partial A_y}{\partial x}+\frac{\partial A_x}{\partial y}+x\frac{\partial^2 A_x}{\partial x\partial y}-y\frac{\partial^2 A_x}{\partial x^2}=0, \tag{A.17}$$

$$\frac{\partial A_y}{\partial y}+x\frac{\partial^2 A_x}{\partial y^2}-\frac{\partial A_x}{\partial x}-y\frac{\partial^2 A_x}{\partial x\partial y}=0, \tag{A.18}$$

respectively. Now, we substitute these expressions for $\frac{\partial A_y}{\partial x}$ and $\frac{\partial A_y}{\partial y}$ into Eq. (A.6), and obtain

$$A_x-x\left(-x\frac{\partial^2 A_x}{\partial y^2}+\frac{\partial A_x}{\partial x}+y\frac{\partial^2 A_x}{\partial x\partial y}\right)+y\left(-\frac{\partial A_x}{\partial y}-x\frac{\partial^2 A_x}{\partial x\partial y}+y\frac{\partial^2 A_x}{\partial x^2}\right)=0, \tag{A.19}$$

$$y^2\frac{\partial^2 A_x}{\partial x^2}-2xy\frac{\partial^2 A_x}{\partial x\partial y}+x^2\frac{\partial^2 A_x}{\partial y^2}-x\frac{\partial A_x}{\partial x}-y\frac{\partial A_x}{\partial y}+A_x=0. \tag{A.20}$$

We now have an equation containing only the unknown A_x that we can solve.

We begin to solve this equation by again using the method of characteristics. For second order PDEs, it is firstly necessary to determine the type of equation, either hyperbolic, parabolic or elliptic. This is done by calculating the discriminant b^2-4ac, where a,b,c are the coefficients of $\frac{\partial^2 A_x}{\partial x^2},\frac{\partial^2 A_x}{\partial x\partial y},\frac{\partial^2 A_x}{\partial y^2}$ respectively. This will then allow us to perform an appropriate change of variables from (x,y,z) to (ξ,η,z), where ξ and η are the characteristics [81]. The discriminant is

$$b^2-4ac=4x^2y^2-4x^2y^2=0. \tag{A.21}$$

Therefore, the characteristic equation is parabolic and has one repeated solu-

tion, which we take for ξ. The characteristic equation is the ODE [81]

$$y^2\left(\frac{dy}{dx}\right)^2 - 2xy\frac{dy}{dx} + x^2 = 0, \tag{A.22}$$

solving for $\frac{dy}{dx}$ gives

$$\frac{dy}{dx} = -\frac{x}{y}.$$

Hence, from Eq. (A.15), we know that the first characteristic is $\xi = a = x^2 + y^2$. Since there is only one root of the characteristic equation, we have complete freedom in the choice for η, provided that it is not the same as ξ. Given that we know that the symmetric gauge satisfies the commutator $\left[\hat{H}, \hat{L}_z\right] = 0$, and, specifically, that $A_x = y$ is a solution for Eq. (A.20), we choose $\eta = y$. By using the chain rule, we find the derivatives in Eq. (A.20).

$$\begin{aligned}
\frac{\partial A_x}{\partial x} &= 2x\frac{\partial A_x}{\partial \xi}, \\
\frac{\partial A_x}{\partial y} &= 2y\frac{\partial A_x}{\partial \xi} + \frac{\partial A_x}{\partial \eta}, \\
\frac{\partial^2 A_x}{\partial x^2} &= 4x^2\frac{\partial^2 A_x}{\partial \xi^2} + 2\frac{\partial A_x}{\partial \xi}, \\
\frac{\partial^2 A_x}{\partial y^2} &= 4y^2\frac{\partial^2 A_x}{\partial \xi^2} + 4y\frac{\partial^2 A_x}{\partial \xi \partial \eta} + \frac{\partial^2 A_x}{\partial \eta^2} + 2\frac{\partial A_x}{\partial \xi}, \\
\frac{\partial^2 A_x}{\partial x \partial y} &= 4xy\frac{\partial^2 A_x}{\partial \xi^2} + 2x\frac{\partial^2 A_x}{\partial \xi \partial \eta}.
\end{aligned}$$

Substituting into equation (A.20), we get

$$\begin{aligned}
&4x^2y^2\frac{\partial^2 A_x}{\partial \xi^2} + 2y^2\frac{\partial A_x}{\partial \xi} - 8x^2y^2\frac{\partial^2 A_x}{\partial \xi^2} - 4x^2y\frac{\partial^2 A_x}{\partial \xi \partial \eta} + 4x^2y^2\frac{\partial^2 A_x}{\partial \xi^2} + 4x^2y\frac{\partial^2 A_x}{\partial \xi \partial \eta}, \\
&+ x^2\frac{\partial^2 A_x}{\partial \eta^2} + 2x^2\frac{\partial A_x}{\partial \xi} - 2x^2\frac{\partial A_x}{\partial \xi} - 2y^2\frac{\partial A_x}{\partial \xi} - y\frac{\partial A_x}{\partial \eta} + A_x = 0,
\end{aligned}$$

$$x^2\frac{\partial^2 A_x}{\partial \eta^2} - y\frac{\partial A_x}{\partial \eta} + A_x = 0,$$

and completing the change of variables gives

$$\left(\xi - \eta^2\right)\frac{\partial^2 A_x}{\partial \eta^2} - \eta\frac{\partial A_x}{\partial \eta} + A_x = 0. \tag{A.23}$$

We have now completed a change of variables and reduced the complexity of the equation. The next step is to perform a reduction of order through the use

of the known solution $A_x = \eta$. The reduction used is

$$A_x = u\eta, \qquad \frac{\partial A_x}{\partial \eta} = \eta\frac{\partial u}{\partial \eta}, \qquad \frac{\partial^2 A_x}{\partial \eta^2} = \eta\frac{\partial^2 u}{\partial \eta^2} + 2\frac{\partial u}{\partial \eta},$$

which we substitute into Eq. (A.23) to give

$$\left(\xi - \eta^2\right)\left(\eta\frac{\partial^2 u}{\partial \eta^2} + 2\frac{\partial u}{\partial \eta}\right) - \eta^2\frac{\partial u}{\partial \eta} - \eta u + \eta u = 0,$$

$$\eta\left(\xi - \eta^2\right)\frac{\partial^2 u}{\partial \eta^2} + \left(2\xi - 3\eta^2\right)\frac{\partial u}{\partial \eta} = 0. \tag{A.24}$$

We now make the substitution $v = \frac{\partial u}{\partial \eta}$, obtaining

$$\eta\left(\xi - \eta^2\right)\frac{\partial v}{\partial \eta} + \left(2\xi - 3\eta^2\right)v = 0. \tag{A.25}$$

This equation can now be solved separably,

$$\int \frac{1}{v}dv = \int \left[\frac{3\eta^2 - 2\xi}{\eta\left(\xi - \eta^2\right)}\right]d\eta.$$

We decompose the denominator through the use of partial fractions, giving,

$$\begin{aligned}
\frac{3\eta^2 - 2\xi}{\eta\left(\xi - \eta^2\right)} &= \frac{I}{\eta} + \frac{J\eta + K}{\xi - \eta^2}, \\
&= \frac{I\left(\xi - \eta^2\right)}{\eta\left(\xi - \eta^2\right)} + \frac{\left(J\eta + K\right)\eta}{\eta\left(\xi - \eta^2\right)}, \\
3\eta^2 - 2\xi &= I\left(\xi - \eta^2\right) + J\eta^2 + K\eta.
\end{aligned}$$

By comparing coefficients, we see that $K = 0$, $-I + J = 3 \Rightarrow I = -2$, $J = 1$,

$$\frac{3\eta^2 - 2\xi}{\eta\left(\xi - \eta^2\right)} = -\frac{2}{\eta} + \frac{\eta}{\xi - \eta^2}.$$

Returning to the solution of equation (A.25), we find

$$\begin{aligned}
\int \frac{1}{v} dv &= -\int \frac{2}{\eta} d\eta + \int \frac{\eta}{\xi - \eta^2} d\eta, \\
&= -\int \frac{2}{\eta} d\eta - \frac{1}{2} \int \frac{-2\eta}{\xi - \eta^2} d\eta, \\
\ln v &= -2 \ln \eta - \frac{1}{2} \ln \left| \xi - \eta^2 \right| + \ln \left[\alpha \left(\xi \right) \right], \\
&= \ln \eta^{-2} + \ln \left(\xi - \eta^2 \right)^{-\frac{1}{2}} + \ln \left[\alpha \left(\xi \right) \right], \\
&= \ln \left[\frac{\alpha \left(\xi \right)}{\eta^2 \left(\xi - \eta^2 \right)^{\frac{1}{2}}} \right], \\
v &= \frac{\alpha \left(\xi \right)}{\eta^2 \left(\xi - \eta^2 \right)^{\frac{1}{2}}},
\end{aligned}$$

where α is an arbitrary function, and we note that $\xi - \eta^2 = x^2 + y^2 - y^2 = x^2 > 0$, hence, $\xi - \eta^2$ is always positive.

Now that we have a solution to (A.25), we must reverse our substitutions to get a solution for A_x. Firstly, we integrate v to get u,

$$u = \alpha \left(\xi \right) \int \frac{1}{\eta^2 \left(\xi - \eta^2 \right)^{\frac{1}{2}}} d\eta. \tag{A.26}$$

We make the substitution $\eta = \xi^{\frac{1}{2}} \sin \theta$,

$$\begin{aligned}
u &= \xi^{\frac{1}{2}} \alpha \left(\xi \right) \int \frac{\cos \theta}{\xi \sin^2 \theta \left(\xi - \xi \sin^2 \theta \right)^{\frac{1}{2}}} d\theta, \\
&= \xi^{\frac{1}{2}} \alpha \left(\xi \right) \int \frac{\cos \theta}{\xi \sin^2 \theta \left(\xi \cos^2 \theta \right)^{\frac{1}{2}}} d\theta, \\
&= \frac{\alpha \left(\xi \right)}{\xi} \int \frac{1}{\sin^2 \theta} d\theta, \\
&= -\frac{\alpha \left(\xi \right)}{\xi} \cot \theta + \beta \left(\xi \right), \\
&= -\frac{\alpha \left(\xi \right)}{\xi} \cot \left[\sin^{-1} \left(\frac{\eta}{\xi^{\frac{1}{2}}} \right) \right] + \beta \left(\xi \right), \\
&= -\frac{\alpha \left(\xi \right)}{\xi} \frac{\xi^{\frac{1}{2}}}{\eta} \left(1 - \frac{\eta^2}{\xi} \right)^{\frac{1}{2}} + \beta \left(\xi \right), \\
&= -\frac{\alpha \left(\xi \right)}{\xi \eta} \left(\xi - \eta^2 \right)^{\frac{1}{2}} + \beta \left(\xi \right),
\end{aligned}$$

where β is another arbitrary function. Next, we write $A_x = u\eta$, obtaining

$$A_x = \alpha(\xi)\left(\xi - \eta^2\right)^{\frac{1}{2}} + \eta\beta(\xi), \tag{A.27}$$

where we absorb the factor of $-\frac{1}{\xi}$ into α. Finally, we substitute back from (ξ, η, z) to (x, y, z),

$$\begin{aligned} A_x &= \alpha\left(x^2+y^2, z\right)\left(x^2+y^2-y^2\right)^{\frac{1}{2}} + y\beta\left(x^2+y^2, z\right), \\ &= x\alpha\left(x^2+y^2, z\right) + y\beta\left(x^2+y^2, z\right), \end{aligned} \tag{A.28}$$

to give the solution for A_x. We find A_y from equation (A.5),

$$\begin{aligned} A_y =& y\frac{\partial A_x}{\partial x} - x\frac{\partial A_x}{\partial y}, \\ =& y\left[\alpha\left(x^2+y^2, z\right) + 2x^2\alpha'\left(x^2+y^2, z\right) + 2xy\beta'\left(x^2+y^2, z\right)\right] \\ & - x\left[2xy\alpha'\left(x^2+y^2, z\right) + \beta\left(x^2+y^2, z\right) + 2y^2\beta'\left(x^2+y^2, z\right)\right], \\ =& y\alpha\left(x^2+y^2, z\right) - x\beta\left(x^2+y^2, z\right), \end{aligned}$$

giving us solutions for all three components.

We will now verify that the solutions for A_x, A_y, A_z, satisfy the remaining equation, Eq. (A.4)

$$\begin{aligned} & ix\frac{\partial}{\partial y}\left(\frac{\partial A_x}{\partial x} + \frac{\partial A_y}{\partial y} + \frac{\partial A_z}{\partial z}\right) - x\frac{\partial A^2}{\partial y} - iy\frac{\partial}{\partial x}\left(\frac{\partial A_x}{\partial x} + \frac{\partial A_y}{\partial y} + \frac{\partial A_z}{\partial z}\right) + y\frac{\partial A^2}{\partial x} \\ =& ix\frac{\partial}{\partial y}\left(2\alpha + 2x^2\alpha' + 2xy\beta' + 2y^2\alpha' - 2xy\beta' + \frac{\partial \gamma}{\partial z}\right) \\ & - iy\frac{\partial}{\partial x}\left(2\alpha + 2x^2\alpha' + 2xy\beta' + 2y^2\alpha' - 2xy\beta' + \frac{\partial \gamma}{\partial z}\right) \\ & - x\left(4x^2y\alpha\alpha' + 2y\beta^2 + 4y^3\beta\beta' + 2y\alpha^2 + 4y^3\alpha\alpha' + 4x^2y\beta\beta' + 4y\gamma\gamma'\right) \\ & + y\left(2x\alpha^2 + 4x^3\alpha\alpha' + 4xy^2\beta\beta' + 4xy^2\alpha\alpha' + 2x\beta^2 + 4x^3\beta\beta' + 4x\gamma\gamma'\right), \\ =& i\left(4xy\alpha' + 4xy\alpha' + 4x^3y\alpha'' + 4xy^3\alpha'' + 2xy\frac{\partial \gamma'}{\partial z}\right. \\ & \left. -4xy\alpha' - 4x^3y\alpha'' - 4xy\alpha' - 4xy^3\alpha'' - 2xy\frac{\partial \gamma'}{\partial z}\right) = 0, \end{aligned}$$

where a prime denotes differentiation with respect to $\left(x^2+y^2\right)$.

Therefore, the form of the vector potential required for $\left[\hat{H}, \hat{L}_z\right] = 0$ is,

$$\mathbf{A} = \left[x\alpha\left(x^2+y^2, z\right) + y\beta\left(x^2+y^2, z\right), y\alpha\left(x^2+y^2, z\right) - x\beta\left(x^2+y^2, z\right), \gamma\left(x^2+y^2, z\right)\right], \tag{A.29}$$

or, in cylindrical polar coordinates (r,θ,z),

$$\mathbf{A} = \left[r\alpha\left(r^2,z\right), -r\beta\left(r^2,z\right), \gamma\left(r^2,z\right)\right]. \tag{A.30}$$

This form of the vector potential satisfies the condition $\left[\hat{H},\hat{L}_z\right]=0$ for wavefunctions with $\frac{\partial\psi}{\partial x}$, $\frac{\partial\psi}{\partial y}$ and $\frac{\partial\psi}{\partial z}$ all independent of each other. Clearly, vector potentials that are not of the form of Eq. (A.29) do not satisfy the condition. But in order to ensure vector potentials of this form satisfy this condition for an arbitrary wavefunction, we use the properties of the vector potentials to solve the original commutator Eq. (A.3) for an arbitrary wavefunction. This gives

$$\begin{aligned}
\left[\hat{H},\hat{L}_z\right]\psi = -i\Bigg\{ & 2\left(x\alpha+y\beta\right)\frac{\partial\psi}{\partial y} - 2\left(y\alpha-x\beta\right)\frac{\partial\psi}{\partial x} \\
& -2x\left[\left(2xy\alpha'+\beta+2y^2\beta'\right)\frac{\partial\psi}{\partial x}+\left(\alpha+2y^2\alpha'-2xy\beta'\right)\frac{\partial\psi}{\partial y}+2y\gamma'\frac{\partial\psi}{\partial z}\right] \\
& +2y\left[\left(\alpha+2x^2\alpha'+2xy\beta'\right)\frac{\partial\psi}{\partial x}+\left(2xy\alpha'-\beta-2x^2\beta'\right)\frac{\partial\psi}{\partial y}+2x\gamma'\frac{\partial\psi}{\partial z}\right] \\
& -x\psi\frac{\partial}{\partial y}\left(2\alpha+2x^2\alpha'+2xy\beta'+2y^2\alpha'-2xy\beta'+\frac{\partial\gamma}{\partial z}\right) \\
& +y\psi\frac{\partial}{\partial x}\left(2\alpha+2x^2\alpha'+2xy\beta'+2y^2\alpha'-2xy\beta'+\frac{\partial\gamma}{\partial z}\right)\Bigg\} \\
& -x\psi\left(4x^2y\alpha\alpha'+2y\beta^2+4y^3\beta\beta'+2y\alpha^2+4y^3\alpha\alpha'+4x^2y\beta\beta'+4y\gamma\gamma'\right) \\
& +y\psi\left(2x\alpha^2+4x^3\alpha\alpha'+4xy^2\beta\beta'+4xy^2\alpha\alpha'+2x\beta^2+4x^3\beta\beta'+4x\gamma\gamma'\right).
\end{aligned}$$

This simplifies to

$$\begin{aligned}
\left[\hat{H},\hat{L}_z\right]\psi =& ix\psi\frac{\partial}{\partial y}\left(2\alpha+2x^2\alpha'+2y^2\alpha'+\frac{\partial\gamma}{\partial z}\right)-iy\psi\frac{\partial}{\partial x}\left(2\alpha+2x^2\alpha'+2y^2\alpha'+\frac{\partial\gamma}{\partial z}\right), \\
=& i\Bigg(4xy\alpha'+4xy\alpha'+4x^3y\alpha''+4xy^3\alpha''+2xy\frac{\partial\gamma'}{\partial z} \\
& -4xy\alpha'-4x^3y\alpha''-4xy\alpha'-4xy^3\alpha''-2xy\frac{\partial\gamma'}{\partial z}\Bigg), \\
=& 0.
\end{aligned}$$

Thus, the vector potentials of the form Eq. (A.29) fulfill the condition $\left[\hat{H},\hat{L}_z\right]=0$, and, in these gauges, $\hat{L}_z$ is a constant of motion.

Appendix B

Gauge Transformations between Vector Potentials for which L_z is a Constant of Motion

In Appendix A, we found that $\left[\hat{H},\hat{L}_z\right]=0$ only when $\mathbf{A}(\mathbf{r})$ is of the form of Eq. (A.29). We now consider a gauge transformation between two gauges of the form of Eq. (A.29). A vector potential of this form gives the magnetic field

$$\begin{aligned}\mathbf{B}(\mathbf{r}) &= \nabla\times\mathbf{A}(\mathbf{r}),\\ &= \nabla\times[x\alpha+y\beta, y\alpha-x\beta,\gamma],\\ &= \left[2y\gamma'-y\frac{\partial\alpha}{\partial z}+x\frac{\partial\beta}{\partial z}, x\frac{\partial\alpha}{\partial z}+y\frac{\partial\beta}{\partial z}-2x\gamma', 2xy\alpha'-\beta-2x^2\beta'-2xy\alpha'-\beta-2y^2\beta'\right],\\ &= \left[2y\gamma'-y\frac{\partial\alpha}{\partial z}+x\frac{\partial\beta}{\partial z}, x\frac{\partial\alpha}{\partial z}+y\frac{\partial\beta}{\partial z}-2x\gamma', -2\beta-\left(2x^2+2y^2\right)\beta'\right].\end{aligned}$$

Since any modification to β would affect the -2β term in the z-component of $\mathbf{B}(\mathbf{r})$, and $\mathbf{B}(\mathbf{r})$ must be unchanged by gauge transformations, β must be constant in a gauge transformation.

A gauge transformation is given by $\mathbf{A}'(\mathbf{r})=\mathbf{A}(\mathbf{r})+\nabla\chi$ and takes the form

$$\begin{aligned}\nabla\chi &= \mathbf{A}'(\mathbf{r})-\mathbf{A}(\mathbf{r}),\\ &= [x\Delta\alpha+y\Delta\beta, y\Delta\alpha-x\Delta\beta,\Delta\gamma],\\ &= [x\Delta\alpha, y\Delta\alpha,\Delta\gamma],\end{aligned}\tag{B.1}$$

using that $\Delta\beta$ must be zero. We obtain $\chi(\mathbf{r})$ by integrating each of the compo-

nents of the vector $\nabla\chi$ in Eq. (B.1):

$$\begin{aligned}\int x\Delta\alpha dx &= \frac{\lambda\left(x^2+y^2,z\right)}{2},\\ \int y\Delta\alpha dy &= \frac{\mu\left(x^2+y^2,z\right)}{2},\\ \int \Delta\gamma dz &= \nu\left(x^2+y^2,z\right).\end{aligned}$$

Clearly then, the scalar field $\chi(\mathbf{r})$ must be a function $\chi\left(x^2+y^2,z\right)$.

Finally, we demonstrate that $[\mathbf{r}\times\mathbf{j}_p]_z$ is unchanged by gauge transformations between gauges of the form Eq. (A.29). The paramagnetic current density transforms according to $\mathbf{j}'_p(\mathbf{r}) = \mathbf{j}_p(\mathbf{r}) + \rho(\mathbf{r})\nabla\chi$

$$\begin{aligned}\left[\mathbf{r}\times\mathbf{j}'_p\right]_z &= \left\{\mathbf{r}\times\left[\mathbf{j}_p+\rho(\mathbf{r})\nabla\chi\right]\right\}_z,\\ &= \left[\mathbf{r}\times\mathbf{j}_p\right]_z + \left[\mathbf{r}\times\rho(\mathbf{r})\nabla\chi\right]_z,\\ &= \left[\mathbf{r}\times\mathbf{j}_p\right]_z + \left[\mathbf{r}\times\rho(\mathbf{r})\left(x\Delta\alpha, y\Delta\alpha, \Delta\gamma\right)\right]_z,\\ &= \left[\mathbf{r}\times\mathbf{j}_p\right]_z + \rho(\mathbf{r})\left(xy\Delta\alpha - xy\Delta\alpha\right),\\ &= \left[\mathbf{r}\times\mathbf{j}_p\right]_z.\end{aligned}$$

So, when we are in any gauge of the form of Eq. (A.29), and when we transform between any of these gauges, both $\hat{L}_z$ and $[\mathbf{r}\times\mathbf{j}_p]_z$ are unaffected.

Appendix C

Evaluation of Densities for Model Systems

Having solved the Schrödinger equation for our model systems, we must use the resulting wavefunction in order to determine an expression for the particle density and, for the magnetic systems, the paramagnetic current density, in order to study these quantities with the metric space approach to quantum mechanics. In this Appendix, we will evaluate the densities for the model systems that we study in Chapters 3, 4, and 5.

C.1 Conversion of Coordinates

In time-independent quantum mechanics, the particle density is defined as the probability of finding one of the particles in the system within the volume element $d\mathbf{r}_1$ about the point $\mathbf{r}_1$, independently of the positions of the other particles [1]. As such the particle density is a function of one of the particle coordinates. However, Eqs. (3.25), (3.34) and (5.9) for the ground-state wavefunctions of the 2D magnetic Hooke's Atom, ISI system and 3D isotropic, non-magnetic Hooke's Atom respectively are in terms of relative motion and centre of mass coordinates, $(\mathbf{r}, \mathbf{R})$.

Before we can proceed with the calculation of the densities for these systems, we must therefore make a coordinate transformation. Following the approach of Taut *et al.* [42], we will write the centre of mass coordinate in terms of the relative motion coordinate and a particle coordinate.

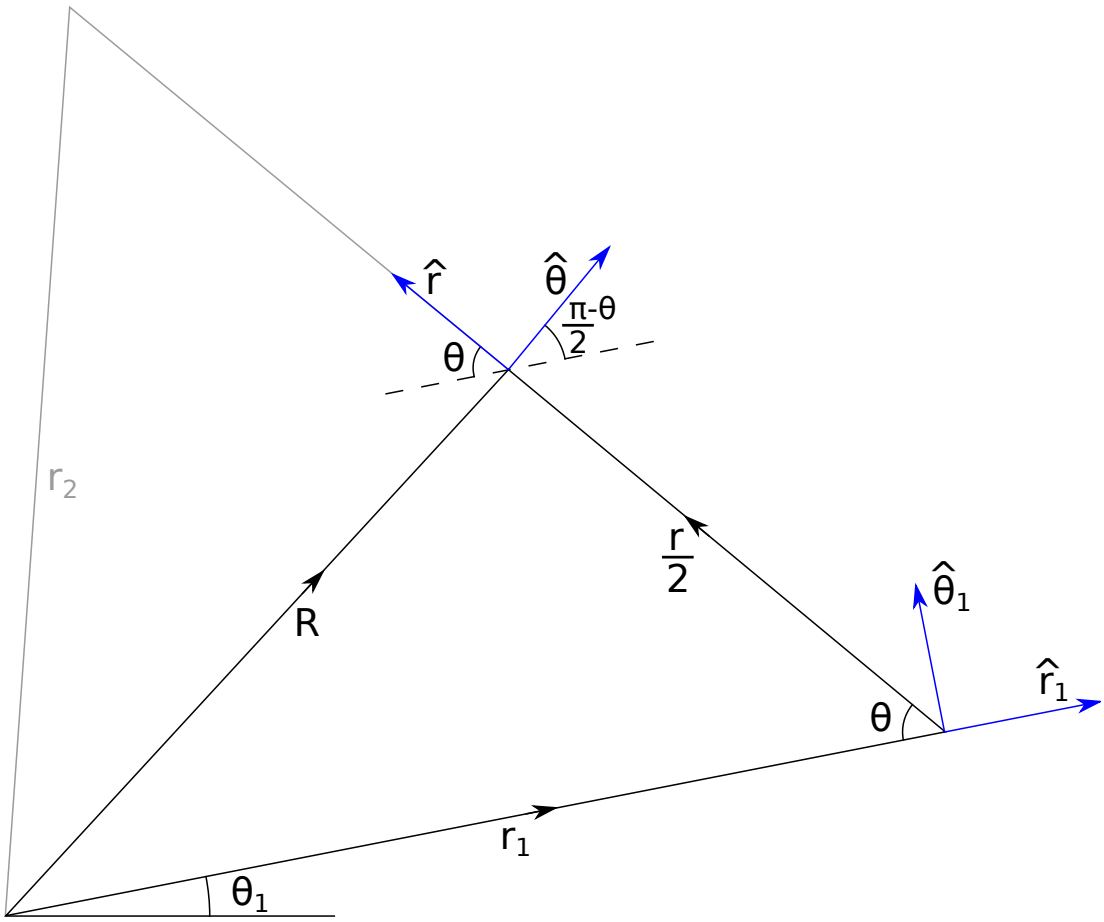

Figure C.1: The relationship between the vectors $\mathbf{R}, \frac{\mathbf{r}}{2}$ and $\mathbf{r}_1$ and the unit vectors for the $\mathbf{r}_1$ and $\mathbf{r}$ coordinates in 2D.

C.1.1 Two Dimensions

In two dimensions, the coordinates $\mathbf{R}, \frac{\mathbf{r}}{2}$ and $\mathbf{r}_1$ form a triangle in the plane, as shown in Fig. C.1. Hence, we can write the coordinate R in terms of the others using the cosine rule,

$$R = \sqrt{r_1^2 + \frac{r^2}{4} - r_1 r \cos\theta}. \tag{C.1}$$

When evaluating the paramagnetic current density, we must also be able to write the unit vectors associated to the relative motion coordinate in terms of the unit vectors for the particle coordinate. From Fig. C.1, we can determine that

$$\hat{r} = -\cos\theta\hat{r}_1 + \sin\theta\hat{\theta}_1, \tag{C.2}$$

$$\begin{aligned}\hat{\theta} &= \cos\left(\frac{\pi}{2} - \theta\right)\hat{r}_1 + \sin\left(\frac{\pi}{2} - \theta\right)\hat{\theta}_1, \\ &= \sin\theta\hat{r}_1 + \cos\theta\hat{\theta}_1.\end{aligned} \tag{C.3}$$

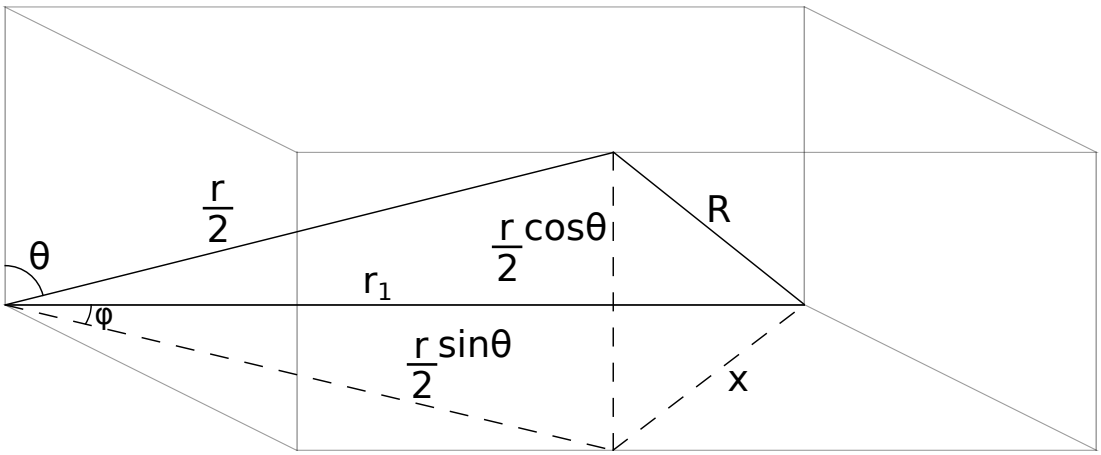

Figure C.2: The relationship between the vectors $\mathbf{R}, \frac{\mathbf{r}}{2}$ and $\mathbf{r}_1$ in 3D.

C.1.2 Three Dimensions

The relationships between the vectors $\mathbf{R}, \frac{\mathbf{r}}{2}$ and $\mathbf{r}_1$ in three dimensions are shown in Fig. C.2. We can determine the length of the line x using the cosine rule,

$$x^2 = r_1^2 + \frac{r^2}{4}\sin^2\theta - r_1 r \sin\theta\cos\phi. \tag{C.4}$$

Hence, using Pythagoras' theorem,

$$\begin{aligned} R^2 &= r_1^2 + \frac{r^2}{4}\sin^2\theta + \frac{r^2}{4}\cos^2\theta - r_1 r\sin\theta\cos\phi, \\ R &= \sqrt{r_1^2 + \frac{r^2}{4} - r_1 r\sin\theta\cos\phi}. \end{aligned} \tag{C.5}$$

C.2 Two-Dimensional Magnetic Hooke's Atom

In terms of the particle and relative coordinates, the ground state wavefunction for the magnetic Hooke's Atom is given by,

$$\psi\left(\mathbf{r}, \sqrt{r_1^2 + \frac{r^2}{4} - r_1 r\cos\theta}\right) = \frac{1}{\pi}\sqrt{\frac{\widetilde{\omega}}{r}} e^{im\theta} e^{-\widetilde{\omega}\left(r_1^2 + \frac{r^2}{4} - r_1 r\cos\theta\right)} u(r), \tag{C.6}$$

using Eq. (3.25) and the fact that this is a 2D system. We will use this form of the wavefunction in order to evaluate the particle and paramagnetic current densities.

C.2.1 Particle Density

We evaluate the particle density of the magnetic Hooke's Atom using [42],

$$\rho(\mathbf{r}_1) = 2\int\int \left|\psi\left(\mathbf{r}, \sqrt{r_1^2 + \frac{r^2}{4} - r_1 r\cos\theta}\right)\right|^2 d\mathbf{r}. \tag{C.7}$$

Inserting Eq. (C.6) into Eq. (C.7) gives,

$$\begin{aligned}\rho(\mathbf{r}_1) &= \frac{2\widetilde{\omega}}{\pi^2} e^{-2\widetilde{\omega}r_1^2} \int_0^\infty e^{-\frac{\widetilde{\omega}r^2}{2}} |u(r)|^2 \int_0^{2\pi} e^{2\widetilde{\omega}r_1 r\cos\theta} d\theta dr, \\ &= \frac{2\widetilde{\omega}}{\pi^2} e^{-2\widetilde{\omega}r_1^2} \int_0^\infty e^{-\frac{\widetilde{\omega}r^2}{2}} |u(r)|^2 \left(\int_0^{\pi} e^{2\widetilde{\omega}r_1 r\cos\theta} d\theta + \int_\pi^{2\pi} e^{2\widetilde{\omega}r_1 r\cos\theta} d\theta\right) dr,\end{aligned}$$

At this point, we note that the theta integrals define a modified Bessel function of the first kind. The definition of a modified Bessel function as an integral is [112]

$$I_n(z) = \frac{1}{\pi}\int_0^\pi e^{z\cos\theta}\cos(n\theta) d\theta. \tag{C.8}$$

Returning to the density, and after recasting the limits of the second theta integral, we have,

$$\begin{aligned}\rho(\mathbf{r}_1) &= \frac{2\widetilde{\omega}}{\pi^2} e^{-2\widetilde{\omega}r_1^2} \int_0^\infty e^{-\frac{\widetilde{\omega}r^2}{2}} |u(r)|^2 \left(\int_0^{\pi} e^{2\widetilde{\omega}r_1 r\cos\theta} d\theta + \int_0^{\pi} e^{2\widetilde{\omega}r_1 r\cos(\theta-\pi)} d(\theta-\pi)\right) dr, \\ &= \frac{2\widetilde{\omega}}{\pi} e^{-2\widetilde{\omega}r_1^2} \int_0^\infty e^{-\frac{\widetilde{\omega}r^2}{2}} |u(r)|^2 \left[I_0(2\widetilde{\omega}r_1 r) + I_0(2\widetilde{\omega}r_1 r)\right] dr.\end{aligned}$$

Hence, the particle density of the magnetic Hooke's Atom is given by,

$$\rho(\mathbf{r}_1) = \frac{4\widetilde{\omega}}{\pi} e^{-2\widetilde{\omega}r_1^2} \int_0^\infty e^{-\frac{\widetilde{\omega}r^2}{2}} |u(r)|^2 I_0(2\widetilde{\omega}r_1 r) dr, \tag{C.9}$$

in agreement with Ref. [42].

C.2.2 Paramagnetic Current Density

With the wavefunction for Hooke's Atom written in terms of the coordinates $\left(\mathbf{r}, \sqrt{r_1^2 + \frac{r^2}{4} - r_1 r\cos\theta}\right)$ in Eq. (C.6), the paramagnetic current density is given by [42]

$$\mathbf{j}_p(\mathbf{r}_1) = -i\int \left[\psi^*\nabla_r\psi - \psi\nabla_r\psi^*\right] d\mathbf{r}. \tag{C.10}$$

The gradient of the wavefunction is

$$\begin{aligned}\nabla_r\psi =& \frac{\partial\psi}{\partial r}\hat{r} + \frac{1}{r}\frac{\partial\psi}{\partial\theta}\hat{\theta},\\ =& \frac{1}{\pi}\sqrt{\widetilde{\omega}}e^{-\widetilde{\omega}r_1^2}\left[e^{im\theta}\frac{\partial}{\partial r}\left(\frac{e^{-\frac{\widetilde{\omega}}{4}r^2}e^{\widetilde{\omega}r_1 r\cos\theta}u(r)}{\sqrt{r}}\right)\hat{r} + \frac{e^{-\frac{\widetilde{\omega}}{4}r^2}u(r)}{r^{\frac{3}{2}}}\frac{\partial}{\partial\theta}\left(e^{im\theta}e^{\widetilde{\omega}r_1 r\cos\theta}\right)\hat{\theta}\right],\end{aligned}$$

and evaluating the derivatives gives

$$\begin{aligned}\nabla_r\psi =& \frac{1}{\pi}\sqrt{\frac{\widetilde{\omega}}{r}}e^{-\widetilde{\omega}r_1^2}e^{im\theta}e^{-\frac{\widetilde{\omega}}{4}r^2}e^{\widetilde{\omega}r_1 r\cos\theta}u(r)\times\\ &\left[\left(-\frac{\widetilde{\omega}r}{2} + \widetilde{\omega}r_1\cos\theta + \frac{1}{u(r)}\frac{du}{dr} - \frac{1}{2r}\right)\hat{r} + \frac{(im - \widetilde{\omega}r_1 r\sin\theta)}{r}\hat{\theta}\right],\end{aligned} \tag{C.11}$$

and for the complex conjugate

$$\begin{aligned}\nabla_r\psi^* =& \frac{1}{\pi}\sqrt{\frac{\widetilde{\omega}}{r}}e^{-\widetilde{\omega}r_1^2}e^{-im\theta}e^{-\frac{\widetilde{\omega}}{4}r^2}e^{\widetilde{\omega}r_1 r\cos\theta}u(r)\times\\ &\left[\left(-\frac{\widetilde{\omega}r}{2} + \widetilde{\omega}r_1\cos\theta + \frac{1}{u(r)}\frac{du}{dr} - \frac{1}{2r}\right)\hat{r} + \frac{(-im - \widetilde{\omega}r_1 r\sin\theta)}{r}\hat{\theta}\right].\end{aligned} \tag{C.12}$$

Forming the terms in the integrand of Eq. (C.10), we have,

$$\begin{aligned}\psi^*\nabla_r\psi =& \frac{1}{\pi^2}\frac{\widetilde{\omega}}{r}e^{-2\widetilde{\omega}r_1^2}e^{-\frac{\widetilde{\omega}}{2}r^2}e^{2\widetilde{\omega}r_1 r\cos\theta}u(r)^2\times\\ &\left[\left(-\frac{\widetilde{\omega}r}{2} + \widetilde{\omega}r_1\cos\theta + \frac{1}{u(r)}\frac{du}{dr} - \frac{1}{2r}\right)\hat{r} + \frac{(im - \widetilde{\omega}r_1 r\sin\theta)}{r}\hat{\theta}\right],\end{aligned} \tag{C.13}$$

and,

$$\begin{aligned}\psi\nabla_r\psi^* =& \frac{1}{\pi^2}\frac{\widetilde{\omega}}{r}e^{-2\widetilde{\omega}r_1^2}e^{-\frac{\widetilde{\omega}}{2}r^2}e^{2\widetilde{\omega}r_1 r\cos\theta}u(r)^2\times\\ &\left[\left(-\frac{\widetilde{\omega}r}{2} + \widetilde{\omega}r_1\cos\theta + \frac{1}{u(r)}\frac{du}{dr} - \frac{1}{2r}\right)\hat{r} + \frac{(-im - \widetilde{\omega}r_1 r\sin\theta)}{r}\hat{\theta}\right],\end{aligned} \tag{C.14}$$

Thus, we form the integrand in Eq. (C.10) by subtracting Eq. (C.14) from Eq. (C.13), and get

$$\psi^*\nabla_r\psi - \psi\nabla_r\psi^* = \frac{2im\widetilde{\omega}}{\pi^2}\frac{1}{r^2}e^{-2\widetilde{\omega}r_1^2}e^{-\frac{\widetilde{\omega}}{2}r^2}e^{2\widetilde{\omega}r_1 r\cos\theta}u(r)^2\,\hat{\theta}. \tag{C.15}$$

Equation (C.15) is a vector represented in the relative motion coordinates. Since we will integrate over this coordinate, we wish to rewrite Eq. (C.15) in terms of the particle coordinates (r_1, θ_1). Substituting the unit vector from Eq. (C.3)

into Eq. (C.15) gives

$$\psi^*\nabla_r\psi - \psi\nabla_r\psi^* = \frac{2im\widetilde{\omega}}{\pi^2}\frac{1}{r^2}e^{-2\widetilde{\omega}r_1^2}e^{-\frac{\widetilde{\omega}}{2}r^2}e^{2\widetilde{\omega}r_1 r\cos\theta}u(r)^2\left(\sin\theta\hat{r}_1+\cos\theta\hat{\theta}_1\right). \tag{C.16}$$

Now we have written the integrand in the desired coordinate system, we can evaluate the paramagnetic current density using Eq. (C.10),

$$\begin{aligned}\mathbf{j}_p(\mathbf{r}_1) &= -i\int_0^\infty\int_0^{2\pi}\frac{2im\widetilde{\omega}}{\pi^2}\frac{1}{r}e^{-2\widetilde{\omega}r_1^2}e^{-\frac{\widetilde{\omega}}{2}r^2}e^{2\widetilde{\omega}r_1 r\cos\theta}u(r)^2\left(\sin\theta\hat{r}_1+\cos\theta\hat{\theta}_1\right)drd\theta,\\ &= \frac{2m\widetilde{\omega}}{\pi}e^{-2\widetilde{\omega}r_1^2}\int_0^\infty\frac{e^{-\frac{\widetilde{\omega}}{2}r^2}u(r)^2}{r}\frac{1}{\pi}\int_0^{2\pi}e^{2\widetilde{\omega}r_1 r\cos\theta}\left(\sin\theta\hat{r}_1+\cos\theta\hat{\theta}_1\right)drd\theta.\end{aligned}$$

For the first term in the theta integral, we have from tables of integrals [112],

$$\int_0^{2\pi}e^{2\widetilde{\omega}r_1 r\cos\theta}\sin\theta d\theta = 0, \tag{C.17}$$

and Eq. (C.8) shows that the second term defines a first order modified Bessel function,

$$\begin{aligned}\mathbf{j}_p(\mathbf{r}_1) =& \frac{2m\widetilde{\omega}}{\pi}e^{-2\widetilde{\omega}r_1^2}\int_0^\infty\frac{e^{-\frac{\widetilde{\omega}}{2}r^2}u(r)^2}{r}\frac{1}{\pi}\left(\int_0^\pi e^{2\widetilde{\omega}r_1 r\cos\theta}\cos\theta d\theta+\int_\pi^{2\pi}e^{2\widetilde{\omega}r_1 r\cos\theta}\cos\theta d\theta\right)\hat{\theta}_1 dr,\\ =& \frac{2m\widetilde{\omega}}{\pi}e^{-2\widetilde{\omega}r_1^2}\int_0^\infty\frac{e^{-\frac{\widetilde{\omega}}{2}r^2}u(r)^2}{r}\left[I_1(2\widetilde{\omega}r_1 r)+I_1(2\widetilde{\omega}r_1 r)\right]\hat{\theta}_1 dr,\end{aligned}$$

Therefore, the paramagnetic current density for the magnetic Hooke's Atom is given by

$$\mathbf{j}_p(\mathbf{r}_1) = \hat{\theta}_1\frac{4m\widetilde{\omega}}{\pi}e^{-2\widetilde{\omega}r_1^2}\int_0^\infty\frac{e^{-\frac{\widetilde{\omega}}{2}r^2}u(r)^2 I_1(2\widetilde{\omega}r_1 r)}{r}dr. \tag{C.18}$$

in agreement with Ref. [42].

C.3 Inverse Square Interaction System

The ground state wavefunction of the Inverse Square Interaction (ISI) system is expressed in terms of the relative motion coordinate and a particle coordinate as,

$$\psi\left(\mathbf{r},\sqrt{r_1^2+\frac{r^2}{4}-r_1 r\cos\theta}\right) = \frac{\widetilde{\omega}}{\pi}\sqrt{\frac{1}{\Gamma(\mu+1)}}\left(\sqrt{\frac{\widetilde{\omega}}{2}}r\right)^\mu e^{im\theta}e^{-\frac{\widetilde{\omega}r^2}{4}}e^{-\widetilde{\omega}\left(r_1^2+\frac{r^2}{4}-r_1 r\cos\theta\right)}. \tag{C.19}$$

C.3.1 Particle Density

By substituting Eq. (C.19) into Eq. (C.7), we see that the particle density of the ISI system is given by,

$$\begin{aligned}\rho(\mathbf{r}_1) =& 2\left(\frac{\widetilde{\omega}}{\pi}\right)^2 \frac{1}{\Gamma(\mu+1)}\left(\frac{\widetilde{\omega}}{2}\right)^{\mu} e^{-2\widetilde{\omega}r_1^2}\int_0^{\infty} r^{2\mu} e^{-\widetilde{\omega}r^2}\int_0^{2\pi} e^{2\widetilde{\omega}r_1 r\cos\theta} r\,d\theta\,dr,\\ =& 2\left(\frac{\widetilde{\omega}}{\pi}\right)^2 \frac{1}{\Gamma(\mu+1)}\left(\frac{\widetilde{\omega}}{2}\right)^{\mu} e^{-2\widetilde{\omega}r_1^2}\times\\ & \int_0^{\infty} r^{(2\mu+1)} e^{-\widetilde{\omega}r^2}\left(\int_0^{\pi} e^{2\widetilde{\omega}r_1 r\cos\theta} + \int_{\pi}^{2\pi} e^{2\widetilde{\omega}r_1 r\cos\theta}\right) d\theta\,dr.\end{aligned}$$

We again use Eq. (C.8) in order to introduce a modified Bessel function and obtain an expression for the density,

$$\rho(\mathbf{r}_1) = \frac{4\widetilde{\omega}^2}{\pi}\frac{1}{\Gamma(\mu+1)}\left(\frac{\widetilde{\omega}}{2}\right)^{\mu} e^{-2\widetilde{\omega}r_1^2}\int_0^{\infty} r^{(2\mu+1)} e^{-\widetilde{\omega}r^2} I_0(2\widetilde{\omega}r_1 r)\,dr. \tag{C.20}$$

C.3.2 Paramagnetic Current Density

The wavefunction of the ISI system is given by Eq. (C.19). The gradient of this wavefunction is,

$$\begin{aligned}\nabla_r\psi =& \frac{\partial\psi}{\partial r}\hat{r} + \frac{1}{r}\frac{\partial\psi}{\partial\theta}\hat{\theta},\\ =& \frac{\widetilde{\omega}}{\pi}\sqrt{\frac{1}{\Gamma(\mu+1)}}\left(\sqrt{\frac{\widetilde{\omega}}{2}}\right)^{\mu} e^{-\widetilde{\omega}r_1^2}\times\\ & \left[e^{im\theta}\frac{\partial}{\partial r}\left(r^{\mu}e^{-\frac{\widetilde{\omega}r^2}{2}}e^{\widetilde{\omega}r_1 r\cos\theta}\right)\hat{r} + r^{\mu-1}e^{-\frac{\widetilde{\omega}r^2}{2}}\frac{\partial}{\partial\theta}\left(e^{im\theta}e^{\widetilde{\omega}r_1 r\cos\theta}\right)\hat{\theta}\right],\\ =& \frac{\widetilde{\omega}}{\pi}\sqrt{\frac{1}{\Gamma(\mu+1)}}\left(\sqrt{\frac{\widetilde{\omega}}{2}}r\right)^{\mu} e^{im\theta}e^{-\widetilde{\omega}\left(r_1^2+\frac{r^2}{2}-r_1 r\cos\theta\right)}\times\\ & \left[\left(\frac{\mu}{r}-\widetilde{\omega}r+\widetilde{\omega}r_1\cos\theta\right)\hat{r} + \frac{(im-\widetilde{\omega}r_1 r\sin\theta)}{r}\hat{\theta}\right],\end{aligned}$$

and for the complex conjugate,

$$\begin{aligned}\nabla_r\psi^* =& \frac{\widetilde{\omega}}{\pi}\sqrt{\frac{1}{\Gamma(\mu+1)}}\left(\sqrt{\frac{\widetilde{\omega}}{2}}r\right)^{\mu} e^{-im\theta}e^{-\widetilde{\omega}\left(r_1^2+\frac{r^2}{2}-r_1 r\cos\theta\right)}\times\\ & \left[\left(\frac{\mu}{r}-\widetilde{\omega}r+\widetilde{\omega}r_1\cos\theta\right)\hat{r} + \frac{(-im-\widetilde{\omega}r_1 r\sin\theta)}{r}\hat{\theta}\right].\end{aligned}$$

Forming the terms in the integrand of Eq. (C.10) gives

$$\psi^*\nabla_r\psi = \left(\frac{\widetilde{\omega}}{\pi}\right)^2 \frac{1}{\Gamma(\mu+1)} \left(\sqrt{\frac{\widetilde{\omega}}{2}}r\right)^{2\mu} e^{-\widetilde{\omega}\left(2r_1^2+r^2-2r_1 r\cos\theta\right)} \times \left[\left(\frac{\mu}{r} - \widetilde{\omega}r + \widetilde{\omega}r_1\cos\theta\right)\hat{r} + \frac{(im - \widetilde{\omega}r_1 r\sin\theta)}{r}\hat{\theta}\right],$$

and

$$\psi\nabla_r\psi^* = \left(\frac{\widetilde{\omega}}{\pi}\right)^2 \frac{1}{\Gamma(\mu+1)} \left(\sqrt{\frac{\widetilde{\omega}}{2}}r\right)^{2\mu} e^{-\widetilde{\omega}\left(2r_1^2+r^2-2r_1 r\cos\theta\right)} \times \left[\left(\frac{\mu}{r} - \widetilde{\omega}r + \widetilde{\omega}r_1\cos\theta\right)\hat{r} + \frac{(-im - \widetilde{\omega}r_1 r\sin\theta)}{r}\hat{\theta}\right].$$

Therefore, the integrand of Eq. (C.10) is

$$\begin{aligned}\psi^*\nabla_r\psi - \psi\nabla_r\psi^* =& 2im\left(\frac{\widetilde{\omega}}{\pi}\right)^2 \frac{1}{\Gamma(\mu+1)} \left(\frac{\widetilde{\omega}r^2}{2}\right)^{\mu} \frac{e^{-\widetilde{\omega}\left(2r_1^2+r^2-2r_1 r\cos\theta\right)}}{r}\hat{\theta},\\ =& 2im\left(\frac{\widetilde{\omega}}{\pi}\right)^2 \frac{1}{\Gamma(\mu+1)} \left(\frac{\widetilde{\omega}r^2}{2}\right)^{\mu} \frac{e^{-\widetilde{\omega}\left(2r_1^2+r^2-2r_1 r\cos\theta\right)}}{r}\left(\sin\theta\hat{r}_1 + \cos\theta\hat{\theta}_1\right).\end{aligned} \tag{C.21}$$

We now evaluate the paramagnetic current density using Eq.(C.10),

$$\begin{aligned}\mathbf{j}_p(\mathbf{r}_1) =& -i\int_0^{\infty}\int_0^{2\pi} 2im\left(\frac{\widetilde{\omega}}{\pi}\right)^2 \frac{1}{\Gamma(\mu+1)} \left(\frac{\widetilde{\omega}r^2}{2}\right)^{\mu} e^{-\widetilde{\omega}\left(2r_1^2+r^2-2r_1 r\cos\theta\right)} \left(\sin\theta\hat{r}_1 + \cos\theta\hat{\theta}_1\right) drd\theta,\\ =& \frac{2m\widetilde{\omega}^2}{\pi}\frac{1}{\Gamma(\mu+1)}\left(\frac{\widetilde{\omega}}{2}\right)^{\mu} e^{-2\widetilde{\omega}r_1^2}\int_0^{\infty} r^{2\mu}e^{-\widetilde{\omega}r^2}\frac{1}{\pi}\int_0^{2\pi} e^{2\widetilde{\omega}r_1 r\cos\theta}\left(\sin\theta\hat{r}_1 + \cos\theta\hat{\theta}_1\right) drd\theta,\\ =& \hat{\theta}_1\frac{2m\widetilde{\omega}^2}{\pi}\frac{1}{\Gamma(\mu+1)}\left(\frac{\widetilde{\omega}}{2}\right)^{\mu} e^{-2\widetilde{\omega}r_1^2}\int_0^{\infty} r^{2\mu}e^{-\widetilde{\omega}r^2}\frac{1}{\pi}\int_0^{2\pi} e^{2\widetilde{\omega}r_1 r\cos\theta}\cos\theta drd\theta,\end{aligned}$$

Noting that the θ integral defines a first order modified Bessel function, we have the following expression for the paramagnetic current density for the ISI system,

$$\mathbf{j}_p(\mathbf{r}_1) = \hat{\theta}_1\frac{4m\widetilde{\omega}^2}{\pi}\frac{1}{\Gamma(\mu+1)}\left(\frac{\widetilde{\omega}}{2}\right)^{\mu} e^{-2\widetilde{\omega}r_1^2}\int_0^{\infty} r^{2\mu}e^{-\widetilde{\omega}r^2} I_1(2\widetilde{\omega}r_1 r). \tag{C.22}$$

C.4 Three-Dimensional Isotropic Hooke's Atom

Using Eq. (5.9) and the coordinates $\left(\mathbf{r}, \sqrt{r_1^2 + \frac{r^2}{4} - r_1 r \sin\theta\cos\phi}\right)$, the ground-state wavefunction for the 3D isotropic Hooke's Atom is

$$\psi\left(\mathbf{r}, \sqrt{r_1^2 + \frac{r^2}{4} - r_1 r \sin\theta\cos\phi}\right) = \frac{1}{2\sqrt{\pi}}\left(\frac{2\omega}{\pi}\right)^{\frac{3}{4}} \frac{u(r)}{r} e^{-\omega\left(r_1^2 + \frac{r^2}{4} - r_1 r \sin\theta\cos\phi\right)}. \tag{C.23}$$

C.4.1 Particle Density

For the density, we have,

$$\rho(\mathbf{r}_1) = \frac{1}{2\pi}\left(\frac{2\omega}{\pi}\right)^{\frac{3}{2}} e^{-2\omega r_1^2} \int_0^\infty |u(r)|^2 e^{-\frac{\omega r^2}{2}} \int_0^\pi \int_0^{2\pi} e^{2\omega r_1 r \sin\theta\cos\phi} \sin\theta d\phi d\theta dr. \tag{C.24}$$

For the ϕ integral we make use of the definition of the modified Bessel function as for the magnetic case, giving,

$$\rho(\mathbf{r}_1) = \left(\frac{2\omega}{\pi}\right)^{\frac{3}{2}} e^{-2\omega r_1^2} \int_0^\infty |u(r)|^2 e^{-\frac{\omega r^2}{2}} \int_0^\pi I_0(2\omega r_1 r \sin\theta) \sin\theta d\theta dr. \tag{C.25}$$

In order to evaluate the theta integral, we use the series expansion of the modified Bessel function [112],

$$I_0(z) = \sum_{k=0}^{\infty} \frac{\left(\frac{z}{2}\right)^{2k}}{(k!)^2}. \tag{C.26}$$

Returning to the density, and using tables of integrals [112],

$$\begin{aligned}
\rho(\mathbf{r}_1) &= \left(\frac{2\omega}{\pi}\right)^{\frac{3}{2}} e^{-2\omega r_1^2} \int_0^\infty |u(r)|^2 e^{-\frac{\omega r^2}{2}} \sum_{k=0}^{\infty} \frac{(\omega r_1 r)^{2k}}{(k!)^2} \int_0^\pi \sin^{2k+1}\theta d\theta dr, \\
&= \left(\frac{2\omega}{\pi}\right)^{\frac{3}{2}} e^{-2\omega r_1^2} \int_0^\infty |u(r)|^2 e^{-\frac{\omega r^2}{2}} \sum_{k=0}^{\infty} \frac{(\omega r_1 r)^{2k}}{(k!)^2} \frac{2^{2k+1}(k!)^2}{(2k+1)!} dr, \\
&= \left(\frac{2\omega}{\pi}\right)^{\frac{3}{2}} e^{-2\omega r_1^2} \int_0^\infty |u(r)|^2 e^{-\frac{\omega r^2}{2}} \frac{1}{\omega r_1 r} \sum_{k=0}^{\infty} \frac{(2\omega r_1 r)^{2k+1}}{(2k+1)!} dr, \\
&= \left(\frac{2\omega}{\pi}\right)^{\frac{3}{2}} e^{-2\omega r_1^2} \int_0^\infty \frac{1}{\omega r_1 r} |u(r)|^2 e^{-\frac{\omega r^2}{2}} \sinh(2\omega r_1 r) dr.
\end{aligned}$$

This form for the density is in agreement with Ref. [92].

C.5 Helium-like Atoms

C.5.1 Particle Density

For the Helium-like atoms, the wavefunction given by Eq. (5.14) is expressed in terms of the coordinates $(2Zr_1, 2Zr_2, \cos\theta)$. Hence, we can calculate the density by integrating out two of these coordinates and transforming the remaining radial coordinate from $2Zr_1$ to r_1. We evaluate the density using the expression,

$$\rho\left(2Z\mathbf{r}_1\right) = 4\pi \int_0^\infty \int_{-1}^1 \left|\psi\left(2Zr_1, 2Zr_2, \cos\theta\right)\right|^2 \left(2Zr_2\right)^2 d\left(2Zr_2\right) d\left(\cos\theta\right). \quad \text{(C.27)}$$

Inserting Eq. (5.14) into this gives,

$$\rho\left(2Z\mathbf{r}_1\right) = \frac{1}{2\pi} \int_0^\infty \int_{-1}^1 e^{-2Z(r_1+r_2)} \left(2Zr_2\right)^2 \times \sum_{\substack{i,j,k,\\ i',j',k'}}^{\substack{i+j+k\leqslant\Omega,\\ i'+j'+k'\leqslant\Omega}} \Big[c_{ijk} c_{i'j'k'} N_{ijk} N_{i'j'k'} L_i^{(2)}\left(2Zr_1\right) L_j^{(2)}\left(2Zr_2\right) P_k\left(\cos\theta\right) L_{i'}^{(2)}\left(2Zr_1\right) L_{j'}^{(2)}\left(2Zr_2\right) P_{k'}\left(\cos\theta\right) \Big] d\left(2Zr_2\right) d\left(\cos\theta\right).$$

The polynomials $L_n^{(\alpha)}(x)$ and $P_n(x)$ obey the orthogonality relations [20, 79]

$$\sqrt{\frac{m!}{(m+\alpha)!}} \sqrt{\frac{n!}{(n+\alpha)!}} \int_0^\infty x^\alpha e^{-x} L_m^{(\alpha)}(x) L_n^{(\alpha)}(x)\, dx = \delta_{mn}, \quad \text{(C.28)}$$

$$\sqrt{\frac{2m+1}{2}} \sqrt{\frac{2n+1}{2}} \int_{-1}^1 P_m(x) P_n(x)\, dx = \delta_{mn}. \quad \text{(C.29)}$$

By using the orthogonality relations (C.28) and (C.29), we can evaluate the integrals in the density, and obtain,

$$\rho\left(2Z\mathbf{r}_1\right) = \frac{e^{-2Zr_1}}{2\pi} \sum_{\substack{i,j,k,\\ i',j',k'}}^{\substack{i+j+k\leqslant\Omega,\\ i'+j'+k'\leqslant\Omega}} \delta_{j,j'} \delta_{k,k'} c_{ijk} c_{i'j'k'} \sqrt{\frac{1}{(i+1)(i+2)(i'+1)(i'+2)}} L_i^{(2)}\left(2Zr_1\right) L_{i'}^{(2)}\left(2Zr_1\right). \quad \text{(C.30)}$$

For the Helium-like atoms, we use the coordinates $(2Zr_1, 2Zr_2, \cos\theta)$, and hence the density is given in terms of the coordinate $2Zr_1$. This is advantageous both for implementing the variational method and calculating the density, as it allows us to use the orthogonality relations (C.28) and (C.29) to evaluate the integrals. The density is expressed in terms of the coordinate r_1 by transforming the coefficients $c_{ijk}, c_{i'j'k'}$ by multiplying them by $(2Z)^{\frac{3}{2}}$.

Bibliography

[1] B. H. Bransden and C. J. Joachain, *Quantum Mechanics*. Pearson, 2000.

[2] R. M. Dreizler and E. K. U. Gross, *Density Functional Theory*. Springer Verlag, 1990.

[3] K. Capelle, "A bird's-eye view of density-functional theory," *Brazilian Journal of Physics*, vol. 36, pp. 1318–1343, 2006.

[4] E. Engel and R. M. Dreizler, *Density Functional Theory: An Advanced Course*. Springer Verlag, 2011.

[5] A. Einstein, "Über einen die erzeugung und verwandlung des lichtes betreffenden heuristischen gesichtspunkt," *Annalen der Physik*, vol. 17, no. 6, pp. 132–148, 2015.

[6] M. Born, "Zur quantenmechanik der stovorgnge," *Zeitschrift fr Physik*, vol. 37, no. 12, pp. 863–867, 1926.

[7] G. F. Giuliani and G. Vignale, *Quantum Theory of the Electron Liquid*. Cambridge University Press, 2005.

[8] E. Merzbacher, *Quantum Mechanics*. John Wiley & Sons, 198.

[9] P. Ehrenfest, "Bemerkung ber die angenherte gltigkeit der klassischen mechanik innerhalb der quantenmechanik," *Zeitschrift fr Physik*, vol. 45, no. 7-8, pp. 455–457, 1927.

[10] A. I. M. Rae, *Quantum Mechanics*. Taylor & Francis, 2008.

[11] E. Noether, "Invariante variationsprobleme," *Nachr. v. d. Ges. d. Wiss. zu Göttingen, Math-phys. Klasse*, pp. 235–257, 1918.

[12] L. N. Hand and J. D. Finch, *Analytical Mechanics*. Cambridge University Press, 2008.

[13] W. Kohn, "Nobel lecture: Electronic structure of matter-wave functions and density functionals," *Rev. Mod. Phys.*, vol. 71, pp. 1253–1266, Oct 1999.

[14] K. Burke, "Perspective on density functional theory," *The Journal of Chemical Physics*, vol. 136, no. 15, pp. –, 2012.

[15] P. Hohenberg and W. Kohn, "Inhomogeneous electron gas," *Phys. Rev.*, vol. 136, pp. B864–B871, Nov 1964.

[16] W. Ritz, "Über eine neue methode zur lösung gewisser variationsprobleme der mathematischen physik," *Journal für die reine und angewandte Mathematik*, vol. 135, pp. 1–61, 1909.

[17] A. J. Coleman, "Structure of fermion density matrices," *Rev. Mod. Phys.*, vol. 35, pp. 668–686, Jul 1963.

[18] T. L. Gilbert, "Hohenberg-kohn theorem for nonlocal external potentials," *Phys. Rev. B*, vol. 12, pp. 2111–2120, Sep 1975.

[19] J. E. Harriman, "Orthonormal orbitals for the representation of an arbitrary density," *Phys. Rev. A*, vol. 24, pp. 680–682, Aug 1981.

[20] "NIST Digital Library of Mathematical Functions." http://dlmf.nist.gov/, Release 1.0.9 of 2014-08-29.

[21] M. Levy, "Universal variational functionals of electron densities, first-order density matrices, and natural spin-orbitals and solution of the v-representability problem," *Proceedings of the National Academy of Sciences*, vol. 76, no. 12, pp. 6062–6065, 1979.

[22] H. Englisch and R. Englisch, "Hohenberg-kohn theorem and non-v-representable densities," *Physica A: Statistical Mechanics and its Applications*, vol. 121, no. 12, pp. 253 – 268, 1983.

[23] W. Kohn and L. J. Sham, "Self-consistent equations including exchange and correlation effects," *Phys. Rev.*, vol. 140, pp. A1133–A1138, Nov 1965.

[24] R. O. Jones and O. Gunnarsson, "The density functional formalism, its applications and prospects," *Rev. Mod. Phys.*, vol. 61, pp. 689–746, Jul 1989.

[25] J. P. Perdew and Y. Wang, "Accurate and simple analytic representation of the electron-gas correlation energy," *Phys. Rev. B*, vol. 45, pp. 13244–13249, Jun 1992.

[26] J. P. Perdew, K. Burke, and M. Ernzerhof, "Generalized gradient approximation made simple," *Phys. Rev. Lett.*, vol. 77, pp. 3865–3868, Oct 1996.

[27] J. P. Perdew, K. Burke, and M. Ernzerhof, "Generalized gradient approximation made simple [phys. rev. lett. 77, 3865 (1996)]," *Phys. Rev. Lett.*, vol. 78, pp. 1396–1396, Feb 1997.

[28] J. Tao, J. P. Perdew, V. N. Staroverov, and G. E. Scuseria, "Climbing the density functional ladder: Nonempirical meta–generalized gradient approximation designed for molecules and solids," *Phys. Rev. Lett.*, vol. 91, p. 146401, Sep 2003.

[29] P. J. Hasnip, K. Refson, M. I. J. Probert, J. R. Yates, S. J. Clark, and C. J. Pickard, "Density functional theory in the solid state," *Philosophical Transactions of the Royal Society of London A: Mathematical, Physical and Engineering Sciences*, vol. 372, no. 2011, 2014.

[30] S. D. Wong, M. Srnec, and M. L. e. a. Matthews, "Elucidation of the fe(iv)=o intermediate in the catalytic cycle of the halogenase syrb2," *Nature*, vol. 499, pp. 320–323, 2013.

[31] M. D. Knudson, M. P. Desjarlais, R. W. Lemke, T. R. Mattsson, M. French, N. Nettelmann, and R. Redmer, "Probing the interiors of the ice giants: Shock compression of water to 700 gpa and 3.8 $\mathbf{g}/\mathrm{cm}^3$," *Phys. Rev. Lett.*, vol. 108, p. 091102, Feb 2012.

[32] U. von Barth and L. Hedin, "A local exchange-correlation potential for the spin polarized case. i," *Journal of Physics C: Solid State Physics*, vol. 5, no. 13, p. 1629, 1972.

[33] O. Gunnarsson and B. I. Lundqvist, "Exchange and correlation in atoms, molecules, and solids by the spin-density-functional formalism," *Phys. Rev. B*, vol. 13, pp. 4274–4298, May 1976.

[34] O. Gunnarsson and B. I. Lundqvist, "Erratum: Exchange and correlation in atoms, molecules, and solids by the spin-density-functional formalism," *Phys. Rev. B*, vol. 15, pp. 6006–6006, Jun 1977.

[35] A. K. Rajagopal and J. Callaway, "Inhomogeneous electron gas," *Phys. Rev. B*, vol. 7, pp. 1912–1919, Mar 1973.

[36] A. H. MacDonald and S. H. Vosko, "A relativistic density functional formalism," *Journal of Physics C: Solid State Physics*, vol. 12, no. 15, p. 2977, 1979.

[37] E. Runge and E. K. U. Gross, "Density-functional theory for time-dependent systems," *Phys. Rev. Lett.*, vol. 52, pp. 997–1000, Mar 1984.

[38] C. A. Ullrich and Z. Yang, "A brief compendium of time-dependent density functional theory," *Braz. J Phys.*, vol. 44, no. 1, pp. 154–188, 2013.

[39] G. Vignale and M. Rasolt, "Density-functional theory in strong magnetic fields," *Phys. Rev. Lett.*, vol. 59, pp. 2360–2363, Nov 1987.

[40] G. Vignale and M. Rasolt, "Current- and spin-density-functional theory for inhomogeneous electronic systems in strong magnetic fields," *Phys. Rev. B*, vol. 37, pp. 10685–10696, Jun 1988.

[41] K. Capelle and G. Vignale, "Nonuniqueness and derivative discontinuities in density-functional theories for current-carrying and superconducting systems," *Phys. Rev. B*, vol. 65, p. 113106, Feb 2002.

[42] M. Taut, P. Machon, and H. Eschrig, "Violation of noninteracting $\mathscr{V}$-representability of the exact solutions of the schrödinger equation for a two-electron quantum dot in a homogeneous magnetic field," *Phys. Rev. A*, vol. 80, p. 022517, Aug 2009.

[43] E. I. Tellgren, S. Kvaal, E. Sagvolden, U. Ekström, A. M. Teale, and T. Helgaker, "Choice of basic variables in current-density-functional theory," *Phys. Rev. A*, vol. 86, p. 062506, Dec 2012.

[44] J. D. Ramsden and R. W. Godby, "Intrinsic exchange-correlation magnetic fields in exact current density functional theory for degenerate systems," *Phys. Rev. B*, vol. 88, p. 195115, Nov 2013.

[45] E. H. Lieb and R. Schrader, "Current densities in density-functional theory," *Phys. Rev. A*, vol. 88, p. 032516, Sep 2013.

[46] E. I. Tellgren, S. Kvaal, and T. Helgaker, "Fermion n-representability for prescribed density and paramagnetic current density," *Phys. Rev. A*, vol. 89, p. 012515, Jan 2014.

[47] A. Laestadius and M. Benedicks, "Nonexistence of a hohenberg-kohn variational principle in total current-density-functional theory," *Phys. Rev. A*, vol. 91, p. 032508, Mar 2015.

[48] M. Frchet, "Sur quelques points du calcul fonctionnel," *Rendiconti del Circolo Matematico di Palermo*, vol. 22, no. 1, pp. 1–72, 1906.

[49] F. Hausdorff, *Set Theory*. Chelsea Publishing Company, 1937.

[50] W. A. Sutherland, *Introduction to Metric & Topological Spaces*. Oxford University Press, 2009.

[51] R. E. Megginson, *An Introduction to Banach Space Theory*. Springer, 1998.

[52] W. A. Sutherland, "Introduction to metric & topological spaces: Supplementary material." http://global.oup.com/booksites/content/9780199563081/.

[53] C. J. Isham, *Lectures on Groups and Vector Spaces for Physicists*. World Scientific Publishing Company, 1989.

[54] C. J. Isham, *Lectures on Quantum Theory*. Imperial University Press, 1995.

[55] H. Hahn, "ber folgen linearer operationen," *Monatshefte fr Mathematik und Physik*, vol. 32, no. 1, pp. 3–88, 1922.

[56] S. Banach, "Sur les oprations dans les ensembles abstraits et leur application aux quations intgrales," *Fund. Math.*, vol. 3, pp. 133–181, 1922.

[57] L. Longpré and V. Kreinovich, "When are two wave functions distinguishable: A new answer to Pauli's question, with potential application to quantum cosmology," *International Journal of Theoretical Physics*, vol. 47, pp. 814–831, 2008.

[58] I. D'Amico, J. P. Coe, V. V. França, and K. Capelle, "Quantum mechanics in metric space: Wave functions and their densities," *Phys. Rev. Lett.*, vol. 106, p. 050401, Feb 2011.

[59] J. Hubbard, "Electron correlations in narrow energy bands," *Proceedings of the Royal Society of London A: Mathematical, Physical and Engineering Sciences*, vol. 276, no. 1365, pp. 238–257, 1963.

[60] F. H. L. Essler, H. Frahm, F. Göhmann, A. Klümper, and V. E. Korepin, *The One-Dimensional Hubbard Model*. Cambridge University Press, 2010.

[61] I. Nagy and I. Aldazabal, "Metric measures of interparticle interaction in an exactly solvable two-electron model atom," *Phys. Rev. A*, vol. 84, p. 032516, Sep 2011.

[62] P. M. Sharp and I. D'Amico, "Metric space formulation of quantum mechanical conservation laws," *Phys. Rev. B*, vol. 89, p. 115137, Mar 2014.

[63] P. M. Sharp and I. D'Amico, "Metric-space analysis of systems immersed in a magnetic field," *Phys. Rev. A*, vol. 92, p. 032509, Sep 2015.

[64] P. M. Sharp and I. D'Amico, 2015. in progress.

[65] C. S. Kubrusly, *The Elements of Operator Theory*. Springer, 2009.

[66] D. Burago, Y. Burago, and S. Ivanov, *A Course in Metric Geometry*. American Mathematical Society, 2001.

[67] R. B. Griffiths, *Consistent Quantum Theory*. Cambridge University Press, 2002.

[68] E. Artacho, "Comment on "quantum mechanics in metric space: Wave functions and their densities"," *Phys. Rev. Lett.*, vol. 107, p. 188901, Oct 2011.

[69] I. D'Amico, J. P. Coe, V. V. França, and K. Capelle, "D'amico *et al.* reply:," *Phys. Rev. Lett.*, vol. 107, p. 188902, Oct 2011.

[70] J. Javanainen, J. H. Eberly, and Q. Su, "Numerical simulations of multiphoton ionization and above-threshold electron spectra," *Phys. Rev. A*, vol. 38, pp. 3430–3446, Oct 1988.

[71] P. Elliott, J. I. Fuks, A. Rubio, and N. T. Maitra, "Universal dynamical steps in the exact time-dependent exchange-correlation potential," *Phys. Rev. Lett.*, vol. 109, p. 266404, Dec 2012.

[72] C. Cohen-Tannoudji, B. Diu, and F. Laloë, *Quantum Mechanics*. John Wiley & Sons, 1977.

[73] M. Taut, "Two electrons in an external oscillator potential: Particular analytic solutions of a coulomb correlation problem," *Phys. Rev. A*, vol. 48, pp. 3561–3566, Nov 1993.

[74] I. D'Amico and G. Vignale, "Exact exchange-correlation potential for a time-dependent two-electron system," *Phys. Rev. B*, vol. 59, pp. 7876–7887, Mar 1999.

[75] M. Taut, "Two electrons in a homogeneous magnetic field: particular analytical solutions," *Journal of Physics A: Mathematical and General*, vol. 27, no. 3, p. 1045, 1994.

[76] V. Fock, "Bemerkung zur quantelung des harmonischen oszillators im magnetfeld," *Zeitschrift fr Physik*, vol. 47, no. 5-6, pp. 446–448, 1928.

[77] C. G. Darwin, "The diamagnetism of the free electron," *Mathematical Proceedings of the Cambridge Philosophical Society*, vol. 27, pp. 86–90, 1 1931.

[78] R. B. Dingle, "Some magnetic properties of metals. i. general introduction, and properties of large systems of electrons," *Proceedings of the Royal Society of London A: Mathematical, Physical and Engineering Sciences*, vol. 211, no. 1107, pp. 500–516, 1952.

[79] M. Abramowitz and I. A. Stegun, *Handbook of Mathematical Functions with Formulas, Graphs, and Mathematical Tables*. New York: Dover, ninth dover printing, tenth gpo printing ed., 1964.

[80] G. Frobenius, "Über die integration der linearen differentialgleichungen durch reihen.," *J. reine angew. Math.*, vol. 76, pp. 214–235, 1873.

[81] E. Kreyzig, *Advanced Engineering Mathematics*. John Wiley & Sons, 2006.

[82] J. P. Coe, A. Sudbery, and I. D'Amico, "Entanglement and density-functional theory: Testing approximations on hooke's atom," *Phys. Rev. B*, vol. 77, p. 205122, May 2008.

[83] L. Quiroga, D. Ardila, and N. Johnson, "Spatial correlation of quantum dot electrons in a magnetic field," *Solid State Communications*, vol. 86, no. 12, pp. 775 – 780, 1993.

[84] A. Thirumalai and J. S. Heyl, "Hydrogen and helium atoms in strong magnetic fields," *Phys. Rev. A*, vol. 79, p. 012514, Jan 2009.

[85] A. Thirumalai, S. J. Desch, and P. Young, "Carbon atom in intense magnetic fields," *Phys. Rev. A*, vol. 90, p. 052501, Nov 2014.

[86] W. Desrat, B. A. Piot, D. K. Maude, Z. R. Wasilewski, M. Henini, and R. Airey, "W line shape in the resistively detected nuclear magnetic resonance," *Journal of Physics: Condensed Matter*, vol. 27, no. 27, p. 275801, 2015.

[87] S. Owerre and J. Nsofini, "A toy model for quantum spin hall effect," *Solid State Communications*, vol. 218, pp. 35 – 39, 2015.

[88] M. Mehring, J. Mende, and W. Scherer, "Entanglement between an electron and a nuclear spin $\frac{1}{2}$," *Phys. Rev. Lett.*, vol. 90, p. 153001, Apr 2003.

[89] S. Takahashi, R. Hanson, J. van Tol, M. Sherwin, and D. Awschalom, "Quenching spin decoherence in diamond through spin bath polarization," *Phys. Rev. Lett.*, vol. 101, p. 047601, Jul 2008.

[90] J. P. Coe, V. V. França, and I. D'Amico. Private Communication.

[91] J. P. Perdew, R. G. Parr, M. Levy, and J. L. Balduz, "Density-functional theory for fractional particle number: Derivative discontinuities of the energy," *Phys. Rev. Lett.*, vol. 49, pp. 1691–1694, Dec 1982.

[92] P. M. Laufer and J. B. Krieger, "Test of density-functional approximations in an exactly soluble model," *Phys. Rev. A*, vol. 33, pp. 1480–1491, Mar 1986.

[93] C. Filippi, C. J. Umrigar, and M. Taut, "Comparison of exact and approximate density functionals for an exactly soluble model," *The Journal of Chemical Physics*, vol. 100, no. 2, pp. 1290–1296, 1994.

[94] M. Born and R. Oppenheimer, "Zur Quantentheorie der Molekeln," *Annalen der Physik*, vol. 389, pp. 457–484, 1927.

[95] G. W. Kellner, "Die ionisierungsspannung des heliums nach der schrdingerschen theorie," *Z. Physik*, vol. 44, pp. 91–109, 1927.

[96] E. A. Hylleraas, "ber den grundzustand des heliumsatoms," *Z. Physik*, vol. 48, p. 469, 1928.

[97] E. A. Hylleraas, "Neue berechnung der energie des heliums im grundstande, sowie des tiefsten terms von ortho-heliium," *Z. Physik*, vol. 54, p. 347, 1929.

[98] G. W. F. Drake, "High precision theory of atomic helium," *Physica Scripta*, vol. 1999, no. T83, p. 83, 1999.

[99] H. A. Bethe and E. E. Salpeter, *Quantum Mechanics of One- and Two-Electron Atoms*. Dover Publications, 1977.

[100] A. J. Thakkar and T. Koga, "Ground-state energies for the helium isoelectronic series," *Phys. Rev. A*, vol. 50, pp. 854–856, Jul 1994.

[101] M. Khan, "Low-lying s-states of two-electron systems," *Few-Body Systems*, vol. 55, no. 11, pp. 1125–1139, 2014.

[102] J. D. Baker, D. E. Freund, R. N. Hill, and J. D. Morgan, "Radius of convergence and analytic behavior of the $\frac{1}{Z}$ expansion," *Phys. Rev. A*, vol. 41, pp. 1247–1273, Feb 1990.

[103] Y. Accad, C. L. Pekeris, and B. Schiff, "s and p states of the helium isoelectronic sequence up to $z = 10$," *Phys. Rev. A*, vol. 4, pp. 516–536, Aug 1971.

[104] J. P. Coe, K. Capelle, and I. D'Amico, "Reverse engineering in many-body quantum physics: Correspondence between many-body systems and effective single-particle equations," *Phys. Rev. A*, vol. 79, p. 032504, Mar 2009.

[105] W. Kohn, A. D. Becke, and R. G. Parr, "Density functional theory of electronic structure," *The Journal of Physical Chemistry*, vol. 100, no. 31, pp. 12974–12980, 1996.

[106] A. D. Becke and M. R. Roussel, "Exchange holes in inhomogeneous systems: A coordinate-space model," *Phys. Rev. A*, vol. 39, pp. 3761–3767, Apr 1989.

[107] M. Taut, A. Ernst, and H. Eschrig, "Two electrons in an external oscillator potential: exact solution versus one-particle approximations," *Journal of Physics B: Atomic, Molecular and Optical Physics*, vol. 31, no. 12, p. 2689, 1998.

[108] R. W. Godby, M. Schlüter, and L. J. Sham, "Accurate exchange-correlation potential for silicon and its discontinuity on addition of an electron," *Phys. Rev. Lett.*, vol. 56, pp. 2415–2418, Jun 1986.

[109] M. J. P. Hodgson, J. D. Ramsden, J. B. J. Chapman, P. Lillystone, and R. W. Godby, "Exact time-dependent density-functional potentials for strongly correlated tunneling electrons," *Phys. Rev. B*, vol. 88, p. 241102, Dec 2013.

[110] J. P. Coe, *Entanglement and density-functional theory in two-electron systems*. PhD thesis, University of York, June 2009.

[111] H.-K. Rhee, R. Aris, and N. R. Amundson, *First order Partial Differential Equations*. David & Charles, 2001.

[112] I. S. Gradshteyn and I. M. Ryzhik, *Table of Integrals, Series and Products*. Academic Press, 2000.